Table of Contents

List of figures

List of abbreviations

3-O-MG	3-O-Methylglucose
ACT	Artemisinin Combination Therapy
AdoMetDC	S-Adenosyl Methionine Decarboxylase
ALBA	Always Lowers Binding Affinity
APAD	3-Acetylpyridine Adenine Dinucleotide
Apiap2	Apicomplexan AP2
AP2/ERF	Apetala2/Environmental Response Factors
ARID	AT-Rich Interaction Domain
ARK	Aurora Related Kinase
AUC	Area Under Curve
BDP	Bromodomain Protein
CAF	CCR4-Associated Factor
Camp	Cyclic Adenosine Monophosphate
CDK	Cyclin Dependent Kinase
CDPK	Calcium Dependent Protein Kinase
CRK	Cdc2-Related Protein Kinase
CSP	Circumsporozoite Protein
DE	Differentially Expressed
DFMO	DL-A-Difluoromethylornithine
EBA	Erythrocyte Binding Antigen
EG	Early-Stage Gametocytes
eIF	Eukaryotic Translation Initiation Factor
F-6-P	D-Fructose-6-Phosphate
FC	Fold Change
G-6-P	D-Glucose-6-Phosphate
GAN	Gene Association Network
GAP	Glideosome Associated Protein
GDV1	Gametocyte Development Protein 1
GEO	Gene Expression Omnibus
GMEP	Global Malaria Eradication Program
GPI	Glycosylphosphatidylinositol
GRENITS	Gene Regulatory Network Inference Using Time Series
GRN	Gene Regulation Network
HAT	Histone Acetyl Transferase
HDAC	Histone Deacetylase
HKMT	Histone Lysine Methyl Transferase
HP1	Heterochromatin Protein 1
Hpi	Hours Post Invasion
HRMT	Histone Arginine Methyl Transferase
IDC	Intraerythrocytic Developmental Cycle
IFM2	Inoculation Fluid Medium 2
IMC	Inner Membrane Complex
iRBC	Asexual Blood Stage Infected Erythrocytes
LG	Late-Stage Gametocytes
LSD	Lysine-Specific Demethylase
LysoPC	Lysophosphatidylcholine
malERA	Malaria Eradication Agenda
MAP	Mitogen Activated Protein Kinase
MCM	Mini-Chromosome Maintenance Complex
MMV	Medicines for Malaria Venture
MRK	MO15-Related Protein Kinase
mRNP	mRNA-Ribonucleoprotein
MSP	Merozoite Surface Protein
NBT	Nitro Blue Tetrazoliumchloride
NEK	Never in Mitosis Associated-Kinase

NPP	New Permeability Pathways
ODC	Ornithine Decarboxylase
ORC	Origin Recognition Complex
PABP	Poly-Adenylate Binding Protein
PBE	Puf Binding Elements
PBS	Phosphate Buffered Saline
PCNA	Proliferating Cell Nuclear Antigen
PES	Phenazine Ethosulphate
PHD	Plant Homeo Domain
PK	Protein Kinase
PKA	cAMP-Dependent Protein Kinase
PKB	Rac-Beta Protein Kinase
PKG	cGMP-Dependent Protein Kinase
pLDH	Parasite Lactate Dehydrogenase
Pol	Polymerase
PPKL	Protein Phosphatase with Kelch-Like Domains
Puf	Pumillo-Family
PV	Parasitophorous Vacuole
RBC	Human Erythrocytes
RC	Replicative Complex
Rh	Reticulocyte Binding Homolog
RIFIN	Repetitive Interspersed Family
RON	Rhoptry Neck Protein
S/B	Signal Above Background
S/N	Signal Over Noise
SAP	Sin3-Repressing Complex
SERA	Ser Repeat Antigen
SRPK	SR-Protein Kinase
STEVOR	Subtelomeric Variant Open Reading Frame
SUB	Subtisilin
SVM	Support Vector Machine
TCA	Tricarboxylic Acid
TCP	Target Candidate Profile
TPP	Target Product Profile
TFBS	Transcription Factor Binding Site
TR	Translational Repression
TSS	Transcription Start Site
UTR	Untranslated Region
WHO	World Health Organization

Chapter 1

Literature review

1.1 Defining the global malaria burden and eradication strategies

Malaria impacts global health and economy and resulted in 216 million cases and 445000 mortalities in 2016 (1). The disease has been targeted for eradication through the concerted efforts of the World Health Organization (WHO) (1) and the continuation of flagship programs including the Malaria Eradication Agenda (malERA) (2) of the Roll Back Malaria campaign (3). Together, these endeavors emphasize an integrative, transdisciplinary approach that aims to improve available strategies targeting the parasite that causes malaria, the *Anopheles* mosquito vector transmitting the parasite and characterizing the transmission reservoir formed by these organisms (2).

The current elimination strategies are based on lessons learnt from both successful and unsuccessful previous attempts at malaria elimination. The Global Malaria Eradication Program (GMEP, 1955–1969) focused almost completely on indoor residual spraying (4), as the information on the feeding habits of the diverse *Anopheles* mosquito species was not available at that time (5,6). Subsequently, research into vector dynamics has identified important health and efficacy concerns in using “gold-standard” vector control methods. This resulted in adoption of integrated vector management as proposed by the WHO (7,8), which combines a number of interventions including long lasting insecticide treated nets and indoor residual spraying (7,9). Current vector control strategies are seen as the main factor that has led to dramatic decreases in malaria case numbers (1). However, confounding factors for sustained success with vector control include development of insecticide resistance (10) and changing biting behavior and migration dynamics of several of the *Anopheline* species that carry malaria parasites (5,6).

The apicomplexan *Plasmodium* parasites that transmit malaria contribute their own sets of challenges and problems to malaria eradication. In 2015, the results of the phase III clinical trial of the first malaria vaccine candidate, the RTS,S/AS01 vaccine, were published (11). The vaccine contained a region of recombinant *P. falciparum* circumsporozoite protein, which is essential for establishing a malaria infection in humans (12,13). Disappointingly, although the vaccine was able to reduce the symptomatic

malaria burden, it is far from completely effective and only offers transient protection (14). In addition, no effective vaccine candidate that also prevents transmission of *Plasmodium* parasites has entered clinical trials (1). The most effective interventions against the parasite to date have been the successes of the antimalarial drugs treating the symptoms of malaria infection (15).

The chemical interventions currently recommended by the WHO are mostly derivatives from natural products that had been used to treat malaria for centuries (16,17). The initial natural products, quinine and artemisinin, gave rise to subsequent generations of antimalarials, the 4- and 8-aminoquinolones; 4-methanolquinolines or artemisinin derivatives, respectively (15). These derivatives form the bulk of the current recommended treatment regime as artemisinin combination therapies (ACTs) (1), combining the rapid activity of artemisinin derivatives with the longer-lasting activity of, for instance, the quinoline compounds (18). The potent activity of artemisinin and its derivatives is believed to stem from Fe^{3+} (released by hemoglobin digestion) activating the drug *in vivo* (19), before alkylation of multiple parasite proteins result in the pleiotropic toxicity characteristic of this compound class (20). For the quinine-derivatives, the main mode-of-action is believed to be interference with the parasite's ability to effectively sequester toxic heme moieties formed by hemoglobin digestion (18). Alternatively, the use of an artemisinin derivative is also recommended in conjunction with compounds targeting enzymes in the folate biosynthesis pathway of the parasite, dihydrofolate reductase (targeted by pyrimethamine) or dihydropteroate synthase (targeted by sulphadoxine), although widespread resistance to the antifolates preclude their use in most clinical settings (21). The emergence of artemisinin resistance in Southeast Asia (22) and a case of reduced parasite clearance following treatment in Africa (23) resulting in decreased efficacy of the drug, raises serious concerns surrounding the continued use of ACTs as front-line treatment of malaria.

These issues with the current interventions against the parasite have encouraged research into novel chemical scaffolds, resulting in promising drug candidates entering clinical development, most notably MMV048, OZ439, KAE609, KAF156 and DSM265 (15). The infectious, virulent nature of the parasite, however, necessitates the continual population of the antimalarial drug and vaccine candidate development pipeline, as proposed by the Medicines for Malaria Venture (MMV, www.mmv.org) if the goal of global malaria eradication is to be met (24). To this point, descriptions of effective lead chemical

compounds (target candidate profiles, TCP) and potential medicines (target product profiles, TPP) were clearly defined and is used as a guided system for desirable attributes of the next generation of antimalarial medicines (25). For TCPs, multi-stage and -species activity, effective in targeting the spread of malaria as well as the symptomatic treatment of the disease, are emphasized (25). It is expected that identification of essential genetic moieties in the parasite (26) as well as identification of the druggable genome of the parasite (27) would overcome many of the previous obstacles in understanding drug activity that made it difficult to achieve the TCP and TPP guidelines. However, understanding the impact of antimalarials on the parasite is still incomplete without a solid knowledge base concerning the biology of the parasite.

1.2 Causative agent of malaria and its complex life cycle

Malaria in humans is currently known to be caused by five *Plasmodium* species, *P. falciparum, P. vivax, P. ovale, P. malariae and P. knowlesi.* Among these species, *P. falciparum* and *P. vivax* are the most widespread and contribute the highest number of infections and mortalities (1,28,29). *P. vivax* also contributes to the parasitic infectious reservoir by forming dormant hypnozoites in the liver that cause recurring malaria (30). *P. falciparum* is still globally responsible for the highest number of infections and mortalities (1) and, as the subject of this study, will be discussed in detail.

P. falciparum parasite infection in humans is initiated by the injection of ~20-200 sporozoites from feeding female *Anopheles* mosquitoes into the human host, where the parasites glide through the skin into the bloodstream using an actin-myosin motor (31). Continuing this gliding motility, sporozoites can migrate to the liver within two minutes of the initial transmission (12). In the liver the parasites traverse hepatocytes by first forming nonreplicative transient vacuoles before invading host cells, replicating within parasitophorous vacuoles (PV) to avoid degradation by host cell lysosomes (31). During this exoerythrocytic development in human hepatocytes, sporozoites asexually replicate to form a hepatic schizont before dividing into merozoites; these are released into the vasculature to subsequently invade erythrocytes, initiating the intraerythrocytic developmental cycle (IDC) (12) (Figure 1.1).

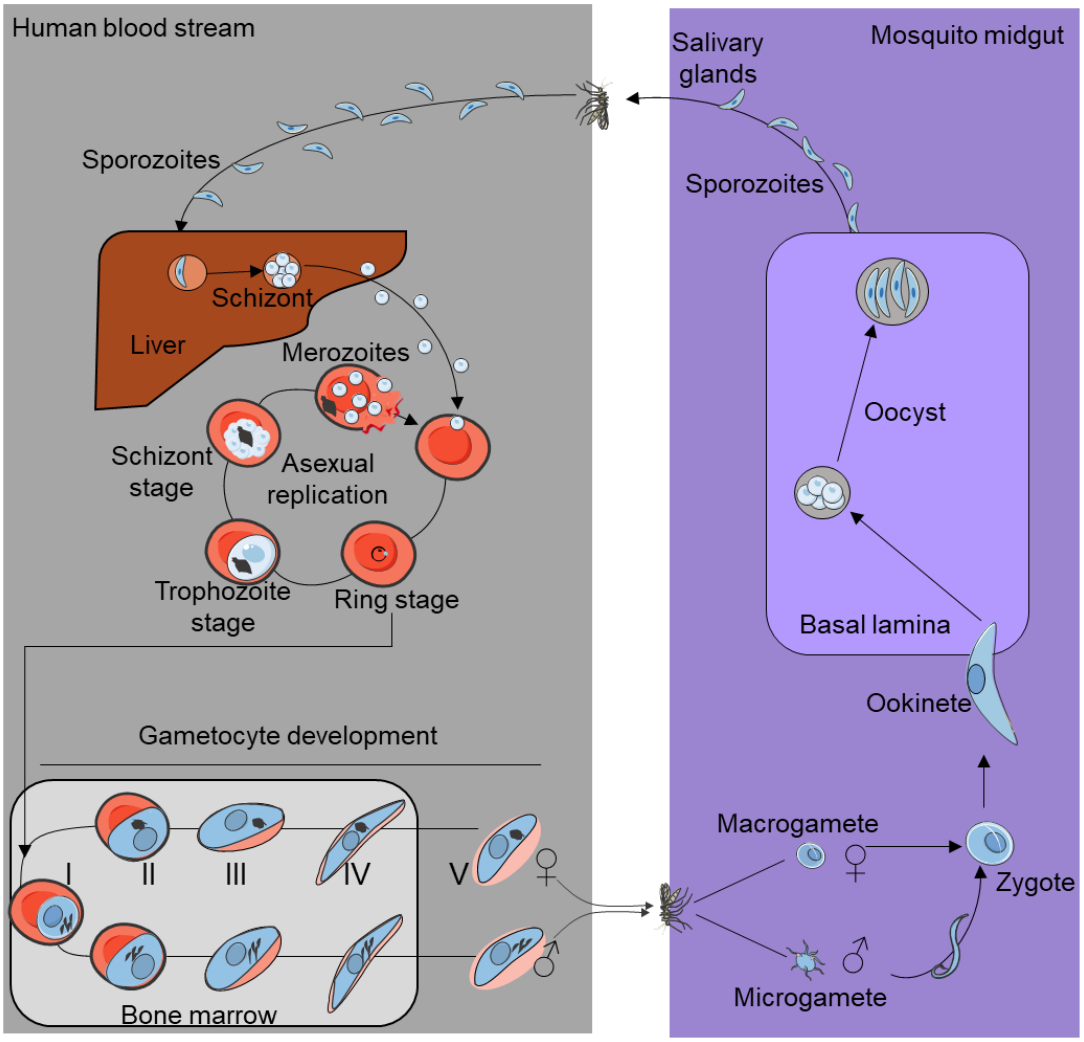

Figure 1.1: The *P. falciparum* parasite life cycle. The parasite completes a complex life cycle traversing both the *Anopheles* mosquito vector and human host. In the human host, the parasite first develops in the hepatocytes before invading erythrocytes, where the parasites can either complete the asexual developmental cycle or differentiate through five stages of gametocytogenesis. The mature gametocyte stages are then able to transmit to feeding *Anopheles* mosquitoes.

In the first few hours after invasion of the erythrocytes, parasites are observed as the morphological ring stages, when the parasites are enclosed in a PV (32) and begin to digest the hemoglobin of the erythrocyte at a rate comparable to parasite expansion (19,33). After ~15 hours of development, the parasite's metabolic activity increases, defining a period of increased cell growth as the parasite develops into the trophozoite stage (34). Trophozoite stages extensively remodel the host erythrocyte environment, decreasing the deformability of the cell membrane and making the membrane more permeable to small solutes, creating "new permeability pathways" (NPP) (35). The NPP are induced between 10 and 20 hours post-invasion (hpi) and have a broad substrate-specificity, being especially permeable to organic and inorganic monovalent ions (36). During the trophozoite stage, the parasite also contains a single mitochondrion (32), which is capable of glucose metabolism via a conventional tricarboxylic acid (TCA) cycle,

although the ring, trophozoite and schizont stages rely heavily on glycolysis for energy production (37–39). Compared to the uninfected erythrocyte, glucose metabolism and lactic acid production rates within an infected erythrocyte increases about 100-fold (40). Trophozoites also convert host hemoglobin into hemozoin through the digestion of heme in the digestive vacuole at an increased rate compared to ring stages, resulting in the characteristic pigmentation that can be observed morphologically during trophozoite stages (33,35,36).

Between 22 and 30 hpi, the parasite initiates DNA synthesis, signaling entry into schizogony (41,42). Multiple rounds of DNA synthesis and nuclear mitosis result in a pre-segmented and multi-nucleated schizont (43). During this process, the parasite's endosymbiotic organelles, the apicoplast and mitochondrion (44), are also replicated and distributed into the newly forming merozoites, with one of each organelle per cell (45). This takes place at ~40 hpi, after which cytokinesis and segmentation occurs, forming 16-32 haploid merozoites that are released about 8 hours later (46,47).

A small proportion (<10%) of intraerythrocytic parasites are stochastically committed to undergo sexual development during each cycle, ultimately forming mature gametocytes that are capable of transmission to a feeding *Anopheles* mosquito (48) (Figure 1.1). The developing gametocytes are morphologically and functionally different from asexual parasites on various levels including gene expression profiles (49) and metabolic activities (37,50). The formation of gametocytes is preceded by commitment to sexual development, with increased commitment stimulated through environmental signaling by cyclic adenosine monophosphate (cAMP) (51) and shown to be repressed by host lysophosphatidylcholine (52). These environmental factors then affect epigenetic and genetic factors governing sexual differentiation (53–56). Commitment to sexual development occurs one asexual cycle before gametocyte manifestation, with all of the merozoites from a single schizont committed to gametocytogenesis (57) and additionally becoming either male or female gametocytes (58).

Following commitment to sexual development in *P. falciparum* parasites, gametocytogenesis proceeds through five morphologically distinct developmental stages over ~14 days, an attribute shared only with the chimpanzee malaria parasite, *P. reichenowi* (59). Stage I gametocytes are morphologically almost indistinguishable from round, pigmented asexual trophozoite stages. Both these forms digest host cell

hemoglobin but stage I gametocytes contain dispersed, elongated hemozoin granules rather than a clump of hemozoin as observed in trophozoites (60). Stage I gametocytes are also sequestered primarily in the bone marrow during infection, compared to trophozoites that sequester in the microvasculature (61–63). Stage II gametocytes are characterized by construction of a subpellicular microtubular membrane (64), which causes a systematic elongation of the parasite. This becomes more pronounced in stage III gametocytes and culminates in crescent-shaped stage IV gametocytes (33,65). In the elongating gametocyte stages, sexual differentiation also becomes morphologically apparent, with female gametocytes containing more dense hemozoin crystals, while the crystals are scattered in male gametocytes (59). Stage IV female gametocytes also contain osmiophilic bodies and both sexes complete hemoglobin digestion by this stage in development (33). Stage V of development, the mature stage, is characterized by depolymerization of the subpellicular microtubule array which results in stage V gametocytes re-entering blood circulation (64) and, after a period of circulating in the blood stream, becoming infectious to feeding *Anopheles* mosquitoes (66).

Following uptake into the mosquito, the changed microenvironment (including an increased pH, decreased temperature and the presence of xanthurenic acid) stimulates the activation of male and female gametocytes to form micro- and macrogametes, respectively (67–69). Microgametogenesis involves three rounds of rapid mitosis and meiosis, resulting in eight flagellated haploid microgametes (70). Macrogametogenesis is associated with extensive macromolecular metabolism to support the developing zygote (71). Micro- and macrogametes from different hosts fuse into a zygote in the mosquito midgut lumen before the zygote undergoes meiosis and develops into a motile ookinete (72). The ookinete makes its way through the mosquito midgut, invading a basal midgut epithelial cell before developing into an oocyst containing multiple sporozoites (72), which, when the oocyst ruptures, migrate back to the salivary glands, ready to infect a new host (72).

Within this complicated life cycle, the cellular fate of the parasite is set for most phases of development, the exception being the point at which (possibly) liver schizonts (73) but primarily asexual parasites commit to either asexual replication or sexually differentiate into gametocytes.

1.3 A bifurcation in cellular fate defines intraerythrocytic *P. falciparum* parasite development: proliferate or differentiate?

The *P. falciparum* parasite is adapted to survive within two vastly different biological hosts and under immense evolutionary pressure by pharmaceutical intervention and host immune responses. One of the key elements of the parasite's evolutionary success is the binary decision determining the fate of the parasite within human erythrocytes. The intraerythrocytic stages will either commit to proliferation, generating additional genetic variation in subsequent generations of parasite populations that allow effective evasion of host or pharmaceutical pressures (74), or sexual propagation, allowing continuation of the parasite's species through transmission to the *Anopheles* mosquito.

1.3.1 Resultant metabolic profile of the respective proliferative or differentiating forms of the parasite

The asexual parasites primarily rely on the fermentative cytosolic glycolytic pathway, presumably for a more rapid production of energy required for the intense proliferation during these stages, similar to what is seen for rapidly proliferating *Saccharomyces cerevisiae* (75). By contrast, slow-maturing *P. falciparum* gametocytes show an increased reliance on the slower but more energy efficient oxidative metabolic pathway, the tricarboxylic acid (TCA) cycle in the mitochondria (37). The shift towards a more energy efficient pathway is proposed to prepare the parasite for development in the mosquito, which requires increased energy levels (76).

In asexual parasites, the glycolytic end-products are primarily lactic acid, pyruvate and alanine that subsequently get exported into the extracellular environment instead of entering into the TCA cycle (37). Although mitochondrial metabolism (TCA cycle) does occur during asexual development (77,78), the primary source for this is glutamine more than glucose (37) and the pathway is not essential for energy production but rather necessary for maintenance of the ubiquinone pathway for pyrimidine biosynthesis and purine salvage (26,76,79) (Figure 1.2).

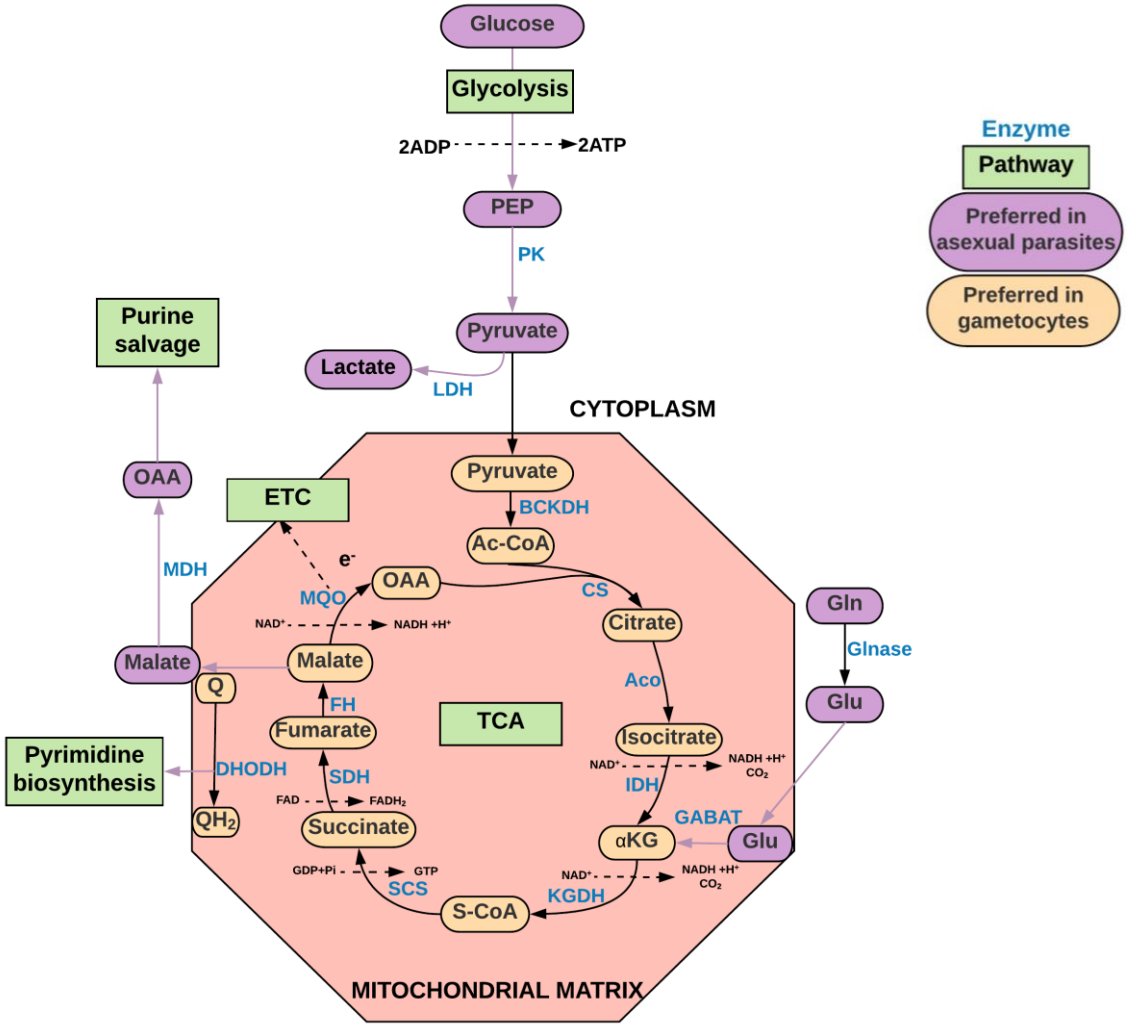

Figure 1.2: *P. falciparum* asexual parasites and gametocytes show different preferences in central carbon metabolic pathways. Asexual parasites metabolize glucose preferentially through glycolysis into pyruvate that gets converted to lactate, while gametocytes show increased reliance on the TCA cycle. The asexual parasite stages do make use of the TCA cycle but preferentially use glutamine as substrate and rather than complete the TCA cycle, export malate for use in purine salvage. Abbreviations: α-ketoglutarate; αKG, aconitase; Aco, branched-chain ketoacid dehydrogenase; BCKDH, citrate synthase; CS, dihydrooratate dehydrogenase; DHODH, fumarate hydratase; FH, GABA transaminase; GABAT, glutamine; Gln, glutaminase; Glnase, glutamate; Glu, isocitrate dehydrogenase; IDH, α-ketoglutarate dehydrogenase; KGDH, lactate dehydrogenase; LDH, malate dehydrogenase; MDH, malate quinone oxidoreductase; MQO, oxaloacetate; OAA, phosphoenolpyruvate; PEP, pyruvate kinase; PK, ubiquinone; Q, ubiquinol; QH2, succinate dehydrogenase; SDH, succinyl-CoA synthetase; SCS, succinyl-CoA; S-CoA.

The parasite is also believed to lack a functional gluconeogenesis pathway, as there are key enzymes missing from the genome (80,81). Instead, most free amino acids are obtained from hemoglobin digestion in the parasite's digestive vacuole of which ~16% are incorporated into parasite proteins, while a large proportion are released into the extracellular environment (82). This process results in potent activity of compounds targeting heme metabolism, like chloroquine, in these stages (83). Hemoglobin is poor in glutamate, methionine, glutamine and cysteine and completely lacks isoleucine; the

parasite cannot survive in media lacking these nutrients (84), but will enter a state of metabolic hibernation in response to amino acid starvation (85).

During gametocyte development, the parasites undergo substantial remodeling of their mitochondria, increasing the number of cristae in the organelles, changing the mitochondrial membrane potential and upregulating genes involved in the TCA cycle and oxidative phosphorylation (37). The substrates entering the TCA cycle also shift from glutamine (in asexual development) to glucose in gametocytes and the TCA cycle also contributes to energy metabolism rather than the ubiquinone pathway (37,39). Gametocytes are also unable to complete development if the TCA cycle is inhibited (37). It has also been shown that the gametocytes have an increased reliance on lipid metabolism, and while it would be tempting to speculate that this is due to increased membrane formation in the mitochondrion (50), it is also possible that lipids are entering the fatty acid synthesis II pathway to support the parasite's development through sporogony (86).

During the extended gametocyte maturation of *P. falciparum* parasites, the extent to which the parasite metabolizes hemoglobin decreases substantially in the late stages (33), resulting in a decreased sensitivity to compounds targeting heme metabolism from stage III-IV of development (87,88). The sensitivity of late-stage gametocytes to compounds targeting most metabolic pathways also decreases dramatically (88), consistent with the mature, circulating stages entering a more metabolically latent stage of development.

Apart from the divergence in metabolism observed during the respective proliferative asexual and differentiating sexual intraerythrocytic parasite stages, a profound but expected difference is observed in the parasite's cell cycle progression which will be discussed below.

1.3.2 Molecular reprogramming: Cell cycle progression in proliferating *Plasmodium* parasites

During the proliferative asexual cycle of intraerythrocytic malaria parasites, each nucleus will undergo multiple replicative cycles, often described as reminiscent of syncytial cell division during early embryogenesis in *Drosophila melanogaster* (89,90). Both processes involve multiple nuclear divisions without observable intervening gap-phases (41,42,46)

(Figure 1.3) within an observable syncytium (91,92). However, the individual nuclei in the syncytium of the developing *Drosophila* undergo synchronized progression through the respective phases of the cell cycle and make use of a cytoplasmic pool of cyclins, imported into the nucleus at the necessary cell cycle checkpoints (89,92). By contrast, the nuclear membrane remains intact during *P. falciparum* cell division, nuclei divide asynchronously *in vitro* (93) and the involvement of cyclins and cyclin dependent kinases (CDKs) in cell division has yet to be clarified, if at all present (94).

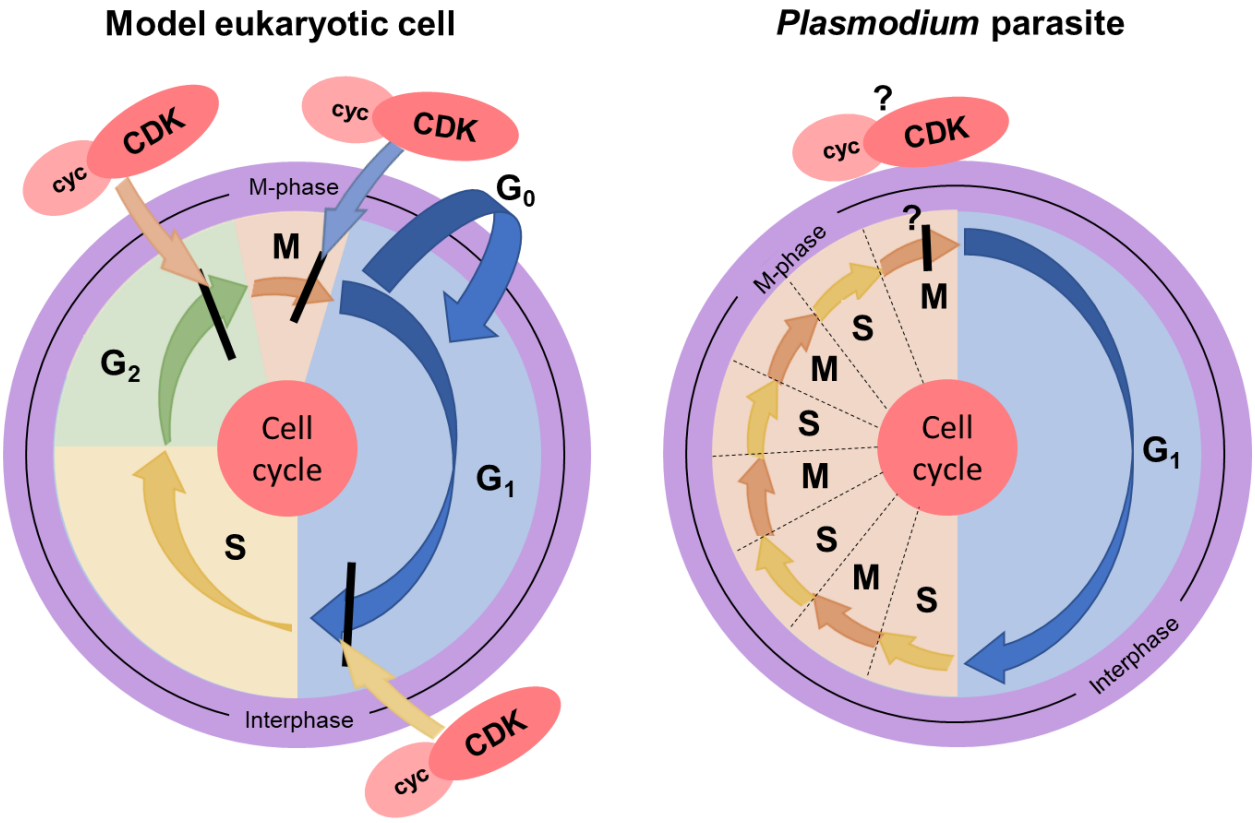

Figure 1.3: Progression and regulation of the model eukaryotic cell cycle compared to the atypical cell cycle observed in *Plasmodium* parasites. Typical eukaryotic cell cycles involve growth and development during G_1 with a cyclin-CDK dependent checkpoint (black bar) at the G_1/S phase transition ensuring controlled DNA synthesis, or alternatively entry into cellular quiescence (G_0). The cell then completes DNA synthesis in S phase before entering the second gap phase (G_2) with a checkpoint ensuring correct replication at the end of the gap phase before the cell divides during mitosis, during which time the final checkpoint ensures correct alignment of chromosomes on the mitotic spindle. Cell cycle checkpoints are uncharacterized in *Plasmodium* with multiple rapid S and M phases observed without intervening gaps and the role of cyclins and CDKs unknown.

Individual nuclei in a single *P. falciparum* schizont can be in different phases of the cell cycle *in vitro* (47,95), although it is believed that the nuclei all undergo a synchronized final round of mitosis before cytokinesis (94,96). This asynchronous nuclear division (95) results in a variable number of progeny produced (96). Coupled with a lack of chromatin condensation during DNA replication (44,94), these attributes make the whole process of tracing cell cycle phases in the parasites considerably complex. DNA replication, signifying entry into S phase in these stages, is therefore postulated to start anywhere

between 22 to 31.5 hpi (41,42,46) and genome duplication takes between 4-5 h per nucleus (47).

Typically, progression through the respective cell cycle phases, for example the G_1/S transition signaled by the initiation of DNA synthesis, is controlled by cell cycle checkpoints, modulated by the activity of specific cyclins and CDKs (Figure 1.3). The classical cell cycle checkpoints are proposed to be missing or alternatively atypical and unique to *P. falciparum* (46,97), with the exact composition and temporal contribution of cyclins and CDK complexes unclear (94,98). Although several cyclins and CDKs have been identified in *P. falciparum* (98–100), for the majority of these molecules, a concrete link between their activity and progression through the cell cycle has not been established.

The three identified cyclins in *P. falciparum* (100) only show 20-33% sequence homology to insect, human and trypanosomastid cyclin proteins, but were showed to activate kinases *in vitro* (100–102). Rather than the specific associations with a cyclin to its associated CDK, allowing coordinated and compartmentalized cell cycle progression as classically observed in metazoa (103), the interactions between cyclins and CDKs in *Plasmodium* parasites are promiscuous (100,104). The best-characterized cyclin involved in the IDC, CYC1 (cyclin H homolog) (100), has been associated to both MO15-related protein kinase (MRK, a proposed CDK7 homolog) (98,100,105) and protein kinase 5 (PK5, proposed homolog of human CDK1 or CDK5) (99,104), although the latter observation is contested (105). In the murine parasite, *P. berghei,* PbCYC1 and PbCYC4 are functionally essential to the progression through the IDC (26) with PbCYC1 abrogation also preventing progression through cytokinesis. No functional association with CDKs has been shown for CYC4 in any of the parasite species. PbCYC3 is dispensable for asexual development but essential for endomitosis in *P. berghei* oocysts and causes deregulation of cdc2-related protein kinase PbCRK3 (102) but no direct functional associations with CDKs have been determined for this cyclin. Although these observations would tie the activity of molecular regulators to general cell cycle progression during the IDC, the inability to observe the parasite's entry into the respective cell cycle phases makes studying phase-specific regulators extremely complicated.

Conversely, sexual development is accompanied by an exit from the proliferative cell cycle. There is evidence to suggest the parasite undergoes some DNA synthesis between

sexual commitment and stage I of gametocyte development (106,107) but no nuclear division occurs following this event, with the slightly increased nuclear content persisting for the duration of gametocyte maturation. The intermediate stages of gametocytes (stages II-IV) still synthesize RNA and proteins, suggesting an active transcriptional and translational environment, but a progressive depression of these processes occurs as the parasite matures (106). This suggests that mature gametocytes are in a latent gap-phase, possibly exited from the cell cycle, awaiting signals from the mosquito to re-enter active development.

1.4 Hard-wired regulation? The extrinsic and intrinsic regulatory signals that shape the bifurcation in parasite biology

Here, the *status quo* of the molecular configuration and regulation underlying the proliferative and differentiating stages of parasite development will be dissected. The mechanisms underlying this developmental bifurcation are an exquisitely controlled interplay of environmental influences and genetic determinants.

1.4.1 Environmental determinants underlying commitment to asexual or sexual development

Second messenger signaling cascades have been associated with numerous stage transitions in the parasite's life cycle, including egress and invasion of merozoites during blood stage infection, initiation of gametogenesis and ookinete motility and midgut invasion (108,109). Modification of the extracellular environment can also either stimulate or prevent entry into gametocytogenesis (52,110). Second messenger signaling by cAMP has been reported to increase the rate of conversion to gametocytes (51,111) while increased host lysophosphatidylcholine decreases conversion (52), consistent with signaling pathways contributing to cell differentiation in other cell types (112,113). This strongly supports the presence of a sensing point during intraerythrocytic development, at which the parasite's environmental conditions are translated to intracellular effectors, influencing its reproductive fate in the following developmental cycle.

The signaling machinery of the parasite, specifically the various kinases and phosphatases that respond to intracellular second messenger concentrations, have been somewhat characterized (98,114). The mechanism by which some signaling kinases regulate signaling processes are still ambiguous, such as the orphan kinase protein kinase 7 (PK7), which both resembles a mitogen activated protein kinase kinase

(MAPKK) and cAMP-dependent protein kinase A (PKA) (98,115), but functionally associates with melatonin signaling and activates the proteasome (116). The cyclic nucleotide dependent kinases in *P. falciparum* include a cGMP-dependent protein kinase (PKG), PKA as well as RAC-beta Ser/Thr protein kinase (PKB) (98). The signaling cascades induced by cyclic nucleotide signaling also show substantial cross-talk with phosphoinositide and Ca^{2+}/calmodulin signaling (117–119). The Ca^{2+}/calmodulin signaling machinery in *P. falciparum* is divergent from metazoans, with the parasite possessing only one calmodulin kinase homolog, PK2 (120), but several Ca^{2+}dependent protein kinases (CDPKs 1-7), typically found in plant rather than mammalian cells (98,121–123).

Interestingly, CDPKs in *P. falciparum* seem to regulate similar processes as CDPKs in *Arabidopsis thaliana.* An increase in intracellular Ca^{2+} in response to changes in the extracellular environment activates processes to restore the physiological state (108), in this case by activating signal transduction pathways through Ca^{2+} binding proteins, the CDPKs. These molecules act as regulators of stress signaling and development in the plant (124) and modulate entry into diverse stages of development in the parasite, with CDPK1 (125), CDPK5 (126) and CDPK7 (123) essential for asexual intraerythrocytic development, CDPK3 (127) for oocyst development and CDPK4 (70) for microgametogenesis. With this extensive Ca^{2+}signaling machinery, it is surprising that the majority of influx and efflux machinery regulating Ca^{2+} homeostasis in the parasites is completely uncharacterized (108). Although second messenger signaling has been associated to both progression through the parasite's cell cycle (119), signaling continuation of asexual proliferation, and extracellular signals stimulating increased commitment to gametocytogenesis (52), specific signaling cascades have not been linked to the point of commitment to either proliferation or differentiation. However, environmental signaling is not the only factor controlling entry into gametocytogenesis, but rather enables translation of the environmental input into the controlled expression of the parasite's genes, to carry out the specific biological functions of the respective reproductive mechanisms (53,128,129).

1.4.2 Controlled gene expression underlying differentiation or proliferation in the parasite

The unique biological adaptations of asexually proliferating or sexually differentiating *P. falciparum* parasites are enabled through core regulatory mechanisms resulting in

coordinated and controlled expression of particular gene sets (49,128). The parasite's genome comprises ~5500 genes, including 57 ncRNA that have not been functionally characterized and ~2000 gene products with unknown function (80,101,130). The parasite's exceptional genetic control is highlighted by the rapid loss of gene products that confer a growth advantage *in vivo,* like genes contributing to cytoadherence and gametocytogenesis, following laboratory adaptation (131,132). The regulation of gene expression itself has unique features in the parasite and is orchestrated by a variety of factors, including transcriptional, epigenetic, post-transcriptional and post-translational control mechanisms.

1.4.2.1 Transcriptional control

The transcriptomes of both the asexual and sexual stages of parasite development show marked evidence of precise transcriptional regulation. In asexually replicating parasites, a monophasic, stage specific expression of ~90% of the parasite's genome immediately precedes translation of most transcripts (128,133). In gametocytes, transcriptional control is evident from expression of gametocyte-specific (49) and sex-specific (134) markers. The core elements of transcriptional control in eukaryotes, conserved in *Plasmodium* parasites, are comprised of *cis*-acting elements inherent in the DNA sequence and *trans*-acting regulatory proteins that bind *cis*-regulatory elements to modulate levels of transcription (135).

Cis-regulatory elements are classified according to their distance from the transcription start site (TSS), which include the canonical promoter, promoter-proximal elements and distance-independent elements (135). In *P. falciparum*, the identification of *cis*-regulatory elements like a classical TATA-box is particularly challenging due to the AT-rich genome (136). Despite these challenges, the preferred transcription initiation site in asexual forms of *P. falciparum* parasites was identified as the conventional TA dinucleotide, allowing RNA pol II binding (136). Factors influencing promoter strength have also been identified with both the local GC-content surrounding the promoter and nucleosome positioning near the promoter shown to affect strength of transcription of specific genes (137). Several *cis*-acting regulatory motifs upstream of the promoter have also been identified in *Plasmodium* (138–141), implying involvement of promotor-proximal or distance independent elements in regulating gene expression in the parasite. Particularly, some motifs have been associated with either the transcription of genes during specific asexual life cycle stages (139) or related to biological functions within the parasite, including a

motif enriched during sexual development, 5' AGACA (138). Although a number of the regulatory motifs have been characterized in terms of their *trans*-acting factors (139,142), limited information is available as to the functions of *cis*-acting motifs as enhancing or silencing elements.

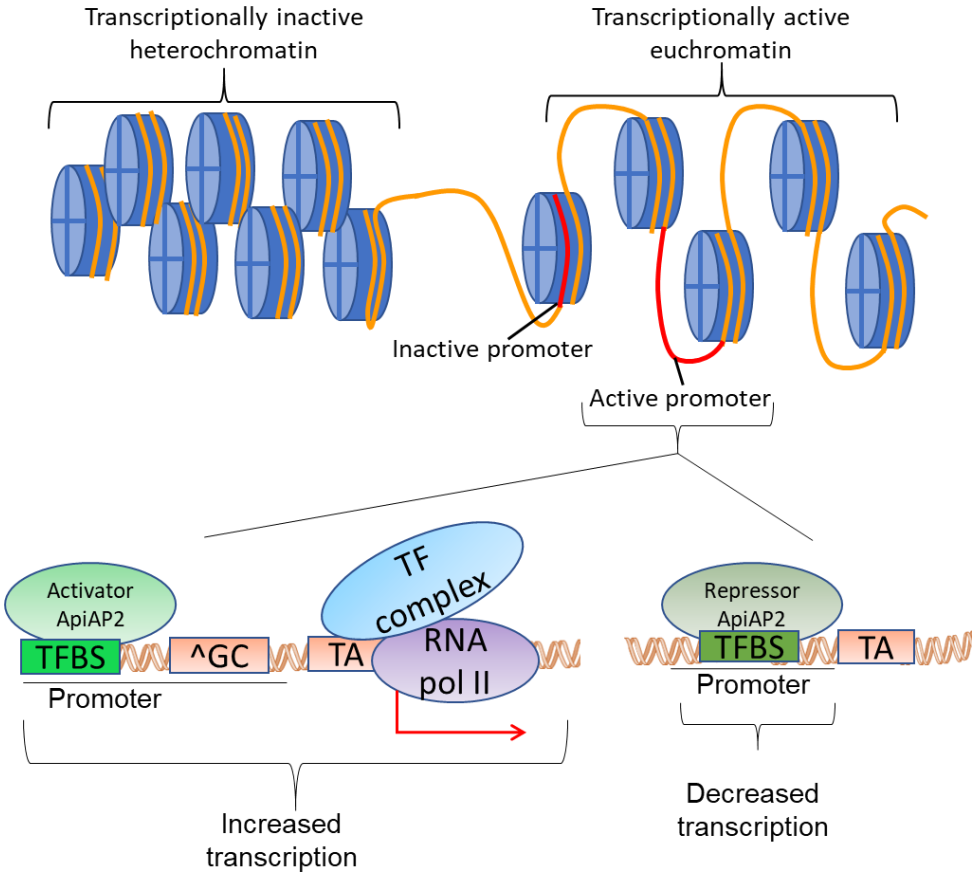

Figure 1.4: Transcriptional control in *P. falciparum* parasites. Chromatin structure (nucleosome occupancy and position) and binding of *trans*-acting factors like ApiAP2 transcription factors to specific *cis*-elements in gene promoters (TFBS) as well as local increases in GC content (^GC) influence transcriptional activity by general transcription factors (TF complex) and RNA pol II of parasite genes during development.

Although not classic *trans*-acting factors, epigenetic factors regulating chromosomal structure have also been found to contribute to transcriptional control in eukaryotes (143). In most eukaryotic organisms, chromatin packaging via nucleosome formation regulates access of transcription factors to gene promoters, thereby regulating levels of gene expression (144), a feature suspected to be conserved in *P. falciparum* parasites. The contribution of chromatin remodeling to transcriptional control by nucleosome occupancy and positioning is well-described for the asexual replication cycle of *P. falciparum* parasites (145–147) (Figure 1.4). In *P. falciparum,* the core histone complex is retained from eukaryotes, including H2A, H2B, H3 and H4, along with several variant forms of these, but H1 is absent in these parasites. This decreases the overall compaction of chromatin structure in the parasite (148,149) and results in a mostly transcriptionally

active, euchromatic chromatin state during asexual development aided by the AT-rich genome and shorter nucleosome spacing (146). During the IDC, transcriptional fluctuations are also influenced by nucleosome occupancy in the 5'-intergenic regions, with decreased nucleosome occupancy in promotor regions generally corresponding to higher relative mRNA levels for those genes (147) and lower nucleosome occupancy observed during active transcription in trophozoite stages (145,150).

Given the tight transcriptional control observed during the IDC, specific transcription factors are expected to contribute substantially to parasite development. However, the *P. falciparum* parasite has a well-documented scarcity of most conserved eukaryotic transcription factor families, with only putative members of helix-turn-helix and zinc-finger families predicted *in silico* (130,151). Only the MYB1 transcription factor has been functionally validated and shown to be essential during asexual development (152). Rather, the parasite relies on a family of 27 transcription factors that are homologs of the Apetala2/Environmental Response Factors (AP2/ERF) family (153) from *A. thaliana* that can act as either transcriptional activators or repressors (154) (Figure 1.4). In contrast to AP2 proteins from plants in which the number of AP2 domains relate to activating or repressive functions for the transcription factors, the Apicomplexan AP2 (ApiAP2) transcription factors in *P. falciparum* contain a varied number of AP2 domains, not associated with specific repressive or activating functions (155,156).

During the IDC, 21 of the 27 ApiAP2 transcription factors are expressed, including some with roles in specific morphological stages, contributing to the overall transcriptional pattern observed during asexual replication (26,151). These transcription factors are also the only transcription factors in *Plasmodium* known to associate with specific *cis*-acting regulatory motifs in the parasite genome (142); this allowed association of possible molecular regulators to the extraordinarily well-controlled transcriptional pattern observed in asexual replication (142). Despite these molecular regulators of transcription contributing invaluable data towards understanding gene expression in the parasite, there are also subsets of genes for which mRNA and protein levels are not well correlated, suggesting active post-transcriptional control in *P. falciparum* parasites (157,158).

1.4.2.2 Post-transcriptional control

P. falciparum parasites make use of most conventional post-transcriptional control mechanisms including alternative splicing, post-transcriptional modifications, mRNA

stabilization and mRNA decay, with the exception of RNA interference, which is absent from malaria parasites (159–161). Prior to export to the cytoplasm, conventional processing mechanisms include adding a 7-methylguanosine cap, 3' poly-A tail and splicing of pre-mRNA. In *P. falciparum,* genes routinely undergo alternative splicing (162–164), which is suspected to aid in translational regulation of active isoforms and sequence variation in antigenic genes that aid the parasite in immune evasion (164).

Once processed mRNA enters the cytoplasm, the fate of the molecules diverges (Figure 1.5). mRNA can either be stabilized by a mRNA-ribonucleoprotein (mRNP) complex, resulting in translational repression, degraded or translated into proteins. These mRNA dynamics could finally be captured with the development of a genetically engineered system for capturing the interplay between post-transcriptional control mechanisms, as since the parasites lack an active pyrimidine salvage pathway (165), classical evaluation of post-transcriptional mechanisms was not previously possible (166–169). The evaluation of these mRNA dynamics showed that total abundance of mRNA in *P. falciparum* parasites is the result of both active transcription and subsequent transcript stabilization (141).

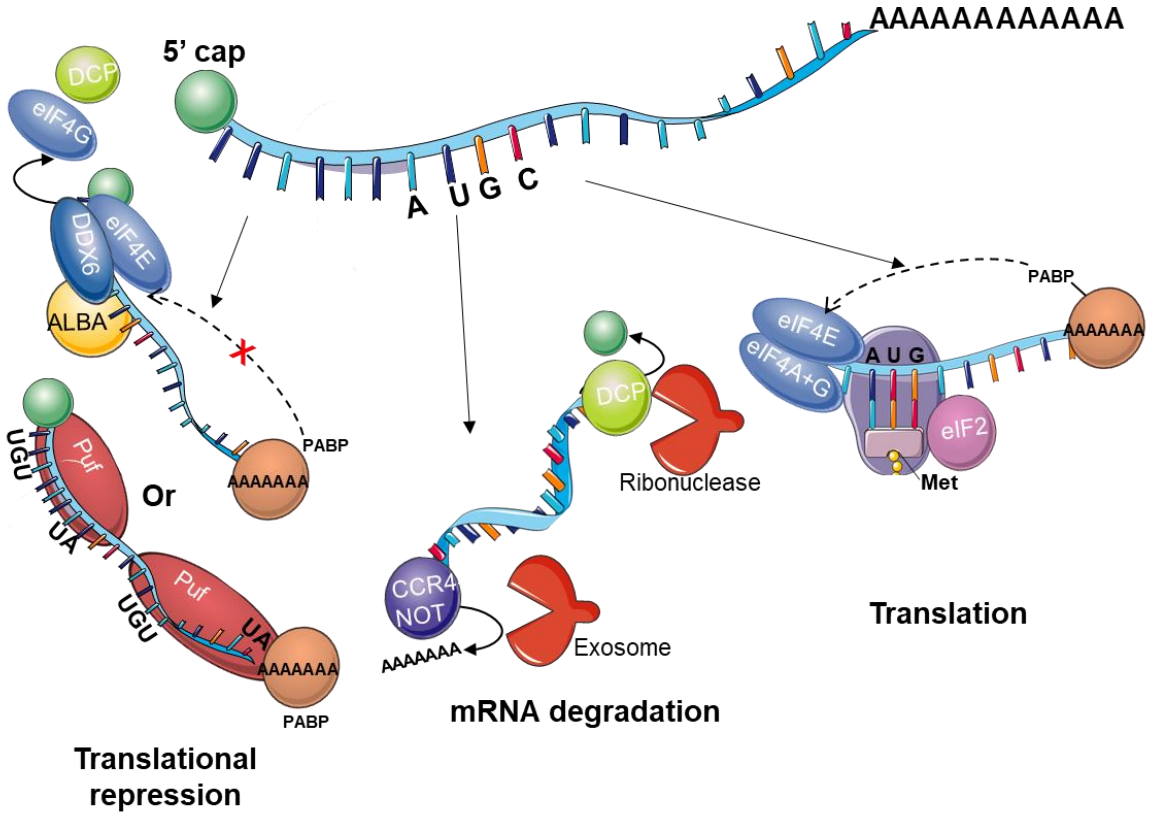

Figure 1.5 Post-transcriptional fates of mRNA in *P. falciparum* parasites. Once the processed mRNA enters the cytoplasm, mRNA can either be stabilized by a mRNA-ribonucleoprotein (mRNP) complex, degraded or translated into proteins. Abbreviations: decapping proteins; DCP, eukaryotic translation initiation factors; eIF, DDX6/DHH1 DNA helicase; DDX6, always lowers binding affinity proteins; ALBA, Pumilio-family proteins; Puf, poly-adenylate binding protein; PABP, CCR4-NOT complex; CCR4 NOT.

The stabilization of transcripts by mRNP complexes prevent mRNA decay and can also function in preventing translation of the transcript when bound to translational repressors (160) (Figure 1.5). The complexes act as *trans*-acting translational regulators in *Plasmodium,* including a DOZI-CITH complex (DDX6/DHH1 DNA helicase in *P. falciparum*) and pumillo-family (Puf) proteins (160,170). The DOZI-CITH complex functions by allowing binding of eukaryotic translation Initiation Factor (eIF) 4E and the poly(A)-binding protein (PABP) but exclusion of eIF4G and degradation factors (171), preventing effective initiation of translation and mRNA decay (Figure 1.5). One of the proteins in the DOZI-CITH complex, a Musashi homologue, prevents binding of eIF4G to PABP in neuronal stem cells (172), effectively preventing translation initiation, a mechanism suspected to be conserved in *Plasmodium* (171). Puf proteins act as an additional, DOZI-independent mechanism of translational repression, binding to Puf binding elements (PBE's) in both the 5'- and 3'-untranslated regions (UTRs) of *Plasmodium* transcripts containing the conserved motif $UGUX_{3\text{-}5}UA$ to, in most cases, repress translation (173).

The DOZI-CITH complex is associated with the 'Always lowers binding affinity' (ALBA) proteins that are bound to mRNA of specific subsets of genes during the IDC, suggesting they contribute toward the lack of transcript and protein correlation for some expressed genes, particularly ALBA1 (174). During sexual development, female gametocyte transcripts also undergo post-transcriptional control reminiscent of metazoan egg cells, in which stabilized, translationally repressed transcripts are hoarded for early embryogenesis during which transcription is absent (71,175). This translational repression is facilitated by the DOZI-CITH complex in *P. berghei* (171,176), with evidence suggesting this mechanism, as well as repression by PUF2, is also present in *P. falciparum* (134,177) enabling the immediate translation of proteins necessary for zygote development during gametogenesis (71). Without stabilizing factors bound to mRNA, the molecules are short-lived (178) and will be quickly degraded, which in turn can also regulate the parasite's biological functions (179).

In *Plasmodium*, mRNA degradation follows a 5'-3' direction with 5' decapping performed by the DCP1 or DCP2 decapping enzymes and the mRNA subsequently degraded by ribonucleases (178). Alternatively, 3'-5' deadenylation is modulated by the CCR4-NOT complex associated with CCR4-NOT associated factor 1 (CAF1), the deadenylating subunit associated with translational control during the IDC (179). Deadenylated

transcripts are then degraded by the exosome, a complex consisting of core proteins and associated exoribonucleases, including RNaseII, that are responsible for RNA processing, quality control and decay (160). During the IDC, mRNA half-life lengthens significantly towards schizogony (178), corresponding to stage-specific increased transcript stabilization, although majority of the total transcript abundance is due to nascent transcription (180). Gene editing studies conducted on CAF1 also showed deregulation of genes necessary for egress and invasion, causing defects in merozoite formation (179). An analogous analysis has not been performed on the sexual stages of development. Barring repressive post-transcriptional control mechanisms of stabilization or decay, the mRNA will be translated into proteins.

The parasite makes use of most conventional eukaryotic translational components, including the 60S and 80S ribosomes as well as tRNAs, aminoacyl-tRNA synthetases and translation factors (181). The parasite does, however, make use of structurally distinct rRNAs during different stages of development (182). The existence of A-rRNA (for human liver and asexual intraerythrocytic development stages) versus S- and O-rRNA (associated with sporozoites and ookinetes) suggests an adaptive mechanism to controlling translation in the different host environments (175).

The eukaryotic translation initiation process, conserved in *P. falciparum,* involves recruitment of eIF4E, eIF4A and eIF4G to form the eIF4F complex (183–185). Subsequently, eIF4F interacts with the poly(A)-binding protein, forming a closed-loop complex that enables efficient translation while preventing mRNA decay (160). Next, the 80S ribosomal subunit and methionine-tRNA are loaded onto the start codon, directed by eIF2 (185). This interaction has been disrupted in *P. falciparum* in response to starvation by phosphorylation of the eIF2-α subunit, resulting in a delayed global translational response during the IDC (85). The elongation factors EF1-α, -β, -γ, -δ as well as eukaryotic peptide release factors that terminate transcription have been annotated, but all lack further functional characterization (160). The asexually replicating parasites express ~80% of their genome in a “just in time” pattern of translation (128), a relationship that has not been probed for sexual development. However, a degree of translational control is implied by the partitioning of specific proteins into male and female gametocytes (134,186,187).

1.4.2.3 Post-translational control

Once proteins are translated, several aspects of their functions can be affected by post-translational modifications (188). Various types of protein modification have been detected in *P. falciparum* parasites, including SUMOylation (189), ubiquitination (190), glycosylation (191), glutathionylation (192) and nitrosylation (193). As in other organisms, the ubiquitination and SUMOylation modifications are expected to play a role in proteasome targeting (190) and glutathionylation is expected to modulate redox-status of the parasite proteins (192,194), but little functional information is available regarding these modifications (188). By contrast, protein lipidation (including prenylation, myristoylation, glycosylation and palmitoylation) (195), phosphorylation, acetylation and methylation have been studied more extensively (188) (Figure 1.6).

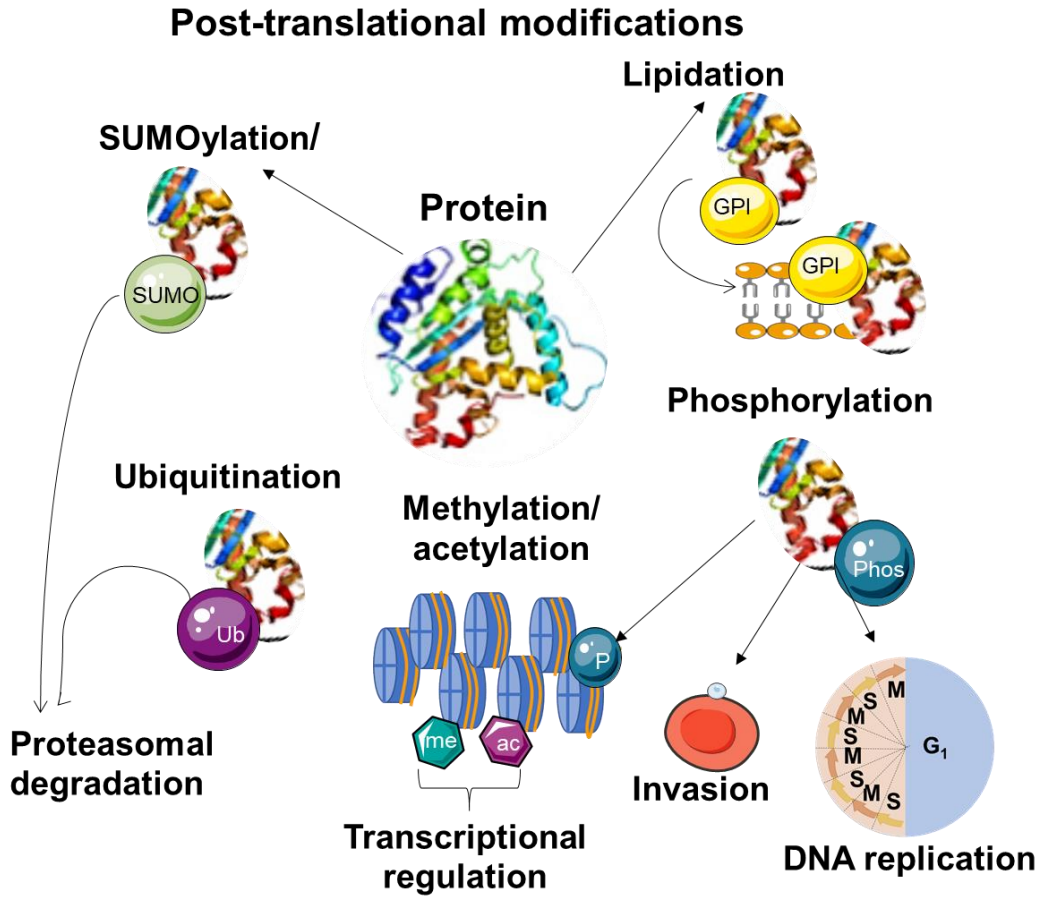

Figure 1.6: Post-translational modification with known functional effects in *P. falciparum* parasites. *P. falciparum* parasite proteins are modified extensively, with these modifications resulting in functional outcomes i.e. localization through lipidation (GPI-anchors), degradation through SUMOylation or ubiquitination, diverse cellular processes influenced by phosphorylation (Phos/P) or transcriptional regulation through by methylation (me) or acetylation (ac) of histones.

Of the different protein lipidations found in *P. falciparum* for modulating association with lipid membranes, palmitoylation occurs the most frequently (196) although glycosylphosphatidylinositol (GPI) anchor attachment is by far the best studied and

functionally characterized (197). GPI biosynthesis is carried out by glycolytic enzymes, a major function of the pathway during the IDC (197). This modification is expected to be critical for asexual development, with merozoite surface protein (MSP) 1 and 2, essential proteins for erythrocyte invasion, attached to the cell surface via GPI-anchors (198). Several proteins involved in signaling cascades within the cell are lipidated, suggesting that this modification, like phosphorylation, could also be important for cellular signaling responses (188,199).

The reversible phosphorylation of proteins regulates a plethora of cellular processes, modulated by kinases and phosphatases (200). Specifically, the phosphorylation of proteins involved in housekeeping processes of asexual proliferation, including DNA replication, transcription, etc. as well as parasite-specific processes (cytoadhesion, invasion) is expected to play a role in their regulation (201). Protein kinases in *P. falciparum* are considerably diverged from mammalian kinases, with the prominent metazoan Tyr kinases presumed absent from the parasite (despite presence of Tyr phosphorylation in the parasite proteome (202,203)). By contrast, a considerably expanded FIKK-kinase (containing Phe-Ile-Lys-Lys motifs) family exists, which is conserved within Apicomplexa (98). Apicomplexans also use CDPKs (as discussed earlier) that are absent from most metazoans but conserved in plants and alveolates (98). The *Plasmodium* parasite also encodes a small complement of 67 protein phosphatases (114), that along with kinases also regulate histone and 14-3-3 protein phosphorylation (204).

Acetylation and methylation modifications serve as co-regulators for numerous important cellular functions (205). Although a variety of nuclear and cytoplasmic proteins are acetylated in *P. falciparum* parasites (206), the best studied examples of these post-translational modifications are found on histones to functionally regulate transcription (207). The deposition and removal of acetylation marks are controlled by histone acetyl transferases (HATs) and histone deacetylases (HDACs), respectively, while bromodomain-containing proteins interact with and interpret the acetylations, acting as so-called histone “readers” (208). Typically, the addition of an acetyl group to a histone lysine residue neutralizes the positive charge of the amino acid, breaking the electrostatic interaction between the lysine residue and the negatively charged phosphate backbone of the DNA (205). This “loosening” of the chromatin structure is usually characteristic of transcriptionally active euchromatin (208). Contrary to acetylation, histones can be mono-

, di- or trimethylated at lysine residues and mono- or dimethylated at arginine residues and the number of methyl groups can have profoundly different effects on transcriptional activity (205). Methyl groups can be deposited on either lysine or arginine residues by histone lysine methyltransferases (HKMTs, SETs in *P. falciparum* (209)) or histone arginine methyl transferases (HRMTs) and removed by the respective demethylases (208).

The acetylation and methylation of histones, both within the "tails" that protrude from the nucleosome structure and within the histone core (e.g. H3K56ac) have been characterized extensively, particularly their involvement in cell cycle development (205,208). The *P. falciparum* genome also contains four predicted HATs, with GCN5 associated with H3K9 and H3K14ac (210), specifically contributing towards H3K9ac in actively transcribed genes during the late stages of the IDC (211,212). The readers of these modifications, bromo-domain proteins binding acetylated histones and chromo-, Tudor and Plant homeodomain (PHD)-containing proteins that bind methylated histone residues are also present in the *P. falciparum* genome (151). Methylated Lys are mostly read by chromodomain-containing proteins and are associated with either facultative or constitutive heterochromatin (205). Facultative heterochromatin is typically transcriptionally silent during particular phases of a cell's development, while constitutive heterochromatin is characteristic of permanently silenced genes, usually associated with telomeres or centromeres of chromosomes (205). Together, a better understanding of these transcriptional, post-transcriptional and post-translational control mechanisms have laid bare the underlying molecular mechanisms for numerous biological processes governing parasite development.

1.5 Specific transcriptional regulators define asexual proliferation and sexual differentiation

The vastly different developmental profiles characterizing the life cycle of the intraerythrocytic parasites implies the presence of a bifurcation switch enabling development into either the asexual or sexual forms. This switch comprises a complex process triggered by low levels of a host-derived phospholipid, lysophosphatidylcholine (52), which initiates a cascade of transcriptional control mechanisms enabling gametocyte differentiation, including 1) epigenetic regulation and 2) activity of specific transcription factors. Here, these two mechanisms of regulation and specifically the

molecular regulators controlling entry into asexual proliferation or sexual differentiation respectively are discussed in detail.

1.5.1 Epigenetic control of transcriptional landscape enabling proliferation or differentiation

The specific histone modifications that aid the stage-specific expression characteristic of the *P. falciparum* IDC have been thoroughly described (207,211,213,214). During the IDC, H3K14ac and H3K9ac as well as H3K4me1,2,3 are highly associated with actively transcribed genes (213). A global view of histone mark deposition and transcription has also indicated an association of H4 acetylation marks, H3K56ac and the methylation mark H4K20me1 with an increase in transcriptional activity, suggesting that these marks are also positive modulators of transcription during asexual development (207). Conversely, H3K9me3 and H3K36me2/3 are associated with a decrease in transcriptional activity (213), with H3K9me3 and H3K36me3 specifically associated with silencing variant antigens associated with immune evasion in humans (214,215) and H3K36me2 described as a global repressive mark, decreasing expression of a diverse complement of genes during intraerythrocytic development (213). While the histone post-translational landscape has been described as dynamic during asexual development (207), it also undergoes substantial changes during gametocyte development (216) and commitment. Specifically, disruption of the association of the *ap2-g* transcription factor gene with H3K9me3 allows its active transcription, enabling commitment to gametocytogenesis, as opposed to its association with H3K9me3 resulting in asexual development (53,211).

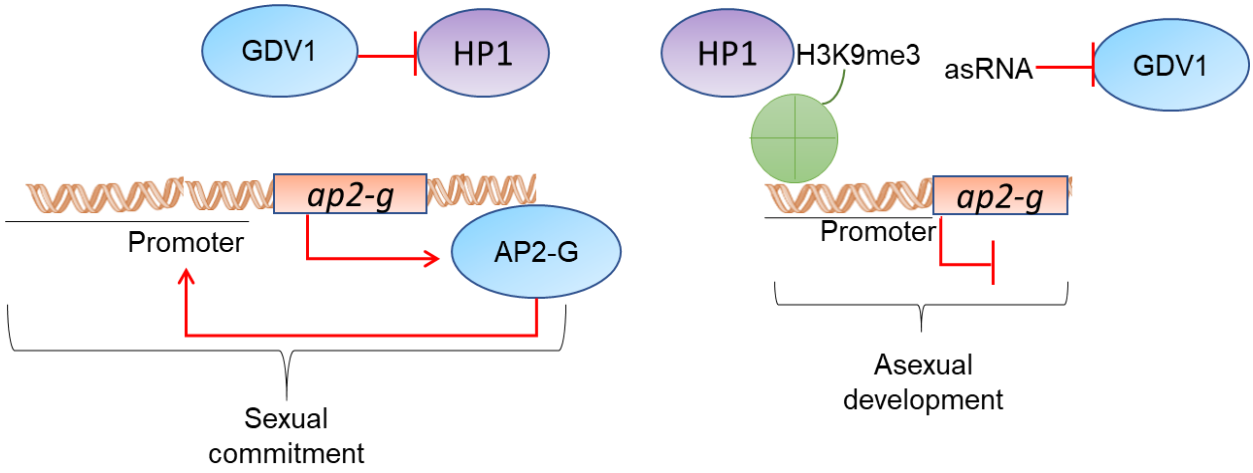

Figure 1.7: Transcriptional regulation of sexual commitment in *P. falciparum*. The repressive histone mark H3K9me3, on the *ap2-g* locus disallows expression of the AP2-G transcription factor. The mark is read by HP1 when the GDV1 transcript is associated with its asRNA, resulting in asexual development. The expression of AP2-G occurs when the H3K9me3 mark is absent and HP1 is associated with the GDV1 protein and AP2-G further forms a positive feedback loop, binding to its own promoter, resulting in commitment to sexual development. Abbreviations: gametocyte development protein 1; GDV1, heterochromatin protein 1; HP1, antisense RNA of GDV1; asRNA.

To date, specific functions have only been associated with a chromodomain protein, heterochromatin protein 1 (HP1), which binds to H3K9me3, regulating antigenic variation and sexual differentiation (55,217) and a bromodomain protein BDP1 that binds H3 acetylation, regulating erythrocyte invasion (218). During asexual development HDA2, HP1 and negative regulation of gametocyte development protein 1 (GDV1) expression by antisense RNA maintains the silenced state of *ap2-g* (54,56), an essential transcription factor enabling commitment to sexual development (Figure 1.7). During commitment, HP1-mediated signaling is antagonized by gametocyte development protein 1 (GDV1) (56), resulting in active transcription of *ap2-g*. Through positive feedback, AP2-G further increases its transcription and ensures sexual development.

1.5.2 Transcription factors play decisive roles in proliferation or differentiation decision

ApiAP2 transcription factors play central roles in multiple stage transitions in the parasite life cycle, enabling differentiation into sexual (53) intraerythrocytic development as well as during the mosquito (219) and liver (220) stages. The process of invasion during the IDC is also mediated by the combined activity of BDP-1 and AP2-I (140,218). The crux of the bifurcation between proliferating and differentiating parasites is believed to be regulation by the AP2-G transcription factor. Expression of AP2-G is essential for commitment to gametocytogenesis as it stimulates expression of several early-stage gametocyte markers (53,129), including Pfs16, which is essential for completion of gametocytogenesis (221). Furthermore, post-transcriptional stabilization of AP2-G targets along with other commitment-associated genes are postulated to be key for transitioning into gametocyte development (141).

Beyond AP2-G, little is known about the factors controlling the gametocyte's development, particularly for *P. falciparum.* In the 48-hour gametocytogenesis process in *P. berghei,* a second transcription factor, AP2-G2 represses transcription of genes that would stimulate invasion in asexual parasites, acting as a downstream regulator to AP2-G (222,223) (Figure 1.8). The *P. falciparum* gametocyte possesses an AP2-G2 ortholog, although it is still functionally uncharacterized (224); and it may still not explain the dramatically increased maturation time of *P. falciparum* gametocytes, suggesting additional mechanisms of control are at play.

The vast biological differences shaped by a bifurcation in the parasite's life cycle have been outlined (Figure 1.8), as a "snapshot" that scratches the surface of deeper understanding of these mechanisms. Some key regulators have been identified that regulate asexual and sexual development, but many aspects remain unanswered including 1) if and how the parasite regulates its progression through its proliferative cycle; 2) the dynamics of transcriptional regulation and expression during gametocytogenesis and whether additional regulators to AP2-G shape the transcriptome; and 3) whether transcriptional regulation is translated to a functional phenotype in these stages, given the extensive post-transcriptional and translational control mechanisms employed by the parasite.

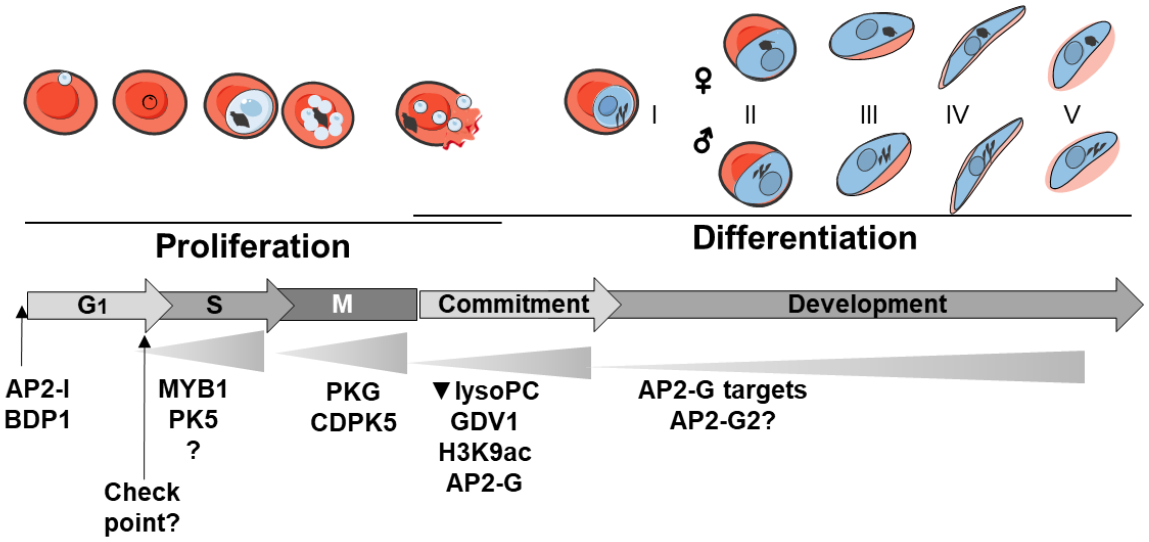

Figure 1.8: Regulatory molecules and biological consequences of parasite proliferation and differentiation. Key biological processes (blocks) and their regulators, previously highlighted in the thesis, shape the transcriptional landscape of parasite development during specific transitions (triangles) although some aspects of regulation have yet to be explored (?).

The work in this thesis models the parasite transcriptome as it progresses through a key point in asexual development, namely the start of DNA replication, to highlight specific molecular regulators that enable the massive cellular expansion that results from parasite proliferation. In sexual development, developmental transitions are not as well studied, and we provide a complete characterization of sexual development and additionally probe specific regulators of sexual development. As an additional level of characterization, the parasite's metabolic phenome during both asexual replication and sexual development, rounds off and builds out the molecular model. In totality, this work details a description of a molecular roadmap of parasite intraerythrocytic development, leading to a more complete understanding of the essential functions of one of the world's most deadly parasites.

1.6 Hypothesis

Transcriptional regulation controls *P. falciparum* intraerythrocytic asexual and sexual development, resulting in observable cellular phenotypes associated with the intricate cellular processes that define proliferation and differentiation.

1.7 Aim

This study aimed to determine transcriptional profiles and investigate regulation of *P. falciparum* asexual proliferation and sexual differentiation and the subsequent quantification of the phenotypic implications of these regulatory mechanisms.

1.8 Objectives

1. Develop and apply a tool to study cell cycle regulation at the G_1/S phase transition in the cell cycle of asexual *P. falciparum* parasites (Chapter 2)

2. Investigate the molecular profile of sexually differentiating *P. falciparum* parasites and regulatory elements that contribute to this process (Chapter 3)

3. Phenotypically evaluate the consequences of the regulated processes of proliferation and differentiation (Chapter 4)

1.9 Outputs related to the thesis

Manuscripts:

1. R van Biljon & J Niemand, R van Wyk, K Clark, B Verlinden, C Abrie, H von Grüning, W Smidt, A Smit, J Reader, H Painter, M Llinás, C Doerig, L Birkholtz. Inducing controlled cell cycle arrest and re-entry during asexual proliferation of *Plasmodium falciparum* malaria parasites (8 November 2018). Nature Scientific Reports.
2. R van Biljon, R van Wyk, L Orchard, J Reader, Werner Smidt, HJ Painter, J Niemand, M Llinás, L Birkholtz. Intricate hierarchical transcriptional control regulates *Plasmodium falciparum* sexual differentiation (2018). Submitted, BMC Biology.

3. R van Biljon, R van Wyk, H von Grüning, L Birkholtz, J Niemand. The carbon and nitrogen phenome of *Plasmodium falciparum* asexual and sexual intraerythrocytic parasites. In preparation.

Conferences:

1. Riëtte van Biljon, Jandeli Niemand, Katherine Clark, Janette Reader, Annél Smit, Lyn-Marié Birkholtz. Probing the unusual cell cycle of intraerythrocytic *Plasmodium falciparum* parasites using DL-α-difluoromethylornithine (DFMO), a cytostatic life cycle stage-specific inhibitor. Poster and Flash talk (both Seminar and Conference) Gordon Research Seminar and Conference on Malaria, Girona, Spain (July 2015)
2. Riëtte van Biljon, Hilde von Grüning, Lyn-Marié Birkholtz, Jandeli Niemand. Phenomics, the missing link: The investigation of the phenome of the human malaria parasite, *Plasmodium falciparum*. Poster presentation. Molecular Approaches to Malaria Conference, Lorne, Australia (February 2016)
3. Riëtte van Biljon, Lindsey Orchard, Roelof van Wyk, Jandeli Niemand, Tanya Paquet, Kelly Chibale, Manuel Llinás, Lyn-Marié Birkholtz. *Plasmodium falciparum* gametocytes undergo tight transcriptional control that shapes their response to drug perturbation. Oral Presentation. MRC Office of Malaria Research Conference, Pretoria, South Africa (August 2016)
4. Riëtte van Biljon, Mariska Naude, Lyn-Marié Birkholtz, Jandeli Niemand. Dynamic evaluation of metabolite transport in the intraerythrocytic life cycle stages of *Plasmodium falciparum* parasites. Poster and Flash talk. BioMalPar Conference, Heidelberg, Germany (May 2017)
5. Riëtte van Biljon, Roelof van Wyk, Lindsey Orchard, Heather Painter, Jandeli Niemand, Manuel Llinás, Lyn-Marié Birkholtz. Unravelling the molecular proliferation and differentiation signals of *Plasmodium falciparum* parasites. Poster presentation. BioMalPar Conference, Heidelberg, Germany (May 2018)

Chapter 2

Evaluating cell cycle progression of asexual *P. falciparum* parasites

2.1 INTRODUCTION

The *P. falciparum* parasite evolved numerous cell biological and biochemical features to adapt and survive in the contrasting environments of its respective insect vector and mammalian host. The progression through successive developmental stages of the asexual life cycle of the *P. falciparum* parasite is tightly controlled (128), allowing for periods of intense proliferation during the rapid IDC, that are responsible for parasite pathogenicity. The IDC is characterized by morphologically traceable stages, but due to asynchronous replication in dividing nuclei, association of these to classical eukaryotic cell cycle phases (G_1, S, G_2 and M phases) has not been clearly established (46,97,225).

The invading merozoite is presumably in G_1 phase and transition from rings to trophozoites (with a 1N DNA copy number) is characterized by chromatin decondensation, similar to the G_1A to G_1B transition in mammalian cells (226). A large increase in RNA and protein levels is seen in early trophozoites (227). DNA synthesis (S phase) occurs in mature trophozoites (1N-2N, ~24 hpi) followed by endocyclic schizogony (46,227–229). The latter is characterized by 3-4 rounds of continuous DNA synthesis in the absence of cytodieresis and cytokinesis, alternating with rapid mitotic phases (M-phase) without a much-extended G_2 phase. This results in a multinucleated schizont (>2N); nuclear division in a single schizont occurs asynchronously (46,228) except for the last round of mitosis, which occurs synchronously for all nuclei, followed by a single segmentation step releasing haploid daughter merozoites after cytokinesis (97).

Metazoan cell cycle progression is typically enforced by the induction of ‘checkpoints’ that allow cells to undergo decision-making, either to progress to the next phase or to exit the cycle and enter a quiescent state until the cycle can be resumed; alternatively resulting in cell death. This quiescence-proliferation decision-making process allows cells to verify completion of each cell cycle phase before entering the next (230). In the G_1 phase, the usually reversible growth factor-dependent restriction point regulates the quiescence (G_0

state) to proliferation switch (231). However, cells can irreversibly exit the division cycle if subsequent cell growth checkpoints, like START in yeast, are not passed (231,232). Understanding the mechanisms underlying this binary decision point is crucial to interpreting an organism's reproductive biology. Cell cycle progression is an orchestrated process involving the activity of growth factors, mitogens and other environmental signals whose central regulators are the cyclins and CDKs. Although protein phosphorylation and degradation by CDKs and cyclins in specific phases of the cell cycle signal progression through mitotic phases in normally proliferating cells (233), the mechanisms governing re-initiation of the cell cycle following cellular quiescence are not well understood.

Cell cycle progression in the parasite is expected to be tightly regulated, considering the phased transcriptional profile observed during the IDC (128), dynamic regulation of its epigenome (207,216) and incorporation of signaling events in cell cycle progression (118,119). Several atypical CDKs, CDK-related proteins, cyclins and other CDK regulators (98,234–236) have been implicated in cell cycle control in *P. falciparum,* although their involvement in the regulation of mitotic signaling cascades typical of other eukaryotes is questioned (46,89). Rather, it is postulated that the parasite employs evolutionary distinct cell cycle regulatory mechanisms; the functions of many of the molecular components needed for cell cycle regulation have not been clarified in *P. falciparum* parasites.

One of the main methods to study the regulation of the cell cycle in other organisms is to synchronize cells to a particular cell cycle phase, then reverse this block and observe various features of the emerging cell. The inability to tightly synchronize the parasite into particular cell cycle phases *in vitro,* with a very tight window and age-range of parasites (46,97), has hampered such mechanistic evaluation of cell cycle progression in *P. falciparum*. However, disruption of polyamine synthesis (regulators of normal cell cycle progression) induces a reversible G_1 arrest, allowing cell cycle kinetic evaluations in these cells (237,238). Disruption of polyamine biosynthesis in *P. falciparum* has been used successfully to tightly (3-5 h window) synchronize the parasites to early trophozoite stages (239) by inducing a cytostatic and reversible block.

Here, we exploit this block to add to the limited toolkit available for cell cycle studies in *P. falciparum*, showing that it correlates to cell cycle arrest in G_1, blocking the G_1/S transition. We characterize the biological processes underlying this block in cell cycle progression,

as well as those needed for the parasite to re-initiate the cell cycle. We conclude that *P. falciparum* parasites can respond to external stimuli and undergo quiescence-proliferation decision-making in the early phases of its cell cycle. This process is coordinated and relies on unique regulatory modules including Ca^{2+} signaling cascades and a pivotal role of PK5 in the regulation of the pre-replicative complex. Cell cycle re-initiation is highly coordinated, the result of successive expression of cell cycle regulators influenced by second messenger signaling (Ca^{2+} and cAMP) from within 3h of reversal of the cell cycle arrest.

2.2 METHODS

2.2.1 *In vitro* cultivation of intraerythrocytic *P. falciparum* parasites

In vitro cultivation of malaria parasites in human erythrocytes (volunteer donation with informed consent) holds ethics approval from the University of Pretoria (EC120821-077). *P. falciparum* (3D7 and NF54) parasites (MRA-102 and MRA-1000 from BEI resources/MR4, www.beiresources.org/MR4home, authenticated and genetically validated as mycoplasma free) were maintained with shaking at 37°C in human erythrocytes, suspended at 5% hematocrit in complete culture medium [RPMI 1640 medium (Sigma-Aldrich) supplemented with 25 mM HEPES (Sigma-Aldrich), 11 mM D-glucose (Sigma-Aldrich), 200 µM hypoxanthine (Sigma-Aldrich), 0.2% (w/v) sodium bicarbonate, 24 µg/ml Gentamycin (Sigma-Aldrich) and 0.5% (w/v) AlbuMAX II] (240,241) under hypoxic conditions (90% N_2, 5% O_2, and 5% CO_2). Parasite development was monitored with light microscopy through Giemsa staining and age-matched to a 2-hourly sampled IDC time course (Appendix file 1, Fig. 1A) and parasites were synchronized by iso-osmotic sorbitol exposure every 48 h for 3 cycles, with two staggered treatments 8 h apart (242). The experiment was repeated as above with Dd2, K1 and HB3 *P. falciparum* parasites (Appendix file 1, Fig 1B). Gametocytogenesis was induced by employing a strategy of concurrent nutrient starvation and a decrease of hematocrit as described in (243).

2.2.2 Perturbation of intraerythrocytic *P. falciparum* parasites with DL-α-difluoromethylornithine (DFMO)

DFMO dose-response analyses in the presence and absence of putrescine dihydrochloride (2 mM) were initiated with ring-stage intraerythrocytic *P. falciparum* parasite cultures (1% hematocrit, 1% parasitemia) using SYBR Green I fluorescence as described (244) measured with a Fluoroskan Ascent FL microplate fluorometer (Thermo Scientific, excitation at 485 nm and emission at 538 nm). Nonlinear regression curves were generated using GraphPad Prism 5. Ring-stage intraerythrocytic *P. falciparum* parasites (5% hematocrit, 3% parasitemia) were treated with DFMO (IC_{90}, 2-10 mM, depending on strain) for 48 h and evaluated morphologically with Giemsa-stained light microscopy (1000x enlarged).

2.2.3 Measurement of nucleic content

The effect of DFMO-induced arrest on parasite DNA content was determined flow cytometrically. Intraerythrocytic *P. falciparum* parasites (~5% parasitemia, 5% hematocrit,

50000 events captured) were treated with DFMO (IC_{90}) from invasion (0 hpi) with samples taken every 6 h until 48 hours after treatment. Alternatively, DFMO treatment (IC_{90}) of 2-10 hpi ring-stage intraerythrocytic *P. falciparum* parasites (~1% parasitemia, 1% hematocrit, 10000 parasitized events captured) was reversed after 24 h with 2 mM putrescine dihydrochloride and proliferation monitored 96 h post DFMO treatment. Cell suspension aliquots were fixed with 1:10 ratio of 0.025% glutaraldehyde (v/v) and cell pellets stained with 10 µl 1:1000 SYBR Green I (v/v) (Invitrogen) for 30 min in the dark at room temperature. Analyses were performed on a Becton Dickenson FACS ARIA with 515-545 nm band pass filters (FL-1 channel, FITC signal) for SYBR Green I (DNA) and analysed using FlowJo vX.0.7. Primary gating was performed based on background fluorescent signal from DNA-free uninfected erythrocytes to obtain the parasite-infected erythrocyte population as an indication of parasitemia. Secondary gating was performed on the parasite-infected erythrocyte population to segregate parasitized erythrocytes by nucleic content with 1 nucleus (1N DNA copy number) corresponding to either ring or early trophozoite forms separated from those corresponding to parasitized erythrocytes containing multiple nuclei (2N, mature trophozoite forms or >2N corresponding to schizont parasites). The effect of DFMO on nuclear division was confirmed by fluorescent microscopy by removing samples from treated and untreated parasites as above before methanol fixation on microscope slides and staining with 10µl 1:1000 SYBR Green I for 30 min in the dark at room temperature. Stained samples were visualized using Zeiss LSM 880 Confocal Laser Scanning Microscope (LSM)–Airyscan detector for super-resolution imaging using a 488 nm laser and 495–550 BP filter.

Cell cycle phase analysis was performed flow cytometrically by investigating both DNA and RNA content as has been described (229) (Appendix file 1, Fig. 2). DFMO treatment was initiated on 2-10 hpi ring-stage parasitized erythrocytes (1% hematocrit, 10% parasitemia) and uninfected erythrocytes (1% hematocrit) for 24 h prior to the addition of putrescine dihydrochloride. Samples were stained with 10 µl 1:1000 SYBR Green I (Invitrogen) for DNA quantification and subsequently with 10 µl Pyronin Y (100 µg/ml) for RNA quantification for 30 min each in the dark at room temperature. Analyses were performed for SYBR Green I (DNA) as described above with Pyronin Y (RNA) measured at 564-606 nm (FL-2 channel, PE signal) (10 000 events of parasitized cells captured). Compensation was calculated from single stained Pyronin Y and single stained SYBR Green I samples.

2.2.4 Oligonucleotide DNA microarray and analysis

Oligonucleotide DNA microarrays were performed in biological duplicate and technical duplicate to analyze the global transcriptome changes of either DFMO-arrested parasites or DFMO-arrested parasites followed by putrescine-reversal using custom microarray slides that contained 12 468 oligos (60-mer, Agilent Technologies) based on the complete *P. falciparum* genome (245,246). Microarray analysis was chosen for investigating the transcriptome of the *P. falciparum* parasites for this thesis as the parasite genome is completely annotated and covered by up to 10 individual probes per gene, giving a good overview of transcriptional changes for the entire *P. falciparum* genome, and for these studies, specific regulation by splicing, antisense and ncRNA were not under investigation. Synchronized ring-stage parasitized erythrocytes (5% hematocrit, 10-15% parasitemia) were incubated with DFMO (IC_{90}) at 37˚C for 24 h prior to sampling (Arrested) or left untreated (Control). Additionally, after 24 h DFMO pressure, the cell cycle arrest was reversed with 2 mM putrescine dihydrochloride (re-initiation time points: RE1=27 h post treatment; RE2=30 h post treatment and RE 3=36 h post treatment) counted from initiation of DFMO treatment. From 50 ml parasite cultures sourced at specific time points, RNA isolation was performed as described (246). For each RNA sample, 5-12 µg total RNA was used to reverse transcribe cDNA as previously described (128,245). RNA samples were incubated at 70˚C for 10 min in the presence of 2 µg/µl each of random nonamer (pdN9) and oligo-DT (dT25) primers before cooling to 4˚C for 10 min. The reverse transcription reaction was carried out with 480 U Superscript III enzyme (Invitrogen, USA) in the presence of 1X FS buffer, 10 mM DTT (both Invitrogen, USA), 1.5 mM dATP and 0.75 mM each of dCTP, dGTP, dTTP and aa-dUTP for 16 h at 42˚C (246). The remaining RNA was hydrolyzed with 1 N NaOH and 0.5 M EDTA at 65˚C for 15 min and the reactions purified with the Wizard SV Gel and PCR Clean-Up system (Promega, USA) according to the manufacturer's protocols. The reference pool containing a mix of all cDNA samples was coupled to Cy3 and individual samples to Cy5 dyes at pH 9.0 (Amersham Biosciences, USA) for 120 min in dark conditions. Dye coupled cDNA was purified using the Zymo DNA Clean & Concentrator Kit (Zymo Research, USA) before samples were hybridized overnight at 65˚C and slides washed as described (128). The slides were scanned using a GenePix™ 4000B (Axon Instruments) scanner.

Initial data processing, including spot finding, was performed using GenePix Pro 5.1 (Acuity). The *P*-values of spots were adjusted to control the false discovery rate with the Benjamini and Hochberg equation (247) with an adjusted *P*-value cut-off of 0.05 applied.

Normalization and the identification of differentially regulated genes was accomplished using R v3.2.3 (www.r-project.org) and Bioconductor (248) with the limma and marray (249) packages. Data normalization included robust-spline within-slide normalization, Gquantile between-slide normalization and the fit of a linear model to obtain $\log_2$(Cy5/Cy3) expression values for each condition. Differentially expressed (DE) genes were defined as those with $\log_2$ fold change ($\log_2$ FC) of 0.5 in either direction. DE genes were calculated between the control and arrested parasites at 24 h and between time-matched arrested (DFMO treated) and reversed (with putrescine following DFMO treatment for 24 h) samples for the re-initiation time points (Appendix file 2). DE genes were validated with qPCR (Appendix file 1, Appendix methods, Fig.3).

2.2.6 Microarray data analyses

Using the hourly IDC transcriptome as a reference time line of global transcript abundance, pearson correlation was used to align the transcriptional profiles of arrested, control and re-initiated parasites to the HB3 IDC transcriptome (Appendix file 2) (128). Where not otherwise stated, data visualization of microarray data was performed using TIGR MeV 4.9.0.

Compound signature clustering was performed on 185 expression patterns found within differential expression datasets for *P. falciparum* parasites treated with 21 compounds in 30 classes (250) to determine genes whose expression patterns were significantly aligned due to the presence of a particular compound. The same process was followed for inclusion of cell cycle arrested and amino acid starved parasites (85). A Support Vector Machine (SVM) was constructed using the SVM function from the e1071 package in R.

The *P. falciparum* transcriptomes for the arrested parasites and those that re-initiated their cell cycle (RE1, RE2 and RE3) were correlated to transcriptomes from model organisms with defined cell cycle phases (Appendix file 4). Yeast transcriptomes for both non-quiescent, normally dividing yeast and quiescent yeast were obtained from the *Saccharomyces* Genome Database (www.yeastgenome.org/expression/microarray) using datasets for Friedlander_2006_PMID_16542486 (251) and Aragon_2006_PMID_16507144 (252). These transcriptomes were mapped to cell cycle phases as defined within the database, with phenotype analysis for mitotic cell cycle phase and associated events. *P. falciparum* orthologs for the yeast genes were identified with InParanoid8 (http://inparanoid.sbc.su.se).

Functional cluster analyses associated with cell cycle events were determined through text mining of PlasmoDB v33 (http://plasmodb.org/plasmo/) (search terms: kinas*, “DNA replication”, “DNA damage”, “DNA repair”, transcription, histon*, ApiAP2, calcium and Ca_2*) and matching resultant gene identifiers (from *P. falciparum* 3D7) with the differential expression dataset for the *P. falciparum* cell cycle arrested and re-initiation transcriptomes (Appendix file 3). For the Ca^{2+} subset, additional gene identifiers were obtained from (108).

2.2.7 Gene association network filtering and coexpression regulation network inference

A gene association network (GAN) was filtered for DE cell cycle associated transcripts in STRING (v10.0) (253). STRING filtering categories contained only evidence based on experimentally determined interactions, coexpression inference, curated database entries and fusion based entries. A combined score threshold equal/greater than 0.8 was imposed on the network.

Construction of a *de novo* putative gene regulation network (GRN) based on inference from gene coexpression across the 3D7 real time transcription and decay dataset from PlasmoDB v33 (101) as described in (141) using the Gene Regulatory Network Inference Using Time Series (GRENITS) package (Bioconductor in R (254)). GRENITS uses a linear interaction model through applying Gibbs variable selection on a Dynamic Bayesian network (254). Genes that were differentially expressed in RE1 and RE2 in the cell cycle-related datasets were probed for regulation by coexpression against the subsequent re-initiated timepoints (RE2 and RE3). The number of links above a varied threshold range and the distribution of interaction strength over probability (Appendix file 5) was used to guide a threshold cut off (>0.25).

The GAN and GRN were merged through combining edges in R and visualized in Cytoscape v.3.5.0. Nodes with single interactions that weren’t identified as regulators (rather as regulated) were not displayed to visually simplify the network.

2.2.8 Data availability

The microarray data has been submitted to the Gene Expression Omnibus with accession number GSE92289 (www.ncbi.nlm.nih.gov/geo/).

2.3 RESULTS

2.3.1 DFMO is an effective tool for arresting *P. falciparum* parasites in their life cycle

Polyamine biosynthesis peaks in a monophasic fashion in intraerythrocytic *P. falciparum* trophozoites (255) resulting in a measurable detection of putrescine in early trophozoites, which increases as the parasite proliferates (Figure 2.1A). Inhibition of polyamine biosynthesis with DFMO at any point prior to the expression of PfAdoMetDC/ODC and DFMO does not elicit off-target effects during life cycle stages where AdoMetDC/ODC is not expressed (246). The treatment window was defined as optimal at any point until ~12 hpi, prior to peak synthesis of AdoMetDC/ODC as target, which results in synchronization of parasites at the early trophozoite stage (Figure 2.1B&C).

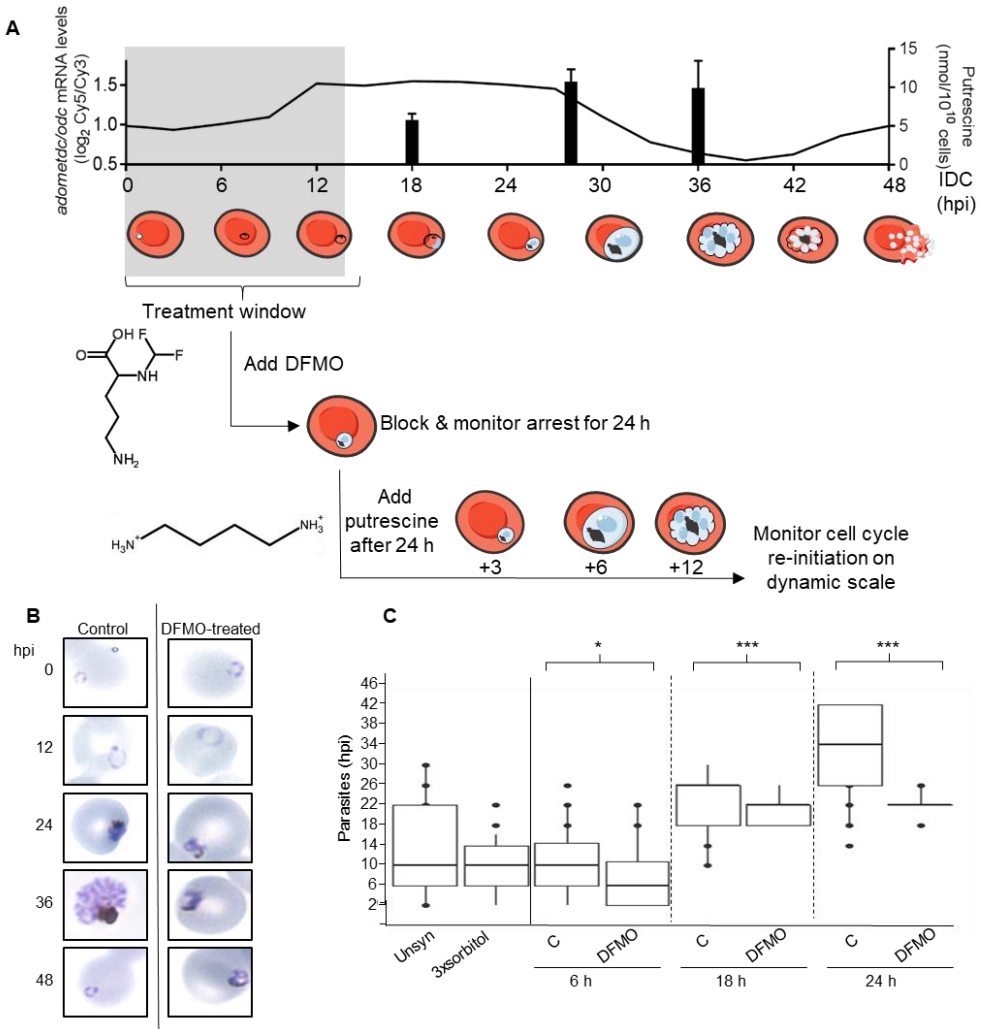

Figure 2.1: Induction of the life cycle arrest caused by DFMO in intraerythrocytic *P. falciparum* 3D7 parasites. (A) mRNA abundance of *adometdc/odc* over the life cycle, with putrescine levels shown as bar graphs. The shaded area indicates the treatment window for cell cycle arrest. Schematics show the normal progression of the life cycle compared to DFMO-induced arrest and reversal. **(B-C)** Morphological evaluation of arrest monitored by Giemsa stained microscopy (1000X enlarged). **(C)** At least 100 individual parasites were morphologically aged to quantify the effects of the arrest, with box and hinges=80% and whiskers=95% of the data.

For initial evaluation and quantification of the synchronization induced by the DFMO-induced life cycle arrest, parasites were evaluated morphologically (Figure 2.1B&C). These data showed the parasite arrested during early trophozoite development ~18-22 hpi, an effect also observed on other strains of *P. falciparum* parasites (Appendix file 1, Fig. 1B). At this point in the life cycle, the parasite starts to pigment slightly more than the ring stages, but the parasite has not yet started to form the hemozoin crystals that are visible within mature trophozoites (Figure 2.1B). DFMO-treated parasites do not form visible hemozoin crystals or merozoites but retain similar morphology for the duration of the 24 h of arrest (Figure 2.1B&C). Quantified, the subjective evaluation of the age range of the parasites after a single DFMO synchronization is within 95% of parasites within a 3-4 h window (18-22 hpi, Fig. 2C), compared to, at best, a 6-10 h window achieved with sorbitol synchronization.

This life cycle arrest was subsequently confirmed and quantified by measurements of SYBR Green I fluorescence as a proxy of nuclear content, using flow cytometry and fluorescence microscopy (Figure 2.2).

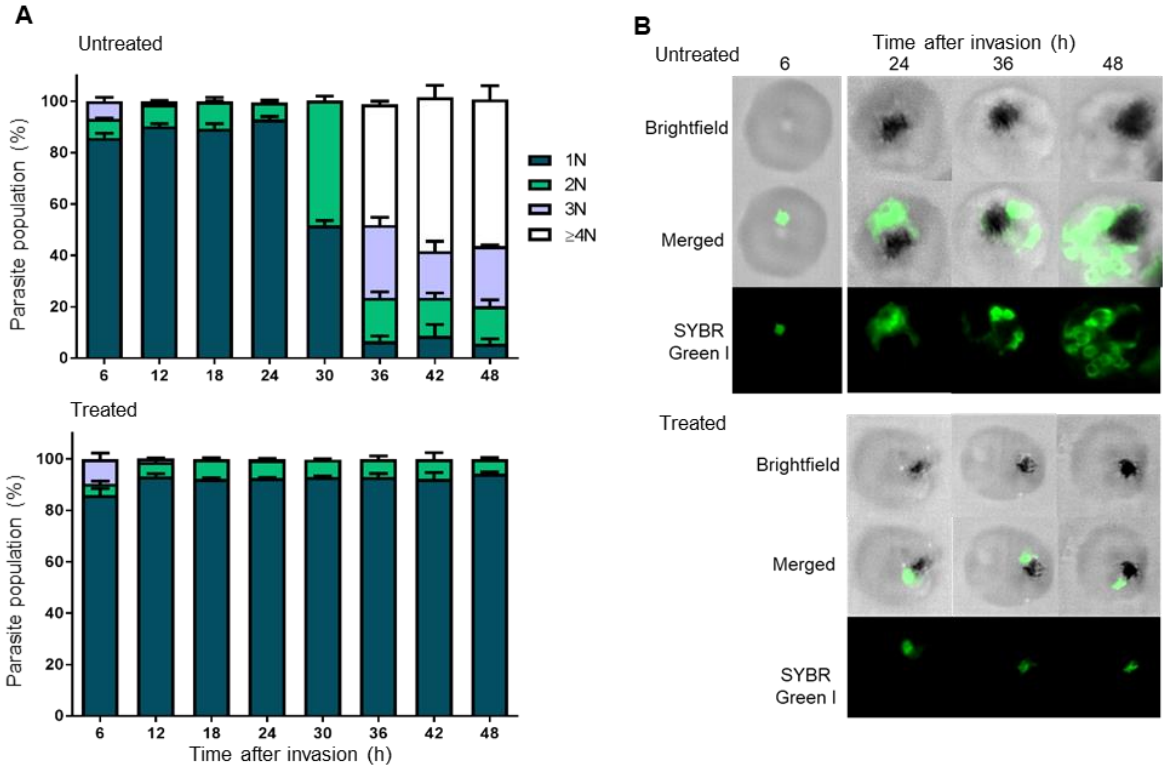

Figure 2.2: Treatment of intraerythrocytic *P. falciparum* 3D7 parasites with DFMO arrests the parasite life cycle before DNA synthesis. Inescapable life cycle arrest following DFMO treatment. Synchronized *P. falciparum* cultures were treated with DFMO (IC_{90}) at 2-6 hpi and **(A)** nuclear content of parasite populations measured by flow cytometry through SYBR Green I fluorescence on a Becton Dickenson FACS Aria with 50000 total events captured. Data are from n=3 biological replicates in technical duplicates, ±S.E**. (B)** DNA content (SYBR Green I fluorescence) was confirmed using fluorescent microscopy on a Zeiss LSM 880 Confocal Laser Scanning Microscope, shown as brightfield image, merged images and SYBR Green I fluorescence images.

After DFMO treatment, 94.3±0.6% of parasites contained a single nucleus (1 N nuclear content) for the entire 48 h period evaluated, indicating that these parasites were synchronized as early trophozoites (Fig. 2.2) prior to DNA synthesis. The remaining treated parasites contained 2N nuclear content, presumably due to pre-existing low levels of polyamines present in the parasites, however, after this was depleted, no further DNA replication was evident. Time-matched, untreated parasites progressed through schizogony, forming multinucleated schizonts (>2 N) from 36 h after invasion onwards. This indicates an absolute requirement of polyamines for DNA synthesis and a complete block in parasite progression to either 1N or maximum 2N, dependent on the availability of polyamines.

2.3.2 The life cycle arrest induced by DFMO has physiological indications of a biologically relevant cell cycle arrest

Classical cell cycle arrest should be fully reversible, with no overt negative perturbation effects and without compromising the cell's viability or capacity to differentiate (97,256). Previously, it had been shown DFMO-treated *P. falciparum* parasites are metabolically viable, capable of ATP synthesis (257), and ultrastructurally unaffected (258). Here, we additionally evaluated the ability of these parasites to differentiate and recover following treatment (Figure 2.3).

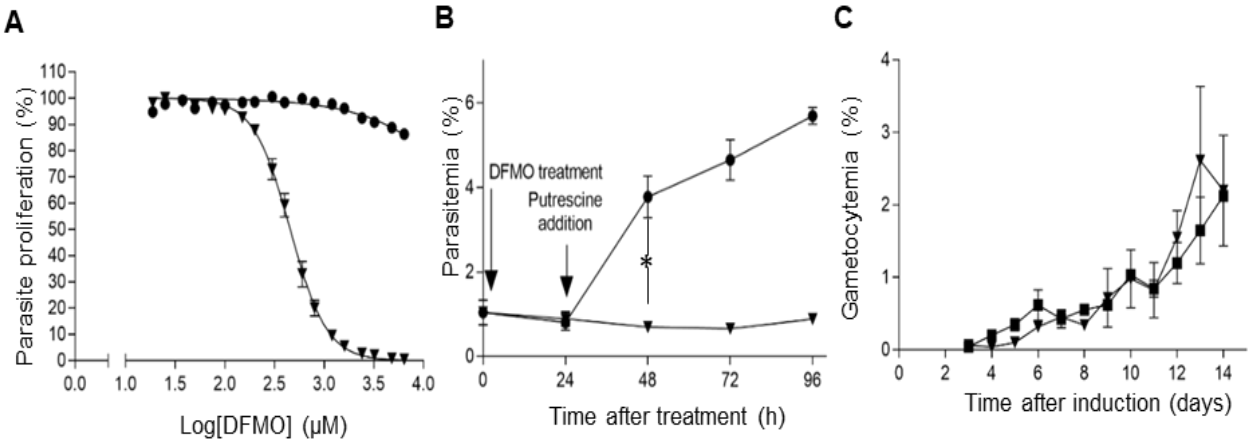

Figure 2.3: Association of the observed cycle arrest to cell cycle arrest in intraerythrocytic *P. falciparum* parasites. In all line graphs- ▼=2 mM DFMO treatment, ■=left untreated and ●=2 mM putrescine addition. **(A)** Reversal of life cycle arrest. Dose-response curves showing the inhibitory effect of DFMO on the proliferation of asexual *P. falciparum* 3D7 parasites *in vitro* in the absence or presence of 2 mM putrescine over 96 h as a percentage of untreated controls from n=6 experiments± S.E. **(B)** The proliferation of ring-stage *P. falciparum* 3D7 parasites were monitored over 96 h in the presence of 2 mM DFMO or addition of 2 mM putrescine dihydrochloride after 24 h of arrest using SYBR Green I fluorescence as measure of parasitemia using flow cytometry with 10000 parasitized events counted, with average proliferation ±S.E. from n=4 experiments in technical duplicate. **(C)** Gametocytemia of *P. falciparum* NF54 cultures over 14 days was measured following arrest with 2 mM DFMO treatment for 24 h using thin smear Giemsa-stained microscope slides with ≥1000 events counted for each sample. Data are averaged±S.E. from n=3 experiments. Where not shown, error bars fall within symbols.

The arrest induced by DFMO is fully reversible by addition of putrescine (taken up by the parasite at non-toxic levels of 2 mM (259)). This is true for the simultaneous addition of putrescine with DFMO (Figure 2.3A) or when putrescine is added after 24 h of DFMO treatment (Figure 2.3B). In DFMO-treated cultures, the parasitemia remained constant over the 96 h monitored, supporting a cytostatic (rather than cytotoxic) response. Putrescine-induced reversal resulted in a significant increase in the parasitemia from 48 h onwards compared to parasites treated with DFMO only ($P \leq 0.05$, n=4) (Figure 2.3B). These parasites developed normally into schizonts, releasing merozoites that subsequently re-invaded erythrocytes with multiplication rates similar to previous experiments (239). We additionally show that these parasites were able to form gametocytes, with comparable gametocytemia at day 14 post-induction, between untreated parasites and those that underwent DFMO synchronization and putrescine rescue ($P > 0.05$, Figure 2.3C). We therefore confirmed that parasites, tightly synchronized in their life cycle, are viable, show no additional signs of overt perturbation and can re-initiate life cycle progression, indicative of a cell cycle arrest.

2.3.3 Cell cycle phase analysis of *P. falciparum* parasites undergoing cell cycle arrest and reversal

The previous observations that DFMO treatment prevented an increase in nucleic content suggested that the arrest in the parasite cell cycle occurs at the boundary between the G_1 and S phase. Flow cytometric analysis based on both DNA (SYBR Green I signal) and RNA (Pyronin Y signal) levels allowed population gating in specific cell cycle phases: G_1, S, and at the G_1/S transition as described in Grimberg *et al.* (229) (Appendix file 1, Fig. 2) as schizogony in *P. falciparum* is characterized by both RNA and DNA synthesis (260,261) (Figure 2.4). Untreated parasites progressed from rings (G_1) to trophozoites (G_1/S) to schizonts (S) and subsequently formed new rings in the next cycle (G_1), with both DNA and RNA levels increasing during schizogony and subsequently decreasing following re-infection of newly formed daughter cells (Figure 2.4).

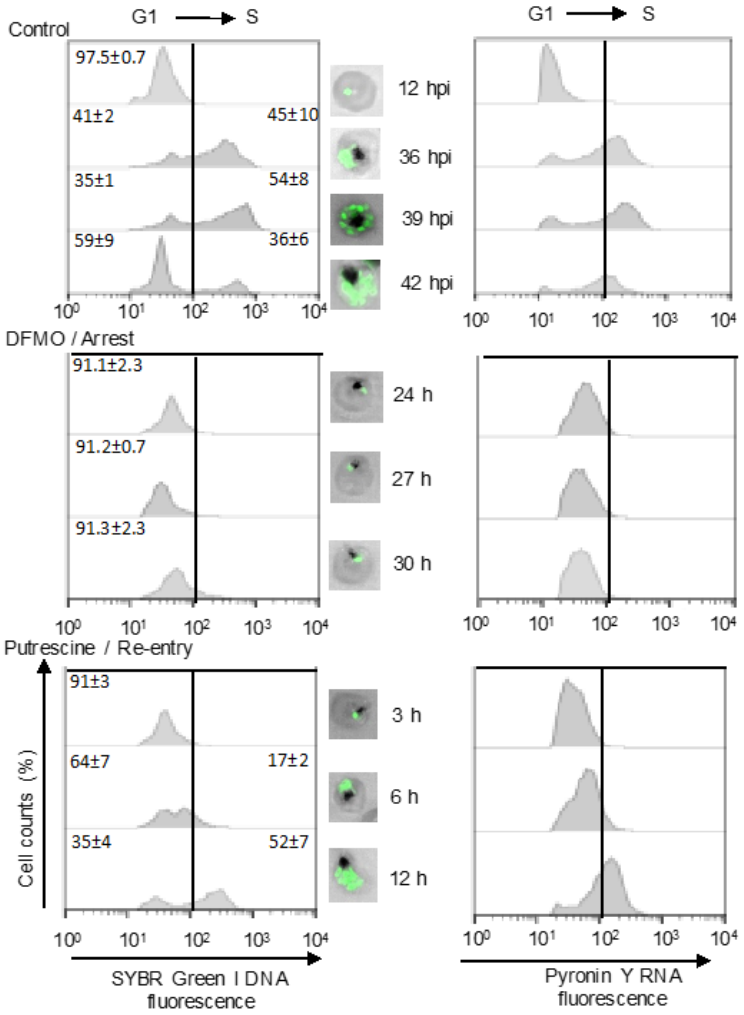

Figure 2.4: Reversible cell cycle arrest occurs at G_1/S phase. Intraerythrocytic *P. falciparum* 3D7 parasites were compartmentalized into different cell cycle phases according to DNA and RNA content as described (229). Ring-stage parasites (1% hematocrit, 10% parasitemia) were treated with DFMO (IC_{90}) for 24, 27 or 30 h or left untreated for control and samples taken at 12 hpi, 36 hpi, 39 hpi, 42 hpi. Additionally, following 24 h of DFMO treatment, putrescine (2 mM) was added to stimulate cell cycle re-initiation, and samples taken 3, 6 and 12 h after reversal. The nucleic acid content of parasitised erythrocytes was determined on a Becton Dickenson FACSAria by consecutive staining with both SYBR Green I (DNA fluorescence) and PyroninY (RNA fluorescence); detected in the FITC or PE channel respectively with >10 000 parasitized erythrocyte events analysed using FlowJo version X.0.7. Compensation values were calculated using single stained samples. Overlaid histograms show a representative sample of biological triplicates. DNA content (SYBR Green I fluorescence) confirmed using fluorescent microscopy on a Zeiss LSM 880 Confocal Laser Scanning Microscope.

DFMO treatment prevented DNA synthesis and >90% of the cell population remained in the G_1 quadrant, confirming that the cell cycle arrest occurred at the end of G_1 or at the G_1/S transition point. Additionally, the concomitant lack of RNA synthesis suggests that these cells exit the cell cycle, which may indicate that parasites enter a quiescent (G_0) state, similar to *S. cerevisiae*, in which transcription will decrease dramatically during cellular quiescence (262) but G_1 cells are still transcriptionally active (263). Putrescine-reversal allowed the cells to re-initiate the cell cycle and resume progression toward schizogony (S phase), with associated increases in DNA and RNA levels observed

already at 6 h post-reversal and appearance of a new generation of ring stages by 24 h (Appendix file 1, Fig 2) post reversal. Collectively, these data indicate that parasites undergo cell cycle arrest at the G_1/S transition, possibly enter a G_0 quiescent state and, upon external polyamine supply, are able to re-initiate proliferation, as seen for mammalian cells in G_1 (237).

2.3.4 Molecular characteristics of a quiescence-proliferation decision point

We exploited the ability to block the cell cycle at the G_1/S transition point to understand the underlying contribution of regulated gene expression to the global transcriptome of parasites at various points in the cell cycle and to interrogate the molecular mechanisms associated with cell cycle arrest in the parasite (Figure 2.5).

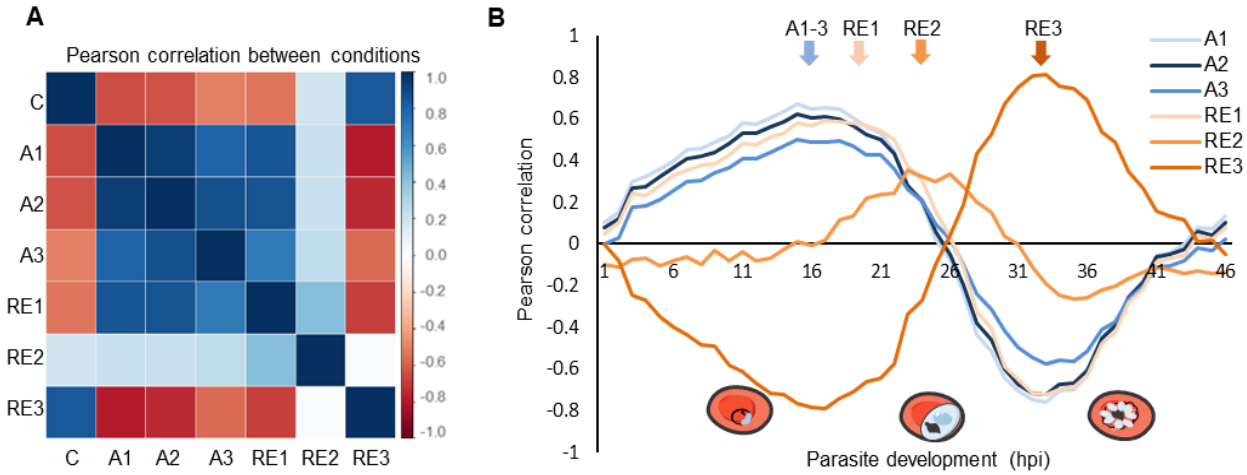

Figure 2.5: The transcriptome profile of cell cycle arrest and re-initiation. Ring-stage intraerythrocytic *P. falciparum* 3D7 parasites were arrested with DFMO (2 mM) for 24 h prior to sampling (A1-3, arrested, sampled at 0, 3 and 6 h after the 24 h DFMO treatment) or left untreated (C, control). Additionally, after 24 h DFMO pressure, the cell cycle arrest was reversed with 2 mM putrescine and sampled after 3 h (RE1), 6 h (RE2) or 12 h (RE3). **(A)** Correlation plot displays the global Pearson correlations within and between each of the treatment conditions. Color intensity indicates strength of correlation from weak (light) to strong (dark). **(B)** Global Pearson correlation to the time-mapped published IDC (128) transcriptome profiles for the arrested samples (A1-3, blue lines), and re-initiated samples (RE1-3, orange lines). Arrows are used to emphasize the peak areas of correlation for the arrested (A1-3) and each RE sample (RE1-3). Representative illustration of parasites shown below graph.

The timeframe of cell cycle arrest and re-initiation was further interrogated by correlating the global transcriptomes of cell cycle arrested and re-initiated parasites to the hourly reference IDC transcriptome (128) (Figure 2.5). Transcriptional profiling of the cell cycle arrested parasites demonstrated a consistent arrested response with strong correlations of r^2=0.8-0.94 between all the cell cycle arrested time points (Figure 2.5A), all correlated to the transcriptomes of late ring/early trophozoites at 15–17 hpi (Pearson r^2 = 0.50–0.67, Figure 2.5B), demonstrating arrest at the G_1/S transition. The transcriptome of the first point of re-entry (RE1) still correlates with the 17 hpi IDC time point (r^2 = 0.59), but the

parasites subsequently rapidly enter S-phase, with re-entry time point 2 (RE2) corresponding to the IDC transcriptome from 22–24 hpi ($r^2 = 0.36$), when parasites initiate DNA synthesis (41,42). This progress towards normal cell cycle progression is further observed with RE3 showing positive correlation from 28 hpi onwards. Further cell cycle progression is observed with RE3 correlating to the 32-35 hpi transcriptomes (35 hpi peak, r^2=0.81). Cell cycle arrest and re-initiation was also evident in the global correlations of the transcriptomes (Figure 2.5B), by RE3 (12 h after reversal), the transcriptome was highly correlated to the 24 h control population (r^2=0.84). Both of these transcriptomes correlated to the 3D7 reference transcriptome at 33-35 hpi, though the RE3 population correlated more closely than the control population (35 hpi peak, r^2=0.81 and r^2=0.65 respectively), possibly due to higher synchronicity in the re-initiated parasite population (258). Finer evaluation of the re-entry will require dynamic evaluation of RNA and DNA synthesis following reversal of DFMO treatment. This confirms that DFMO-induced arrest did not delay parasite development as previously seen with metabolic hibernation through amino acid starvation which extends parasite development rather than arrests it (85) and does not affect the GCN2-sensing pathway markers (including *eif2α*; *pf3d7_1438000* and *eik1*; *pf3d7_1444500,* Appendix file 2); the cell cycle truly arrested at the G_1 phase of the cell cycle (15 hpi) without progression, but addition of putrescine stimulated entry into S phase 6 h after reversal of the arrest and progression through S phase by 12 h after reversal.

Following analysis of the global arrested and re-initiated transcriptomes, DE genes were identified as genes with transcript abundance $-0.5 < \log_2 FC > 0.5$ between arrested and control parasites or arrested and re-initiated parasites. These genes were subsequently probed to better understand transcriptional differences between the conditions and compare the quiescent profile to other chemical perturbations (Figure 2.6).

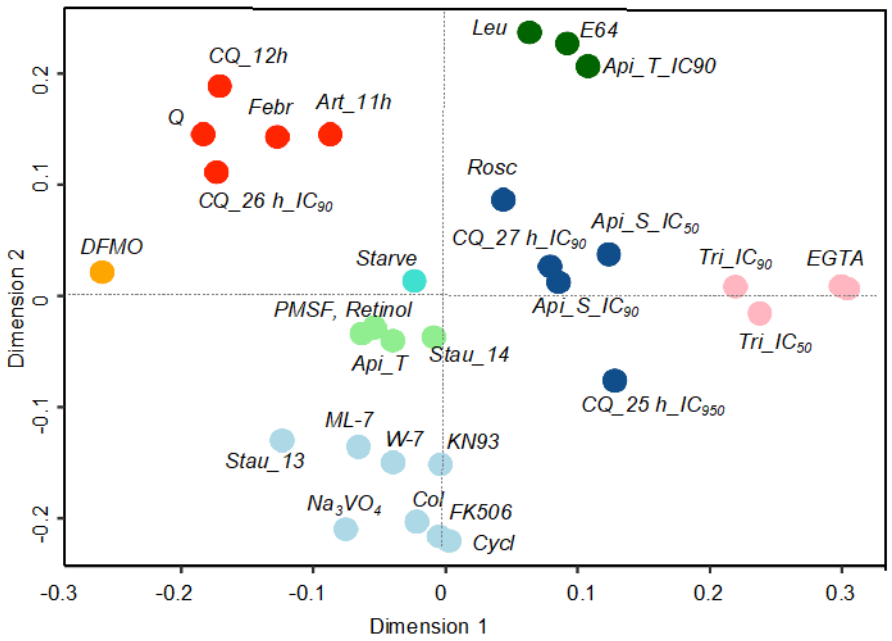

Figure 2.6: Compound transcription signature clustering. Transcriptomes of drug-treated asexual parasites (250) and parasites undergoing amino acid starvation (85) (Starve) were separated with a support vector machine (SVM) classifier and subsequently clustered in order to establish relatedness of chemical perturbations to cell cycle arrested parasites (2 mM DFMO-treated, 24 h, orange circle). Q=quinine, CQ=chloroquine, Stau=straurosporine, Rosc=roscovitine, Api=apicidine, Febr=febrifugine, Art=artemisinin, leu=leupeptine, Tri=trichostatin A, Col=colchicine, Cycl=cyclosporine.

The cell cycle arrested transcriptome was clearly distinct from those obtained under any other reported chemical or physical perturbations (250) (Figure 2.6). Chemical signature clustering of 21 perturbations (250) showed compounds with similar chemical backgrounds or biological effects grouped together, for example, the red grouping containing chloroquine (CQ), quinine (Q) and artemisinin (Art) that all interfere with heme metabolism (18,20). However, the cell cycle arrested transcriptome was fully dissociated from these compounds and the starvation response induced by a lack of isoleucine in parasites cultures (85), indicating a unique transcriptional signature profile for DFMO-induced cell cycle arrest and quiescence in *P. falciparum* parasites.

2.3.5 Characterization of the cell cycle phases of *P. falciparum* parasites

Previous association of molecular components with specific cell cycle phases in *Plasmodium* parasites (264) have proven difficult, owing to the lack of synchronization in the parasite's life cycle. Here, initial characterization was performed using the well-defined yeast transcriptome that has been associated with cell cycle phases (251,265), including the quiescence regulators associated with entry into G_0 (266) (Figure 2.7).

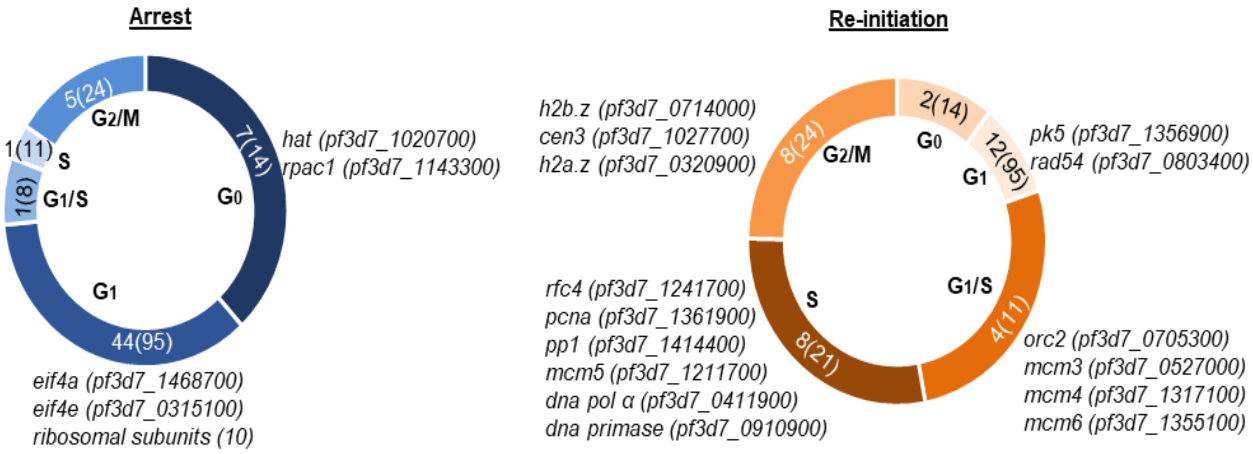

Figure 2.7: Cell cycle analysis of arrested *P. falciparum* parasites. *P. falciparum* parasite arrested (blue) and re-initiated (orange) transcriptomes were matched to cell cycle associated transcripts from non-quiescent and quiescent yeast transcriptomes (251,265,266) (www.yeastgenome.org) according to defined cell cycle phases. The number of matched DE (log_2 fold change of >0.5) genes in each cell cycle phase is indicated with the number of orthologues associated with the cell cycle phase in brackets and darker shades/ bigger portions of the circle corresponding to stronger associations with specific phases.

The 14 orthologous transcripts characteristic of a quiescent, G_0 yeast transcriptome generally showed increased abundance (7 transcripts >0.5 log_2 FC) during cell cycle arrest, including a putative histone acetyl transferase, *pf3d7_1020700* confirming a potentially quiescent phenotype in arrested parasites (Figure 2.7). Transcripts (44/95) associated with the yeast G_1 phase were also increased in abundance during arrest compared to cell cycle re-initiation, corresponding mostly to genes involved in protein synthesis (e.g. ribosomal proteins, *eif4a (pf3d7_1468700)* and *eif4e (pf3d7_0315100)*), suggesting that this timing is conserved between yeast and *P. falciparum* parasites G_1.

A small subset (12/95) of yeast G_1 orthologs related to DNA repair/replication, including the CDK *pk5 (pf3d7_1356900)* and DNA repair protein *rad54 (pf3d7_0803400)*, were rather associated with cell cycle re-initiation, suggesting that these genes do not characterize the same cell cycle phase in the two organisms. As expected, the re-initiated parasite transcriptomes showed the strongest association with the replicative cell cycle phases (S, G_2/M and G_1/S phase transition). Notably, 4/11 of the *P. falciparum* orthologs of transcripts whose decreased levels are associated with the G_1/S checkpoint in yeast are increased as the parasite cell cycle re-initiates (e.g. several transcripts encoding pre-replicative complex components, pre-RC: mini-chromosome maintenance complex subunit 3 (*mcm3), pf3d7_0527000; mcm4, pf3d7_1317100; mcm5, pf3d7_1211700, mcm6, pf3d7_1355100,* & origin recognition complex 2 subunit (*orc2), pf3d7_0705300)* (90). Similarly, proteins involved in DNA synthesis typically expressed during S phase (e.g. DNA polymerase subunits alpha *pf3d7_0411900* & DNA primase *pf3d7_0910900*

and proliferating cell nuclear antigen, *pf3d7_1361900*) are decreased in abundance in the cell cycle arrested, quiescent parasites and increased upon re-initiation into the cell cycle. Together, this data confirms that the parasite quiescence-proliferation decision is associated with some of the molecular descriptors similar to that employed by other unicellular eukaryotes.

2.3.6 Molecular cues govern entry into the proliferative state of *P. falciparum* parasites

While the parasite does share some characteristics with model organisms, the unusual progression of the cell cycle in the parasite would suggest that additional, atypical mechanisms are at play. To investigate possible molecular regulators related to cell cycle regulation, 4 functional clusters were prioritised containing transcripts associated with (i) kinases and phosphatases (228 individual transcripts), (ii) DNA replication (73 transcripts), (iii) transcription and chromatin dynamics (272 transcripts) and (iv) Ca^{2+} signalling associated processes (95 transcripts).

Interrogation of these transcripts allowed molecular characterization of the regulatory molecules associated with early, intermediate and late response of re-initiation, respectively (Figure 2.8A). To better understand the parasite's decision to re-engage its proliferative machinery, the DE transcripts characterizing the earliest point of cell cycle re-initiation (RE1) were interrogated against the cell cycle arrested and re-initiation datasets (Fig. 2.8B).

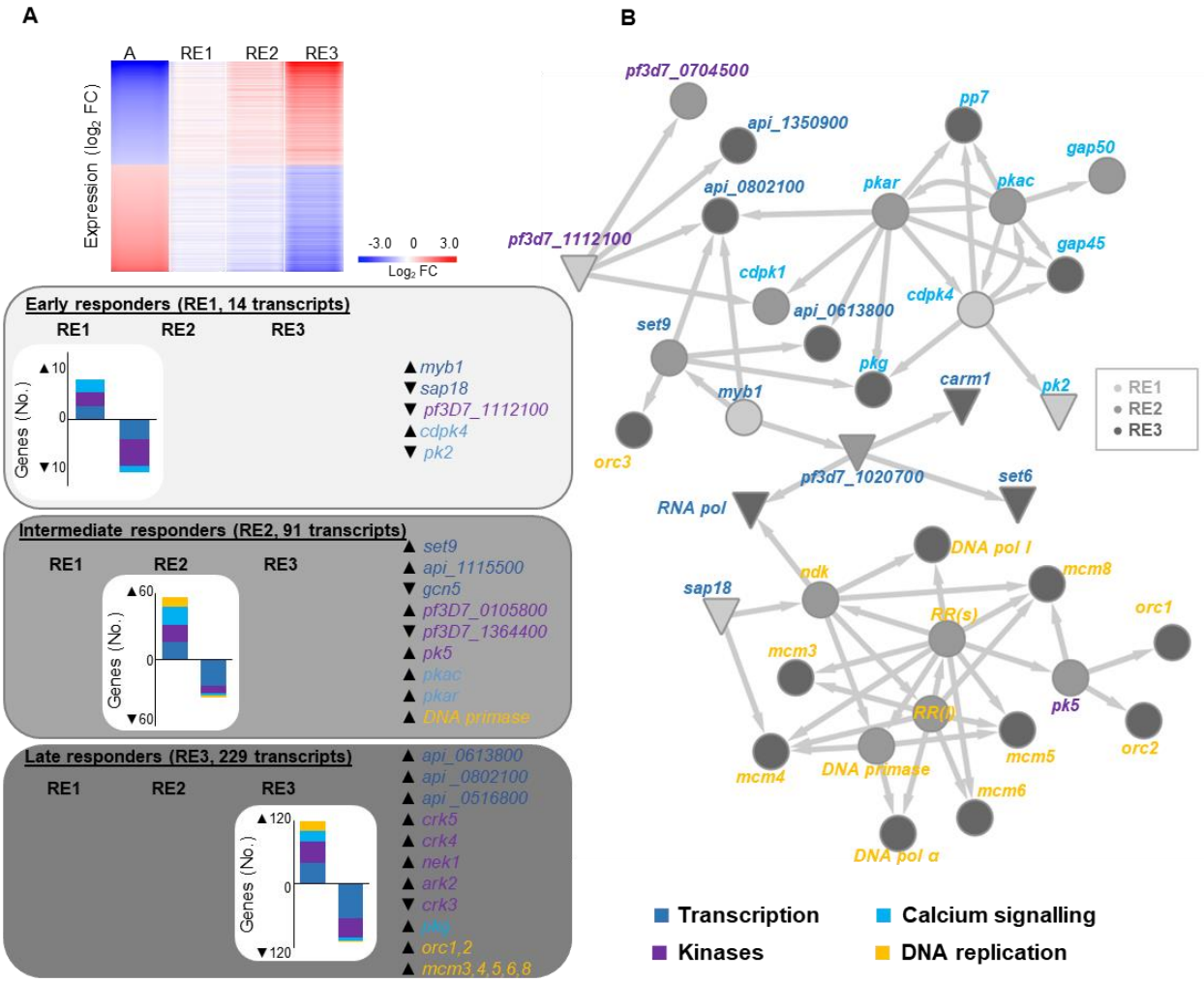

Figure 2.8: Molecular mechanisms controlling cell cycle re-initiation. (A) The transcriptomes of parasites (color-coded key) that re-initiated their cell cycles (RE1-3) were analyzed in context of genes matching key terms associated with cell cycle regulation using PlasmoDB (v33). The expression profiles of genes of interest that were DE in RE1-3 are shown in heatmap, with the number of DE (either increased or decreased abundance) genes associated with specific cell cycle-related functional associations in histograms and genes of interest highlighted in grey boxes. **(B)** A gene association network was constructed between putative regulators of cell cycle re-initiation by combining co-expression analysis (GRENITS, probability linkage score >0.25) and functional association between genes (STRING v 10.0, combined probability score >0.8). Transcripts that were differentially expressed by RE1 (light grey), RE2 (grey) and RE3 (dark grey) are indicated according to their increased (●) or decreased (▼) transcript abundance. Genes are indicated by gene name on the network, (RR=ribonucleoside-diphosphate reductase large (l) subunit, *pf3d7_1437200* and small subunit (s), *pf3d7_1015800, orc3*=conserved unknown protein with ORC3 domain, *pf3d7_1029900*).

Several kinases involved in proliferation/cell division were differentially expressed, 43% of which (63/147) are essential to either *P. falciparum* or *P. berghei* development (26,267) (Figure 2.8A). This included *ark2, nek1*, the cdc-2 related kinases *crk3, crk4* and *crk5* and *pk5,* of which *crk3 & 4* and *pk5* are essential to parasite development (201,267). Other Ca^{2+} sensitive kinases including *pk2* (an essential Ca2+/calmodulin-dependent kinase), *cdpk4* (a cyclin-dependent kinase), *pkac* and *pkar* (catalytic and regulatory subunits of cAMP-dependent PKAs) and cGMP-dependent *pkg*, were also differentially expressed. Of the 27-member ApiAP2 transcription factor family, *pf3d7_1115500* increased during

DNA synthesis, while *pf3d7_0802100, pf3d7_0613800*, and *pf3d7_0516800*, increased during endomitotic division (RE3). Additionally, the MYB1 transcription factor, which is essential for progression into schizogony (152), increased in transcript abundance at re-initiation (RE1). Furthermore, genes that encode proteins involved in epigenetic control are present in the DE set, including decreased levels of histone deacetylase complex subunit (*sap18*) and two histone acetyl transferases (*gcn5* and *pf3d7_1020700*) and increased transcript abundance for the methyl transferase, *set9*. The dynamics of the DE genes was assessed by probing for their occurrence either immediately upon re-entry in RE1 as early responders (14 genes) or subsequently during RE2 (intermediate responders) or RE3 (late responders) (Fig. 2.8B). Re-entry into the cell cycle was characterized by the immediate expression of *myb1* and *cdpk4* upon polyamine supply, whilst *sap18* and *pk2* both display decreased expression upon cell cycle re-entry. After this initial expression of genes, a second subset are associated with RE2 (n=91), including kinases (*pk5, pkac* and *pkar*), *set9*, ApiAP2 *pf3d7_1115500*, DNA primase and an unannotated gene. The latter, *pf3d7_0105800*, contained an Interpro domain associated with cyclin dependent kinases (IPR000789). Genes involved in the late response (RE3) are enriched in transcription factors (3 ApiAP2 family members) and CDKs and Aurora kinases 16 (*crk3, 4, 5* and *ark2*), with increased expression of pre-RC genes *orc1&2* and *mcm3, 4, 5, 6, 8* also evident.

The dynamics in expression of cell cycle-associated genes led us to predict directional relationships between particularly important gene nodes during re-entry through gene association network analysis based on co-expression data obtained at various re-entry time points (Figure 2.8B, full network in Appendix file 1, Fig. 4 and Appendix file 5). Four early responders (*cpdk4, myb1, sap18* and *pf3d7_1112100*) are defined as effectors. *Cdpk4* is a particularly connected node effecting downstream signaling events (e.g. *pk2, pkg, pkac* and *pkar, cdpk1*) with 58 connections to cell cycle related genes involved in Ca^{2+} signaling, transcription, kinases and phosphatases. This suggests that CDPK4 expression could stimulate entry into S phase and lead to the expression of genes essential for completion of schizogony in *P. falciparum*, similar to its requirement for entry into S phase in *P. berghei* gametogenesis (70). *Myb1* shares 12 connections with *cdpk4,* including the two essential ApiAP2 transcription factors (*pf3d7_0802100* and *pf3d7_0613800*), providing a link between signaling events and associated transcriptional regulation. Additionally, *myb1* associates with epigenetic modulators; its expression is associated with histone methyltransferase, *set9* expression and decreased abundance of

a putative histone acetyl transferase (*pf3d7_1020700*) in RE2. The involvement of epigenetic mechanisms is further evident in connections with *sap18*; its decreased abundance is associated with increased levels of genes involved in DNA replication and transcription, including pre-replicative licensing factors (*mcm3-6 & 8*), DNA polymerases and replication factors, with a functional relationship confirmed for *pk5* with members of the pre-replicative complex, *orc1, orc2* and co-expression with *mcm8*. *Pf3d7_1112100* was decreased in abundance by RE1, but it was co-expressed with genes that almost uniformly increased in abundance in RE2, supporting a repressive function for this regulator. Manual annotation revealed the presence of a Bub1/Mad3 motif (IPR015661), typically associated with regulation of the spindle assembly checkpoint in metazoans. The co-expressed genes of this regulator comprised 55 cell cycle related genes, mostly encoding kinases, transcription factors and Ca^{2+} signaling mediators. The gene also co-expressed with *pk6*, a CDK-related kinase, which was increased in abundance during cell cycle arrest and re-initiation. The presence of this regulator within the dataset may indicate the existence of a G_1 cell cycle checkpoint in *P. falciparum*. Taken together, these results suggest that the proliferation decision in *P. falciparum* following exposure to mitogens is mediated by Ca^{2+} signaling pathways, possibly influencing activity of MYB1 that subsequently initiates an epigenetically driven cascade of expression, ultimately enabling DNA replication through expression of the pre-RC.

2.4 DISCUSSION

Here, we used complementary cell biology, transcriptome profiling and gene association analyses to show that *P. falciparum* parasites employ quiescence-proliferation decision-making to enforce cell cycle control, particularly inducing a G_1 restriction point just prior to G_1/S transition. We developed a method to allow cell cycle synchrony in malaria parasites and as such, provide the most effective tool thus far to study cell cycle progression and regulation in malaria parasites. The abrogation of the normal cellular functions of polyamines as cell cycle regulators (268) has successfully been used to induce cell cycle arrest in specific phases (238,269). Inhibition of polyamine metabolism in eukaryotes arrests cells typically at the G_1/S transition (238,269), or prolongs the S phase prior to the G_2/M transition (270) through regulation of checkpoint control elements (271,272). Polyamine-induced cell cycle arrest is fully reversible and considered a physiologically relevant mechanism to study cell cycle checkpoints and associated regulatory mechanisms. The use of this system in malaria parasites resulted in life cycle arrest with an exceptionally tight window of development, associated with the limited production of the biosynthetic AdoMetDC/ODC enzyme (246). This system is further advantageous in its ease of use: cell cycle arrest can be induced by DFMO addition at any point prior to the production of AdoMetDC/ODC, resulting in a broad treatment window and the inhibition can easily be overcome with the addition of exogenous polyamines.

Protists have diverse mechanisms of cell cycle control due to the varied forms of disconnect between evolution of the nucleus and other cytological features (273). The classical mechanisms of control: cell cycle checkpoints, synchronous cell cycle progression and the ability to enter quiescence in response to physiological conditions, have been postulated to be missing or absent, thereby enabling the observed asynchronous endomitotic cycles (46). However, the recent finding that core cell division cycling proteins are conserved in apicomplexan parasites (274) and the ability of malaria parasites to tightly synchronize their asexual replication *in vivo,* imply some endogenous cell cycle control. This is even more evident in the ability of the parasite to enter a dormant state of development under drug pressure (275) or enter metabolic hibernation as a result of amino acid starvation (85), suggesting that malaria parasites are indeed capable of sensing metabolic stressors and relaying this to cell cycle control. The removal of essential cell cycle regulators therefore elicits a unique cellular response in malaria

parasites, indicative of the induction of a growth factor-dependent G_1 restriction point in its cell cycle.

Several lines of evidence support this conclusion. The induction of the G_1 restriction point, blocking the G_1/S transition, results in parasites entering a quiescent, G_0 state: the parasites are ultra-structurally unaffected (258), are metabolically active (257) but unable to synthesize DNA or RNA, characteristic of quiescent cells (263). However, the quiescent phenotype does not mimic artemisinin-resistant dormancy or metabolic hibernation (85,275). Additionally, the quiescence is fully reversible by re-introduction of polyamines, in contrast to other perturbations previously investigated including Roscovitine and L-mimosine, both of which result in irreversible damage to the parasite (97). We did not see any evidence (morphological, functional or molecular) of physiological stress in polyamine-perturbed parasites, and there was no increase nor deficit in the rate of sexual differentiation. As is characteristic of cell cycle restriction points, a prolonged stasis of >96 h does result in parasite death. This all points to the cell cycle quiescence observed being a true reflection of normal cell cycle arrest. On a transcriptional level, this cell cycle quiescence associates with marks from other eukaryotes defining G_1 restriction prior to the G_1/S transition (256) but does not resemble START in yeast (232,251). Comparison of the complete *P. falciparum* transcriptome under cell cycle arrest showed no evidence of DNA damage as the signal for induction of the G_1 restriction point prior to G_1/S transition in malaria parasites. Rather, DNA damage signals like RAD51/54 showed decreased transcript abundance at this point, which is similarly found in the yeast G_1 phase (276). However, the atypical characteristics associated with the parasite's cell cycle organization and divergence in the cell cycle machinery suggest the existence of regulatory mechanisms that are different to those of higher eukaryotes.

The induction of a G_1 restriction point in the *P. falciparum* cell cycle implies that the parasite must be able to sense signals for cell cycle arrest and enter quiescence. Once polyamines are re-introduced into the system, this is translated to mechanisms that enable subsequent re-initiation into the cell cycle for continued proliferation. Such quiescence-proliferation decision-making processes are typically tightly controlled through distinct regulatory mechanisms. Previous strategies focusing on the elucidation of cell cycle regulation mechanisms in *P. falciparum* have mainly relied on homology-based PCR and database mining approaches, which led to the identification of several CDKs, CDK-related proteins, cyclins as well as CDK regulators (99,277,278). These

proteins show promiscuous behavior not found for the respective human or yeast counterparts (100,104) and their involvement in control in *P. falciparum* is unclear (46,279). Of these, our data show the expression of NIMA *(nek1)* and Aurora *(ark2)* kinases during cell cycle progression similar to previous observations (279), tentatively linking their expression to G_1/S transition. The data also confirm the involvement of PK5 in cell cycle progression through regulation of pre-RC components, including regulation of ORC1 through phosphorylation by PK5 (280).

Ca^{2+} and second messenger signaling, although not classical features of cell cycle regulation, seem to be key in progressing into S phase in *P. falciparum* parasites. Co-expression analysis, coupled with the immediate increased abundance of *cdpk4* from the earliest point of cell cycle re-initiation, suggest that the interplay between *cdpk4* and *pk2* may contribute to crossing of the G_1/S boundary. PbCDPK4 is required for DNA replication and progression to S phase in activated *P. berghei* male gametocytes (70) and changes in Ca^{2+} levels are also associated with a G_1/S transition in mammalian cells and yeast (281–283). It is also tempting to speculate that the Crz1p or mammalian NFATc transcription factor ortholog in *P. falciparum* could be MYB1 or one of the ApiAP2 transcription factors associated with PKAr, but these observations still need to be investigated.

In-line with MYB1 being a transcriptional regulator of the parasite's entry into S phase, ablation of its expression leads to death at the trophozoite-schizont transition (152). In addition, MYB1 seems to coregulate putative targets of PK2, PKAc and PKAr, all implicated in progression through S phase from our data. Transcriptional regulation by ApiAP2 transcription factors allowing the parasite to progress through S phase cannot be ruled out, with seven ApiAP2 transcription factors increased in transcript abundance during cell cycle re-initiation. Of these, two *(pf3d7_0802100, pf3d7_0613800)* were linked to cell cycle perturbation in our study and genetically validated as essential for asexual development in *P. falciparum* and *P. berghei* (223) respectively.

The *P. falciparum* parasite also possesses a dynamic epigenome, with several post-translational histone modifications shown to influence transcription and chromatin status over the intraerythrocytic life cycle (207). It is very interesting that SAP18 involved in transcriptional corepression, would be affected by a G_1/S arrest. The protein is functionally associated with *hdac1 (pf3d7_0925700)* and chromatin assembly factor 1

pf3d7_1329300, positing an expected role in the changing chromatin status of the parasite life cycle, which could explain its connection to much of the DNA replication machinery of the parasite. This link is still only predictive but does support the step-wise expression of replication factors in the parasite's progression through S phase, with the functional association between NDK and ribonucleotide reductase during entry into S phase preceding the increased abundance of most of the pre-RC. The regulation of the pre-RC is not well understood outside of the regulation of ORC1 through phosphorylation by PK5 (284,285), which is only expressed later on during re-initiation, preceding increase of ORC1.

Taken together, our data demonstrate the ability of *P. falciparum* parasites to undergo quiescence-proliferation decision making in the initial phases of its cell cycle. Our data show that DNA damage is not a signal for induction of a G_1 restriction point, although its involvement in later phases cannot be excluded. Secondly, growth factor dependency should be considered a contributing feature to cell cycle control in *Plasmodium* spp., thereby inducing quiescence to ensure survival until more favorable conditions are again experienced (85,286). Finally, we show here that the parasite is able to sense signals for cellular senescence-like processes and induce a G_1 block preventing the G_1/S transition. Passing this restriction point seems to be an absolute requirement for cell cycle progression before entering the endocyclic mitotic cycles (46,97). The ensuing endocyclic division however, might not be as well-controlled, causing asynchronous nuclear division, resulting in a varied number of daughter merozoites produced from individual schizonts, reminiscent of early embryonic development in *Drosophila*, which is characterized by syncytial formation after the first 13 rounds of mitosis without cytokinesis (287).

The regulatory mechanisms underlying the quiescence-proliferation decision-making are unique to malaria parasites and involve transcriptional control, Ca^{2+} signaling and effector kinases. With this first set of evidence for cell cycle regulation in *Plasmodium* parasites, the system described will open avenues for future validation of the mechanisms underlying these processes in the parasite. Understanding the underlying mechanisms of parasite proliferation is key in unravelling the parasite's molecular regulators of development, allowing it to make cellular decisions in its complex biological life cycle. Of course, the parasite is also able to forego proliferation, exiting the cell cycle and differentiating into gametocytes. In the next chapter, the consequences and regulators of this decision will be explored.

Chapter 3

Intricate hierarchical transcriptional control regulates *Plasmodium falciparum* sexual differentiation

3.1 INTRODUCTION

Sustained malaria prevalence is ensured through continued human-to-mosquito transmission of *Plasmodium* parasites. The developmental biology of *P. falciparum*, causing the most severe forms of disease in humans, is characterized by a complex, multistage life cycle occurring in both the human host and Anopheline mosquitoes. Two distinct and exclusive developmental phases characterize intraerythrocytic development: rapid, asexual cell division manifesting in pathology, or the stochastic (<10%) (224,288) sexual differentiation into gametocytes, which produces the non-replicative, mature, transmissible forms of the parasite (224). Whilst the IDC is rapid (~48 h) and results in massive cell number expansion, sexual development and differentiation is a prolonged process (~14 days) in *P. falciparum*, characterized by morphologically and functionally distinct gametocyte stages (stages I-V) (59).

Both processes of cell division and differentiation in the parasite are associated with distinct metabolic requirements within specific developmental stages (43) and specific patterns of gene expression that are tightly controlled through complex regulatory systems. These patterns have been investigated to some extent for asexual division where *P. falciparum* parasites use both transcriptional and post-transcriptional processes (160,175,289) to effect a cascade of coordinated, stage-specific gene expression profiles (128). The restrictive presence of only a small family of ApiAP2 transcription factors and the lack of understanding of the specific mechanisms of active transcription remain challenges to interpreting the importance of transcriptional control during the IDC. Although epigenetic control of gene expression is employed for particular gene families (211,214), mRNA dynamics is further influenced by additional post-transcriptional mechanisms (141).

The mechanisms regulating commitment to gametocytogenesis have been somewhat clarified, with host lysoPC restriction as an environmental factor driving gametocyte commitment (52). Activation of AP2-G as molecular master switch (53,222) from an epigenetically silenced state (54,55), results in expression of downstream transcriptional regulators that drive entry into gametocytogenesis (53,129). Gametocyte commitment further requires stabilization of a subset of gametocyte-specific transcripts (141) and AP2-G independent protein export early in sexually committed ring-stage parasites (290). However, comparatively little mechanistic data is available on the molecular mechanisms governing subsequent gametocyte development and maturation.

Some ApiAP2 proteins enable progression into intermediate stages of gametocyte development in the rodent parasite *P. berghei* (223) and *P. falciparum* (291) and translational repression has been described as a mechanism controlling expression of a subset of transcripts for gametogenesis (176). Systematic exploration of gene expression for *P. falciparum* gametocytogenesis is limited to evaluation of the transcriptome (49,134,163,292,293) and proteome (134,186,187,294) captured at only specific developmental snapshots, particularly during the bifurcation in committing asexual parasites to gametocytogenesis (52,129,141), or alternatively evaluation of mature gametocytes in preparation for transmission (134,186,187). Current datasets evaluating the complete gametocyte development process are sparse (49) and preclude dynamic evaluation of the molecular profile associated with the extended gametocyte development process of *P. falciparum* parasites. A detailed, time-resolved single dataset of the transcriptome of each stage of gametocyte development, at a similar high-resolution to that for asexual development, is therefore required to allow comparison of gene expression levels during gametocyte development and maturation.

Here we describe a comprehensive, high quality of the transcriptome of *P. falciparum* parasites during all stages of sexual development. With this high-resolution data, we demonstrate that gametocytes can be completely distinguished from asexual parasites on a transcriptional level. In particular, the data show distinct shifts in transcript abundance associated with morphological stage transition, indicating that gene expression occurs on a time scale consistent with developmental decisions underlying gametocyte development. The data also demonstrated the regulatory effect of specific epigenetic and ApiAP2 transcription factors, implying further transcriptional regulation shapes the gametocyte transcriptome post-commitment. Given the great complexity of

the *P. falciparum* transcriptional program, these data provide a quantitative baseline of gene expression throughout gametocytogenesis in *P. falciparum* and constitutes a highly valuable resource that could be exploited to understand the molecular mechanisms governing cellular differentiation in the parasite.

3.2 METHODS

3.2.1 Parasite culturing and sampling

Asexual *P. falciparum* NF54 parasite cultures (NF54-*pfs16*-GFP-Luc, (295)) that produce an increased number (243) of mosquito-infective (295) gametocytes were maintained at 5-8% parasitemia 37°C in human erythrocytes at 5% hematocrit in RPMI 1640 medium supplemented as described in Section 2.2.1. Synchronous asexual cultures (>95% synchronicity of ring-stage parasites, 6 h window) were obtained by two consecutive cycles (48 h developmental cycles) of treatment with 5% D-sorbitol, each 6-8 h apart.

Gametocytogenesis was induced by employing a strategy of concurrent nutrient starvation and a decrease of hematocrit (243). Ring-stage parasite cultures (>95%) were adjusted to 0.5% parasitemia, 6% hematocrit in RPMI 1640 medium prepared as for growth of asexual parasites but without glucose supplementation (day -3) and maintained under the same hypoxic conditions at 37°C without shaking. After 72 h, the hematocrit was adjusted to 4% (day 0) and after another 24 h, the medium was replaced with normal glucose-supplemented culture medium and gametocytogenesis monitored for a total of 16 days. Contaminating asexual parasites were removed daily with 5% D-sorbitol treatment from day 1 for 15 min at 37°C until asexual forms were no longer visible in culture.

All cultures were maintained with daily medium changes and monitored with Giemsa-stained thin smear microscopy. Parasite samples (30 ml of 2-3% gametocytemia, 4-6% hematocrit) were harvested daily for microarray analysis on days -2 to 13 following gametocyte induction. The samples harvested on days -2 to 7 were isolated from uninfected erythrocytes via 0.01% w/v saponin treatment for 3 min at 22°C, while samples from day 8 to 13 were enriched for late-stage gametocytes via density centrifugation using Nycoprep 1.077 cushions (Axis-Shield, UK). Late-stage gametocyte samples were centrifuged for 20 min at 800x*g* and the gametocyte containing bands collected (243). All parasite samples were washed with phosphate-buffered saline (PBS) (137 mM NaCl, 2.7 mM KCl, 10 mM phosphate, pH=7.4) before storage at -80˚C until RNA was isolated.

3.2.2 RNA isolation, cDNA synthesis and dye labeling

Total RNA was isolated from each parasite pellet with a combination of TriZol treatment and using a Qiagen RNeasy kit (Qiagen, Germany) as described previously (296). The quantity, purity and integrity of the RNA were evaluated by agarose gel electrophoresis

and on a ND-2000 spectrophotometer (Thermo Scientific, USA). For each RNA sample, 3-12 µg total RNA was used to reverse transcribe cDNA as previously described (128,245). RNA samples were incubated at 70˚C for 10 min in the presence of 2 µg/µl each of random nonamer (pdN9) and oligo-DT (dT20) primers before cooling to 4˚C for 10 min. The reverse transcription reaction was carried out by 400 U Superscript III (Invitrogen, USA) in the presence of 1X FS buffer, 10 mM DTT (both Invitrogen, USA), 1.5 mM dATP and 0.75 mM each of dCTP, dGTP, dTTP and aa-dUTP for 1 h at 42˚C before an additional 100 U Superscript III was added and incubated for an additional 1.5 h (297,298). The remaining RNA was hydrolyzed with 0.1 N NaOH at 70˚C for 10 min before the reaction was neutralized with 0.1 N HCl. Synthesized cDNA was purified using the Zymo DNA Clean & Concentrator Kit (Zymo Research, USA) according to the manufacturer's instructions, with the exception that centrifugation steps were carried out at 16000*xg*. cDNA samples were kept in 0.1 M sodium bicarbonate at pH 9.0 and stored at -20˚C until dye labeling. The reference cDNA pool was constructed from a mixture of all the gametocyte samples used in the experiment in a 1:4 ratio with cDNA from a 6-hourly time course of asexual *P. falciparum* 3D7 parasites. The reference pool was coupled to Cy3 and samples to Cy5 dyes at pH 9.0 (Amersham Biosciences, USA) for 120 min in dark conditions in an ozone free environment (299). Dye coupled cDNA was purified using the Zymo DNA Clean & Concentrator Kit (Zymo Research, USA) identically to after cDNA synthesis.

3.2.3 Array hybridization and scanning

Equal amounts of Cy5 and Cy3 coupled cDNA for the single time course at quantities between 150 and 500 ng were added to a hybridization mixture containing 1X GE blocking agent and 1XHI-RPM hybridization buffer (both Agilent Technologies, USA). Hybridization was carried out while rotating at 10 rpm at 65˚C for 17 hours. Before scanning, arrays were washed in first 6X and then 0.06X SSPE, both containing 0.005 % *N*-lauryl-sarcosine (Sigma Aldrich, USA) before being rinsed in acetonitrile. The microarray slides used were optimized in terms of the number of features, sensitivity, and inter-array variability (245) that also included ncRNA (300) and representative of an updated version of the genome's annotation from those used in Chapter 2. Arrays were scanned on an Agilent G2600D Microarray Scanner (Agilent Technologies, USA) with 5 µm resolution at wavelengths of 532 nm (Cy3) and 633 nm (Cy5). Hybridization and scanning was carried out in an ozone free environment (299). Linear lowess normalized signal intensities were extracted using the Agilent Feature Extractor Software version

11.5.1.1 using the GE2_1100_Jul11_no_spikein protocol and all data uploaded onto the Princeton University Microarray Database (https://puma.princeton.edu/).

3.2.4 Data analysis

From the signal intensities loaded on the Princeton University Microarray Database, data were included that had both red and green intensities that were well above background and passed spot filters (P<0.01) and $\log_2$(Cy5/Cy3) expression values were used for further analysis (Appendix file 6). Where not otherwise stated, data were analyzed using TIGR MeV software version 4.9.0 (http://www. Tm4.org/mev.html). Pearson correlation coefficients were calculated in the R statistical package (version 3.2.3) comparing the expression of genes at each time point with every other time point and visualized using the Corrplot package (301) in R. K means clustering was carried out in R using verbose code and Euclidean distance clustering with the optimal number of clusters first determined using a within sum of squares measurement. Genes from clusters that showed differential expression between stages were validated using qPCR (Appendix file 1, Appendix methods, Fig. 5).

For functional analysis of genes (Appendix file 6), gene ontology enrichments per cluster were obtained for biological processes with P<0.05 using curated evidence from PlasmoDB v33 on accessed during July 2017 (http://www.plasmodb.org/). Additional annotations were obtained for genes involved in metabolic pathways from the Malaria Parasite Metabolic Pathways (MPMPdatabase (http://mpmp.huji.ac.il/) and for genes with unknown functions using protein domain searches from the Interpro database (https://www.ebi.ac.uk/interpro). Additional supplementary datasets for translationally repressed genes (134,173), transcripts involved in commitment (52,129,141) and gametocyte proteomes (134,186,187,294) were probed for significant association with clusters of expression using a two-tailed Fisher's exact test to calculate significant association between the datasets. Genes involved in mRNA decay were probed for regulation of decreased transcripts using the GRENITS package in R and the number of links per model, per threshold was evaluated to determine the set probability threshold at >0.4 for these regulators. For comparison between transcript abundance and histone post-translation modifications, supplementary information was sourced for Chipseq experiments conducted by Gupta *et al.* from the GEO datasets for H3K56ac, H4K5/8/12ac (207) as well as Salcedo-Amaya *et al.* for H3K9me3 (211) and Jiang *et al.* 2014 for H3K36me3 (214). The genes associated with the specific histone marks in each of the

publications were then probed for correlation between their transcript abundance during gametocytogenesis and increased presence of the post-translation modification in gametocytes (216).

To determine the involvement of specific ApiAP2 transcription factors in gametocyte development, GRENITS was applied (probability threshold >0.7) to probe the 13 ApiAP2 transcription factors that were increased in abundance during gametocyte development as putative regulators and the total transcriptome as possible regulated genes (254). Following the identification of ApiAP2 transcription factors with putative regulatory activity (*pf3d7_1222600, pf3d7_0934400, pf3d7_0611200, pf3d7_1317200, pf3d7_0516800*), these transcription factors were re-probed as regulators using GRENITS, but including only genes containing the transcription factor's binding site as possible regulated genes (142). For the two transcription factors (PF3D7_0934400, PF3D7_0611200) for which binding sites have not yet been determined, the entire transcriptome was probed as possible regulated genes. The number of links per model, per threshold was evaluated to determine the set probability threshold for each constructed GRENITS network for the regulated genes of each transcription factor.

3.2.5 Data availability

The microarray data has been submitted to GEO with accession number GSE104889 (www.ncbi.nlm.nih.gov/geo/).

3.3 RESULTS

3.3.1 High-resolution transcriptome displays clear distinction between sexual and asexual stages of development

P. falciparum NF54 parasites were induced to form gametocytes and monitored for 16 days from commitment in asexual development to induction and maturation of the sexual stages (Figure 3.1). Tight synchronization of the asexual parasites ensured a coordinated view of gametocytes during development, with the most heterogeneous populations observed in early differentiation (days 2-3). The resultant complete transcriptome of parasites sampled on each day during the entire gametocyte commitment (days -2 to 0) and differentiation process (days 1-13) contains $\log_2$(Cy5/Cy3) expression values for 96-99% of the 5443 genes hybridized on the array, including non-coding RNAs (P<0.01). This therefore comprises a comprehensive and high-resolution dataset of the transcriptome of *P. falciparum* parasites during gametocytogenesis.

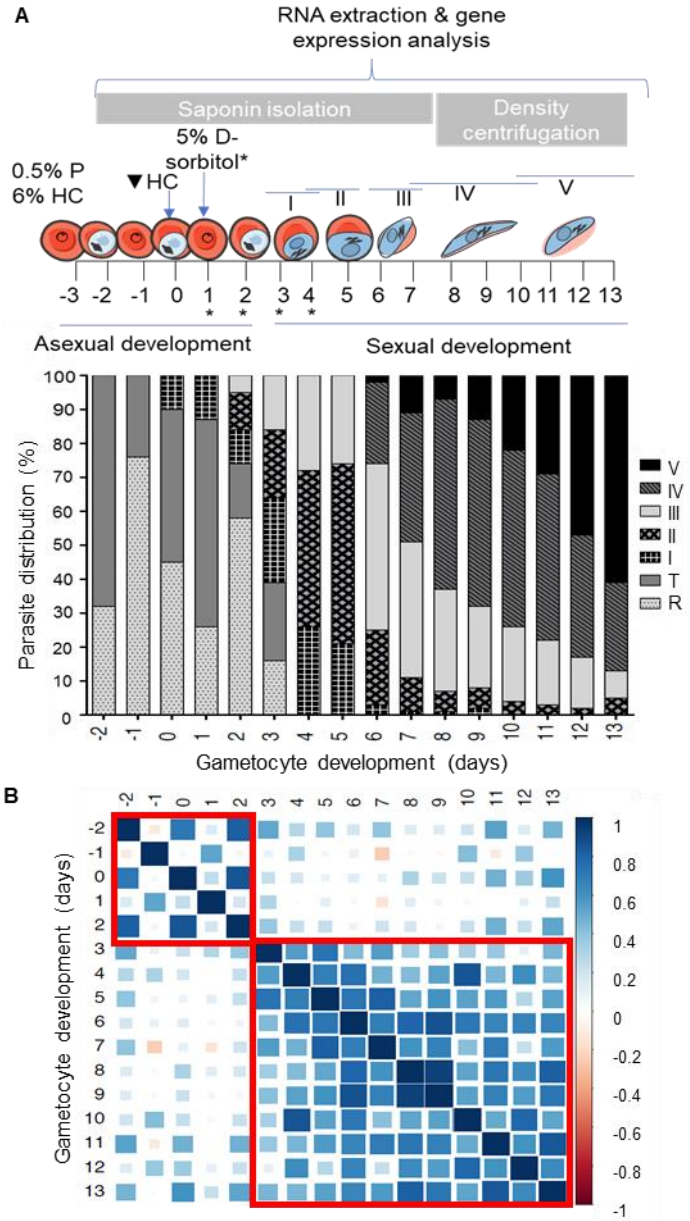

Figure 3.1: The development and associated transcriptome of *P. falciparum* NF54 gametocytes from commitment to maturity. (A) Sampling and culturing strategy and stage distribution of parasites on each day of the time course. Morphological development was monitored from induction (day -2) over 16 days of development using Giemsa-stained thin-smear microscopy. The stage distribution for each day was calculated by counting ≥100 parasites on each day of monitoring. Legend: I-V indicates different stages of gametocyte development, R=ring- and T=trophozoite stage asexual parasites, *=D-Sorbitol synchronization, HC=hematocrit, P=parasitemia. **(B)** Pearson correlation coefficients of the total transcriptomes obtained for each day of development. The 1st red box indicates the pre-gametocytic stages of commitment to gametocytogenesis (majority asexual population) and the 2nd indicates the days corresponding to gametocyte development.

Careful morphological evaluation showed the appearance of gametocytes (60% of population) by day 3 of development (Figure 3.1A). The transcriptome of gametocytes is also distinct from asexual parasites, as evident by a clear shift in global correlation scores between the transcriptomes of asexual parasites (day -2 to 2) and gametocytes (day 3 onward) (Figure 3.1B). Populations containing asexual parasites (days -2 to 2) correlated to each other every 48 h cycle, corresponding to similar points in their development

(r^2=0.54-0.86) and consistent with periodic gene expression changes between the asexual ring and trophozoite stages. Transcriptional divergence between asexual parasites and gametocytes is evident in a loss of the 48 h correlation pattern, with only r^2=0.29 observed between day 1 and 3. During subsequent days of gametocytogenesis, peak correlations are associated within developmentally similar stages e.g. stage I-II with r^2=0.56-0.73 (days 3-5), stage III-IV with r^2=0.51-0.92 (days 6-9), within mature stage V gametocytes r^2=0.50-0.84 (days 10-13) (Figure 3.1A&B). These results show that gametocytes have a different transcriptional program from asexual development, evident in Figure 3.2.

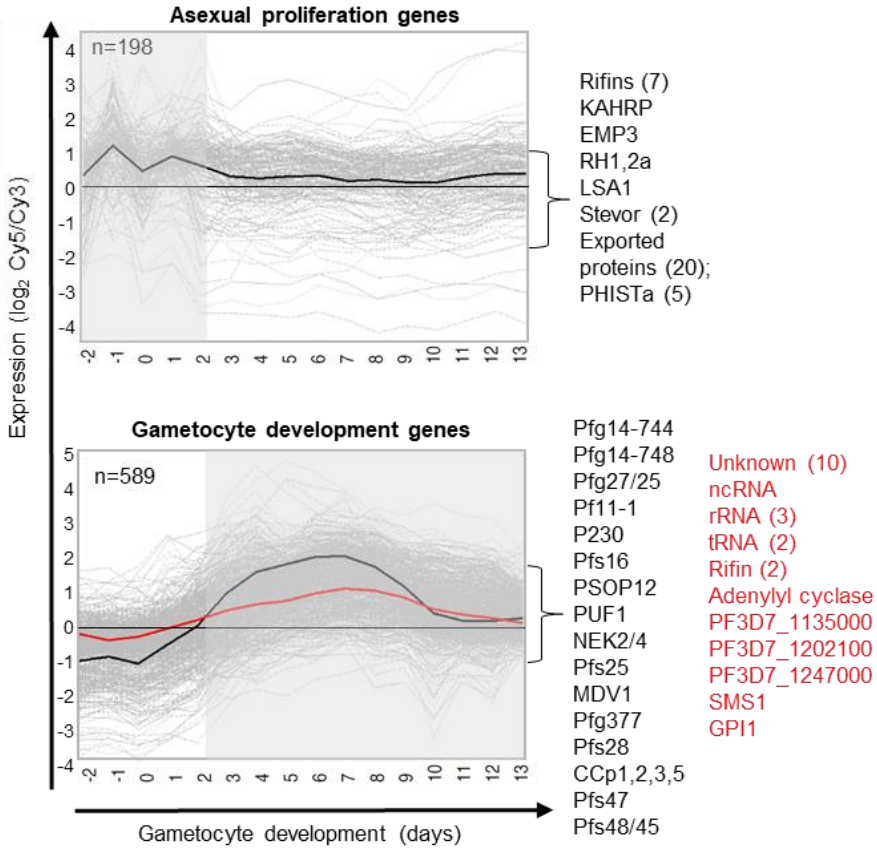

Figure 3.2 Separation of genes associated with either asexual proliferation or gametocyte development. The full range of samples from gametocyte development time points were hybridized against a reference pool of 6 hourly time points over the full asexual development cycle. Abundance of transcripts that were enriched during asexual development (log_2(Cy5/Cy3) of >0.5) and their average abundance (black line) versus gametocytogenesis are shown in top and bottom graphs respectively, with gold standard gametocyte genes (302) shown as black line and gametocyte genes not described previously shown in red.

The specificity and unique nature of the gametocyte transcriptome was validated through cross-hybridization to an asexual reference transcriptome (Figure 3.2, Appendix file 7). The divergence between the transcriptome of asexual parasites and gametocytes was evident in the sole expression of asexual markers (302) (e.g. *kahrp, pf3d7_0202000*; *emp3, pf3d7_0201900*; *rh1, pf3d7_0402300*; *rh2a, pf3d7_1335400*; *LSA1,*

pf3d7_1036400) in asexual parasites (n=198, Figure 3.2, log_2(Cy5/Cy3)>0.5, 95th percentile of differential expression). Conversely, 589 gametocyte-enriched transcripts were identified (log_2(Cy5/Cy3)>0.5, 95th percentile of differential expression, Figure 3.2). This included 85% (35/41) of the "gold standard" gametocyte markers recently reported (302), including genes expressed at the onset of gametocytogenesis (e.g. *pfg14-744, pf3d7_1477300* and *pfg14-748, pf3d7_1477700*) (292), early-stage gametocyte markers (*pfs16, pf3d7_0406200* and *pfg27/25, pf3d7_1302100* (49)) as well as late-stage gametocyte markers (*pfs25, pf3D7_1031000* (303)). The majority of the markers (9/11) associated with mature gametocyte sex-specificity (134) were also present.

However, we identified 24 novel gametocyte-associated transcripts that, to our knowledge, have not been associated with gametocytogenesis before. Of these, 10 encode proteins of unknown function and 5 are highly expressed (log_2(Cy5/Cy3)>0.75; *pf3d7_0911500, pf3d7_1233200, pf3d7_1413300, pf3d7_1133000, pf3d7_1215500*). Moreover, 1 putative ncRNA, 3 rRNA and 2 tRNA transcripts were identified, confirming previous indications that the expression of such RNAs may not only play a role in gametocyte commitment (141) but also in gametocyte development in *P. falciparum.* Together, these data comprise a high-resolution gametocyte transcriptome measurement that allows the temporal evaluation of transcriptional patterns associated with gametocyte development and maturation.

3.3.2 The gametocyte-specific transcriptional program reflects the molecular landscape of gametocyte development

To evaluate the temporal association of gene sets to particular events during gametocyte commitment and subsequent stage-transition during development, the entire 16-day transcriptome dataset was K-means 10 clustered, revealing 2765 transcripts with overall decreased abundance and 2429 with increased abundance during gametocytogenesis. This suggests a more specialized program of gene expression during gametocytogenesis compared to asexual development, with only ~45% of transcripts showing increased abundance during gametocyte development compared to the ~80% of transcripts increased in specific phases of asexual development (128). Furthermore, during gametocytogenesis, specific patterns of transcription are observed, with transcript abundance either maintained (clusters 1-2, 6-7), decreased (clusters 3-5) or increased at

specific points in development (cluster 8-10). These patterns of expression were further evaluated for their functional relevance during gametocyte development (Figure 3.3). Several transcripts that show phase-like expression during asexual replication (days -2 to 2) lose such stage-specific expression profiles during gametocyte development (from day 3 onwards) and maintained throughout development at low levels (cluster 4 & 5, 1723 transcripts, average $\log_2$(Cy5/Cy3) -0.36 to 0.11) or maintained throughout commitment and development (cluster 6 & 7, 1572 transcripts, average $\log_2$(Cy5/Cy3) -0.24 to 0.46). These include the expected gene sets involved in the constitutive process of macromolecular metabolism (e.g. DNA replication, protein modification and RNA metabolism) (49,293). Proliferative processes are decreased (e.g. origin of replication complex protein *mcm4*, *pf3d7_1317100* and cyclin dependent kinase *crk4, pf3d7_0317200*) but by contrast, genes involved in cell differentiation (e.g. *caf40, pf3d7_0507600*; *pblp, pf3d7_0818600)* are maintained throughout gametocytogenesis (Figure 3.3). Beyond these examples, clusters 6 and 7 were also enriched for genes involved in signaling consistent with the involvement of cellular signaling pathways in commitment (52). As these maintained clusters in total comprise 63% of the total transcriptome (3297 of 5194 transcripts), the transcriptional mechanisms resulting in phase-like expression of these genes during asexual development are either not being applied in gametocytes, or additional unique regulatory mechanisms exist in gametocytes to continually express or maintain these transcripts.

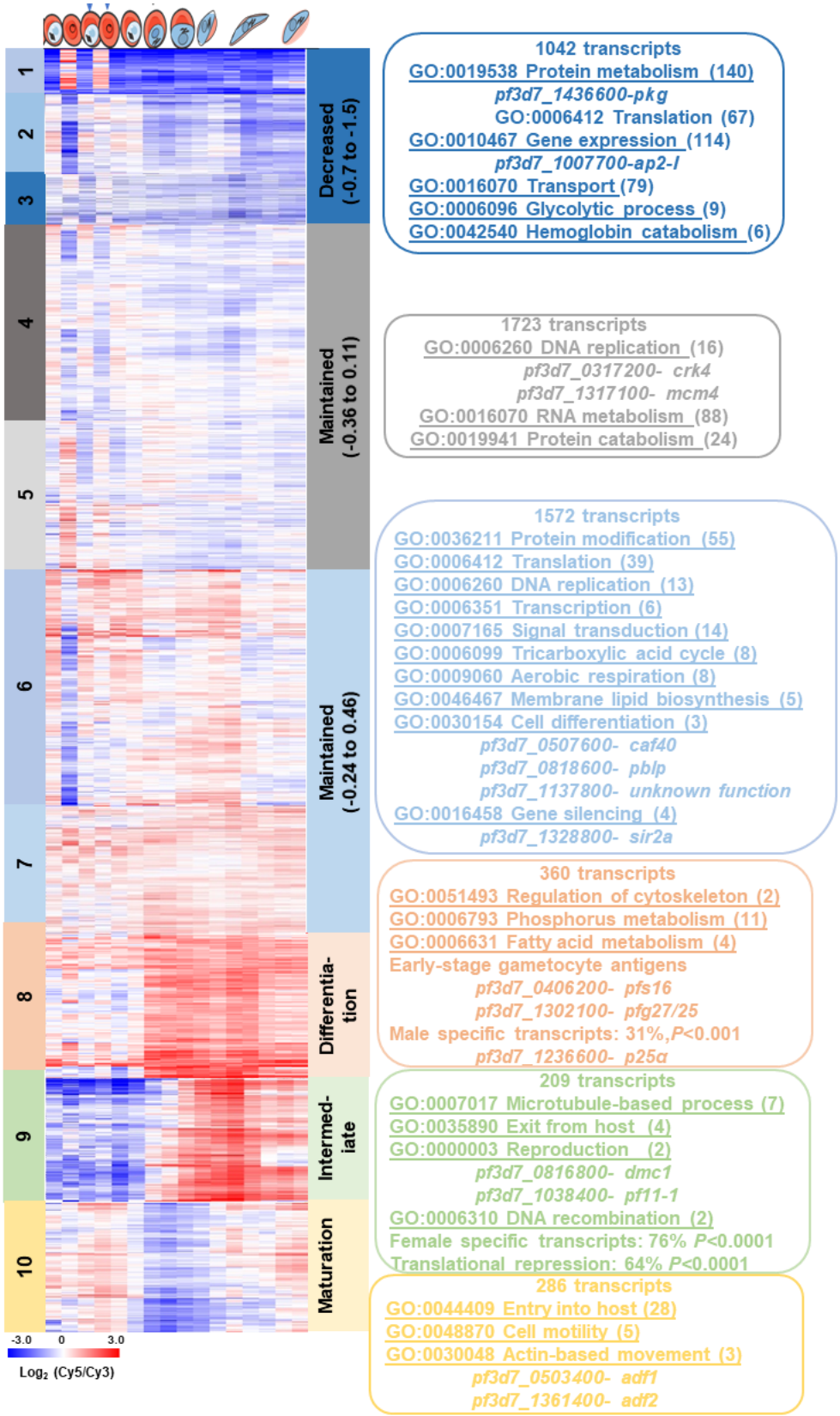

Figure 3.3: Distinct clusters of expression link to biological development of the *P. falciparum* gametocyte. Clusters of genes expressed during gametocyte development following K10 clustering of the total transcriptome (Appendix file 6). Clusters were grouped into phases of decreased, maintained or stage-specific increased expression and translated to enriched biological functions. Biological process enrichment was determined using GO enrichment of each of the clusters (P<0.05) with generic descriptions of the gene sets used to indicate the enriched functions of the genes within each cluster. Significant associations of specific clusters with female, male or translationally repressed transcripts (134) were determined using two-tailed Fisher's exact tests.

A total of 1042 transcripts show a marked decrease during gametocyte differentiation (clusters 1-3, $\log_2$(Cy5/Cy3) -0.7 to -1.5). These gene products are involved in crucial aspects of asexual development that are not as important in gametocytes, including heme metabolism and glycolysis. Conversely, transcripts involved in processes that would be expected to be conserved between asexual and sexual development (gene expression and protein metabolism) were also decreased in abundance. Interestingly, the genes in these clusters also include regulators of egress (*pkg, pf3d7_1436600*) and invasion (*bdp1, pf3d7_1033700*; *ap2-I, pf3d7_1007700*), non-essential functions for the gametocyte maturing in a single erythrocyte.

Genes increased in transcript abundance during gametocyte development showed many of the expected transitions, given the previously observed changes in the gametocyte's biology. The metabolic shift and host cell remodeling associated with gametocyte development is clearly reflected in the transcriptome. The shift to mitochondrial metabolism and fatty acid biosynthesis is evident in the expression of TCA enzymes, cytochrome subunits and acyl-synthase/synthetase enzymes in clusters 6, 7 & 8 (37,50). As expected, gametocyte development (clusters 8, 9) is also characterized by the construction of a rigid subpellilcular microtubule array during the sequestering stages (stages I-IV) of gametocytes (304), evident here by the enrichment of processes related to cytoskeletal formation. The transcripts in these clusters taper down in abundance as the parasite enters stage V of development while actin depolymerization factors 1 and 2 (cluster 10, *pf3d7_0503400, pf3d7_1361400*) transcripts increase as the microtubule network depolymerizes to allow for a more deformable erythrocyte that can re-enter circulation (304). This suggests that very tight regulation of these genes to ensure timely occurrence of parasite sequestration and circulation is still retained *in vitro* within parasites that do not fulfil either of these functions.

Sex differentiation in gametocytes is proposed to be an AP2-G independent process that occurs at the absolute onset of commitment (58,141). The time-resolved transcriptome afforded analysis of the previously described sex-specific transcripts (134) and proteins (134,186,187) associated with stage V gametocytes (735 female-specific transcripts and 528 male-specific transcripts) as well as sex-specific proteins. A significant overrepresentation of male-specific transcripts associate with cluster 8 (31%, $P<0.001$, two-tailed Fisher's exact test), including *p25α* (*pf3d7_1236600*) that is essential for gametocyte differentiation (291).

Female-specific transcripts are only significantly enriched in later stages (III-IV) of gametocyte development (cluster 9, 31%, *P*<0.0001, two-tailed Fisher's exact test) with 85% of these genes showing no detectable proteins in mature gametocytes as this cluster shows significant association with translationally repressed transcripts (64%, *P*<0.0001, two-tailed Fisher's exact test). This translational repression was previously associated with DOZI and Puf2 (134,177) and both *dozi* (*pf3d7_0320800*) and *puf2* (*pf3d7_0417100*) are expressed from the onset of gametocyte emergence in cluster 6 and 8 respectively, preceding the transcription of cluster 9. Translational repression may therefore be imposed already in the intermediate stages of gametocyte development (stages II/III onwards) in preparation of macrogamete formation. This is however, not a general mechanism for all female-specific transcripts, with 31 female specific transcripts associated with detectable protein levels in stage V. These proteins ensure host environment adaptation, by further preparing for gamete generation, expressing gamete-associated genes like *nek4*-kinase (*pf3d7_0719200*) (305) in females and calcium dependent protein kinase *cdpk*4 (*pf3d7_0717500*) and mitogen-activated protein kinase 2 (*map2, pf3d7_1113900*), (70,278) in male gametocytes, further supporting observations that the mature gametocytes contain stored proteins as well as transcripts (134).

3.3.3 Timed regulation of gametocytogenesis enables sex-specific development and life cycle switching

The gametocyte transcriptome is well-timed, expressing specific clusters of genes at specific points in development, suggesting this transcriptional program is important to gametocytes to fulfil their biological functions. In order to better understand this connection, we probed available gametocyte functional genomics datasets concerning: 1) commitment to differentiation (52,129,141) and 2) gametocyte stage transition (267).

3.3.3.1 Both activation and repression events characterize the initial switch to differentiation

The switch between commitment to differentiation from proliferation is associated with the expression of 342 transcripts upon external stimuli (52) resulting in increased commitment to gametocytogenesis. The derepression of AP2-G expression results in further expression of 64 AP2-G-dependent genes (129). A further 808 genes were shown to be actively transcribed or stabilized during commitment to gametocytogenesis (141), resulting in a proposed "on switch" of a combined 1075 unique genes that allow

gametocyte commitment. The time-resolved transcriptome was probed to further characterize this initial switch (Figure 3.3).

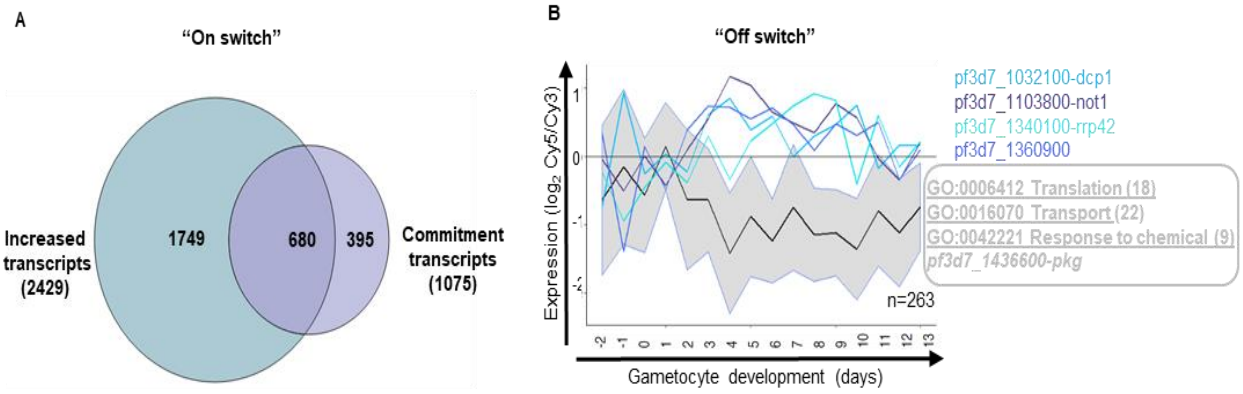

Figure 3.4: An on/off switch characterizes gametocyte development. (A) The genes increased in expression during commitment (52,129,141) were compared to genes increased in expression during gametocytogenesis (Clusters 6-10). **(B)** Within the "on switch", genes involved in mRNA decay were probed for regulation by coexpression using GRENITS in R (probability linkage cutoff of >0.4) against decreased transcripts (Clusters 3-5), forming a possible "off switch" accompanying differentiation, with proposed regulators of decay indicated in legend and mean±SD of decreased genes coexpressed with the mRNA decay genes shown in ribbon plot with GO enrichments indicated in box.

Of the proposed genes involved in commitment, 680 genes (63%) have increased transcript abundance in our data (Figure 3.4). These include epigenetic regulators involved in cell cycle control (e.g. *sir2A, pf3d7_1328800* and *sap18, pf3d7_0711400*) that both potentially contribute to decreased DNA synthesis and a block in proliferation (306) (Figure 2.7B, chapter 2). The remaining 395 transcripts are not expressed during gametocyte development, suggesting these transcripts are short lived and rather just needed during gametocyte commitment. This indicates that these transcripts are essentially important to the switch, but not needed to maintain stage-transition in gametocyte development.

After commitment, progression of gametocyte development also requires transcriptional repression (an "off switch"), as supported by increased repressive epigenetic marks (216) and HP1 occupancy leading to heterochromatin status of early-stage gametocytes (217). However, only 10.6% of the genes associated with the decreased clusters are marked by HP1 (217), suggesting heterochromatin formation is important for the repression of only a subset of decreased transcripts. Additionally, we associate the "off switch" in our data with the increased expression of genes related to mRNA decay including decapping enzyme 1 (*pf3d7_1032100-dcp1*), CCR4-NOT transcription complex subunit 1 *(pf3d7_1103800-not1)*, exosome complex component RRP42 *(pf3d7_1340100)* and a polyadenylate binding protein *(pf3d7_1360900).* Together, these genes co-express with 25% of the 1042 actively repressed transcripts, including *pkg*, implicating involvement of

active mRNA decay as an additional mechanism to repress proliferative markers and allow gametocyte development after commitment.

3.3.3.2 Post-commitment, development and maturation is underpinned by separate transcriptional induction events of essential genes

Once parasites are committed to gametocytogenesis, sexual development does not simply progress due to the presence of the transcripts abundant during commitment. Rather, 35% of transcripts showing well-timed, dynamic abundance changing during development and maturation, suggesting this transcriptional program is important to gametocytes to fulfil their biological functions. These changes are not merely describing the metabolic adjustments and structural changes defining gametocytes. Rather, some inferences can be drawn about transcriptional mechanisms allowing progression through gametocytogenesis (Figure 3.5).

The transcriptional program associated with stage-transition was binned into three distinct phases (Figure 3.5). The first cluster showed a significant association (12 transcripts, *P*=0.0003, two-tailed Fisher's exact test) with genes that elicit a growth phenotype when not expressed in gametocytes from *P. falciparum* or *P. berghei* (267) including early-stage gametocyte markers Pfs16 and Pfg27/25 (224). Surprisingly, this cluster is enriched for 206 genes without functional annotation. However, careful evaluation of these gene products revealed 59 proteins with annotated Interpro domains, including 7 with possible functions in regulating gene expression (*pf3d7_0603600*, possible transcription factor containing an AT-rich interaction domain (ARID)), cell cycle regulation (*pf3d7_1143500; pf3d7_0214300; pf3d7_1006700; pf3d7_0819800*) or regulating sexual development (*pf3d7_0624900*, possible growth arrest specific protein; *pf3d7_0816300,* gamete fusion) suggesting these genes are important for sexual development.

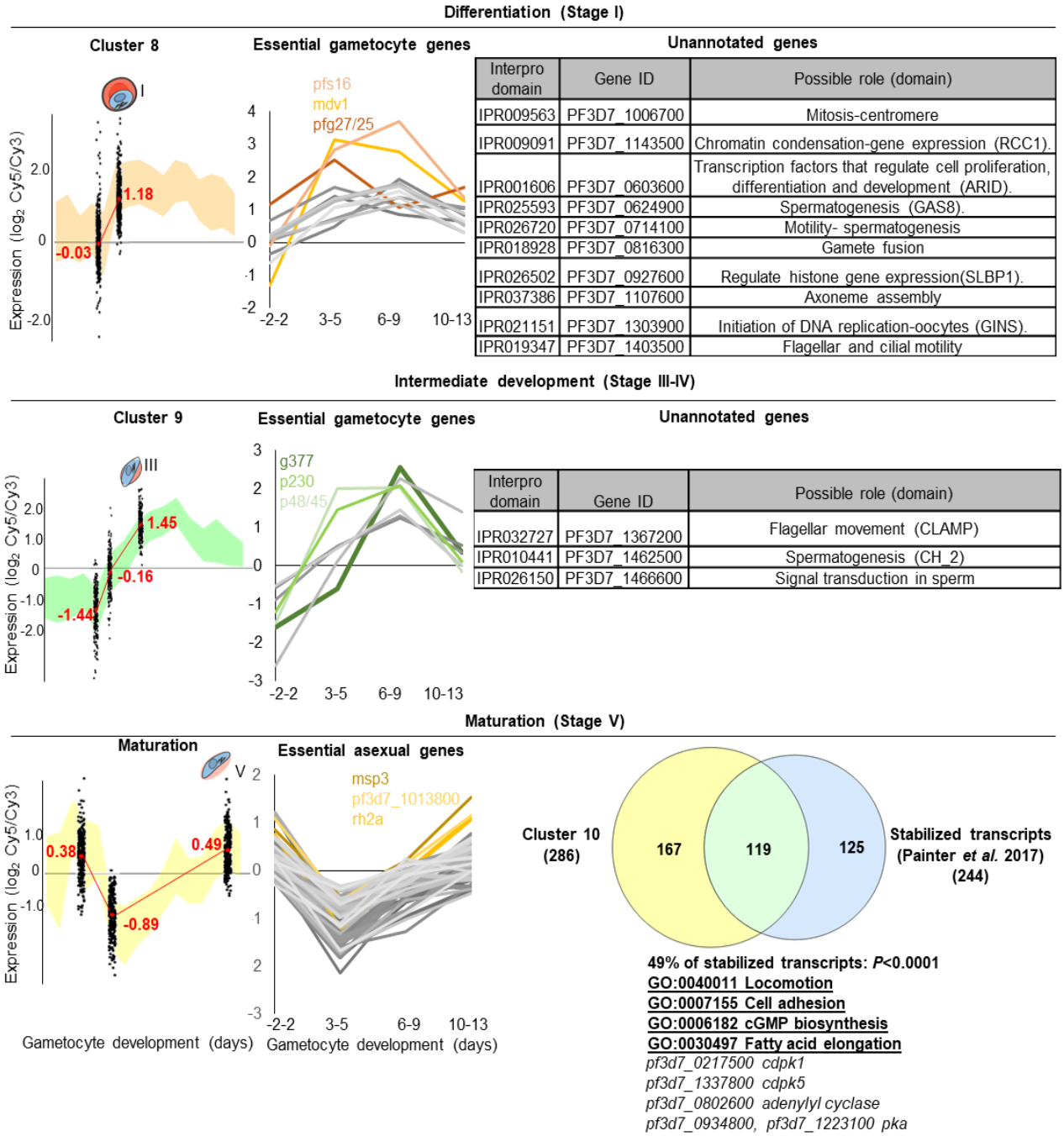

Interpro domain	Gene ID	Possible role (domain)
IPR009563	PF3D7_1006700	Mitosis-centromere
IPR009091	PF3D7_1143500	Chromatin condensation-gene expression (RCC1).
IPR001606	PF3D7_0603600	Transcription factors that regulate cell proliferation, differentiation and development (ARID).
IPR025593	PF3D7_0624900	Spermatogenesis (GAS8).
IPR026720	PF3D7_0714100	Motility- spermatogenesis
IPR018928	PF3D7_0816300	Gamete fusion
IPR026502	PF3D7_0927600	Regulate histone gene expression(SLBP1).
IPR037386	PF3D7_1107600	Axoneme assembly
IPR021151	PF3D7_1303900	Initiation of DNA replication-oocytes (GINS).
IPR019347	PF3D7_1403500	Flagellar and cilial motility

Interpro domain	Gene ID	Possible role (domain)
IPR032727	PF3D7_1367200	Flagellar movement (CLAMP)
IPR010441	PF3D7_1462500	Spermatogenesis (CH_2)
IPR026150	PF3D7_1466600	Signal transduction in sperm

Figure 3.5: Transcriptional patterns indicate regulation of gametocyte development. Points of increased gene expression during gametocyte development are highlighted with expression of individual genes (dots) overlaid over the mean ± SD expression of all genes in the cluster. The average log2(Cy5/Cy3) expression of the genes on days of interest are shown in red. The transcriptional patterns were also shown for essential genes for asexual stage or gametocyte development (267). Further functional annotation of proteins with unknown function in the clusters were probed using Interpro (https://www.ebi.ac.uk/interpro/) domain searches. The maturation cluster was also significantly associated with genes stabilized post-transcriptionally during commitment (141) (*P*<0.0001, two-tailed Fisher's exact test).

Subsequent gametocyte development requires a two-phased shift in gene expression, at the onset of gametocyte development (day 2-3) and during intermediate development (day 5-6). Although this cluster is strongly associated with translational repression, the transcripts that have been detected as proteins (70 transcripts) are also strongly

associated (7 transcripts, *P*=0.004, two-tailed Fisher's exact test) with genes that elicit growth phenotypes when not expressed in gametocytes including the osmiophilic body protein *g377* (*pf3d7_1250100*), *p230* (*pf3d7_0209000*) and *p48/45* (*pf3d7_ 1346700*) (267) (Figure 3.5). The proteins with unknown functions in this cluster include 4 with possible roles in spermatogenesis, particularly ensuring cilliar or flagellar movement.

Gametocyte maturation is further characterized by transcripts that are increased in abundance in committed or asexual parasites but decreased in abundance between days 3-9 and increased in abundance in late-stage gametocytes (stage V days 10-13). This cluster was significantly enriched for transcripts stabilized during commitment (45% of stabilized transcripts, *P*<0.0001, two-tailed Fisher's exact test) (141). For these transcripts, mRNA stabilization is potentially only important during commitment and thereafter, active decay/silencing by transcriptional repression has to be in play to result in this unique expression profile. These genes include the signaling machinery of the parasite (307) *cdpk1* (*pf3d7_0217500*) and adenylyl cyclase (*pf3d7_ 0802600*), along with cAMP-dependent protein kinase A catalytic and regulatory subunits (*pf3d7_0934800, pf3d7_1223100*). Surprisingly, this cluster uniquely but strongly associates (46 transcripts, *P*=0.0021, two-tailed Fisher's exact test) with genes previously shown to be essential for asexual development (267). These essential genes were enriched for products required for invasion, including egress and invasion regulators, *cdpk1* and *cdpk5* (*pf3d7_1337800*) (126,308), with CDPK1 also having a confirmed role in de-repressing female gametocyte transcripts in the mosquito (309), but suggesting a further role for CDPK5 in the mosquito stages as well. Together, these specific patterns of expression suggest that transcriptional control mechanisms could be at play during gametocyte development.

3.3.4 Epigenetic control contributes to timed gene expression during gametocytogenesis

Epigenetic regulation affects commitment to gametocytogenesis (54,55) and distinct quantitative epigenomic post-translational modifications characterize gametocyte development (216). These studies prompted the investigation of modifications that have been linked to transcription in asexual parasites (207,211,214) for their potential additional involvement during gametocytogenesis as novel modifications only involved in gametocytogenesis have not yet been elucidated (Figure 3.6).

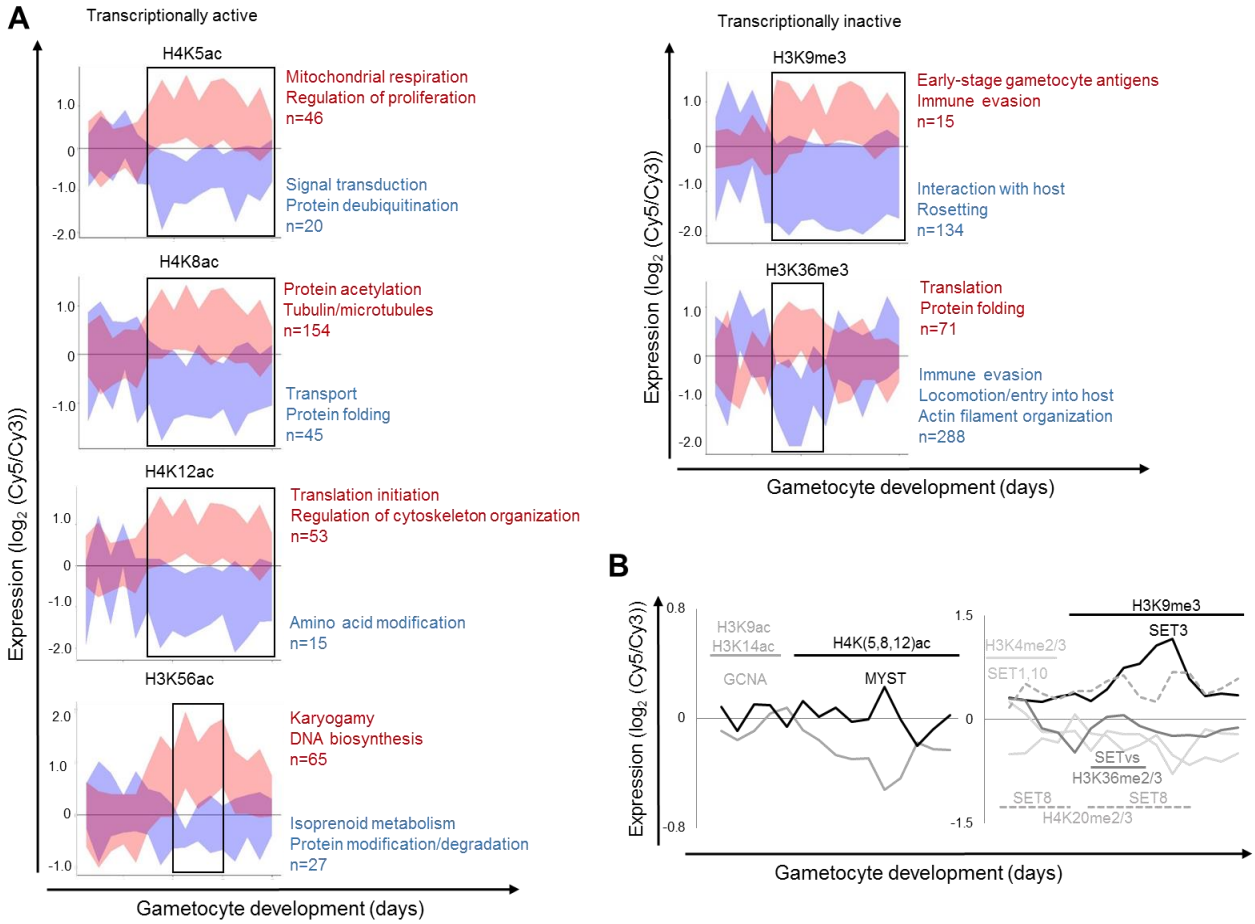

Figure 3.6: The epigenetic landscape of gametocytes contributes towards timed gene expression. **(A)** Epigenetic histone post-translational marks that were shown to be quantitatively biased towards gametocyte development (216) and associated with transcription (207,211,214) were cross-referenced with the expression of their associated genes. For each mark, associated genes were probed for transcriptional profiles corresponding to the increased presence of the mark in gametocyte development (indicated by blocks) with decreased transcripts shown as blue shaded ribbons and increased transcripts shown as red shaded ribbons. **(B)** The expression of histone modifying enzymes responsible for the deposition of specific marks are shown with the corresponding peaks of the marks indicated with straight lines.

The epigenetic landscape of gametocytes changes substantially from asexual parasites, with preferential acetylation of H4 (with the exception of H4K16ac) in gametocytes, but high levels of H3K9 and H3K14 acetylation acting as global activation marks during asexual development (213,216). In our data, a subset of genes usually associated with H4K5/8/12ac (207) showed increased transcript abundance during gametocyte development (Figure 3.6A). As was seen in asexual parasites, H4K8ac most affected transcript levels (310), with 154 transcripts increased in abundance during gametocyte differentiation while a smaller subset (45 transcripts) were anticorrelated to the mark's presence. The transcripts correlated to the H4ac marks were functionally related to gametocyte mitochondrial metabolism (ATP synthesis coupled electron transport, GO:0042773, *P*=0.025) and morphological differentiation (microtubule-based movement, GO:0007018, *P*=0.037). The decreased presence of H3K9 and H3K14 acetylation in

gametocytes also corresponds to decreased transcript abundance of GCN5 acetyl transferase (212) *(pf3d7_0823300)* during gametocyte development (Figure 3.6B). By contrast, MYST acetyl transferase *(pf3d7_1118600)*, which is primarily responsible for H4 acetylation (149,311) was expressed at higher quantities, peaking in stage III-IV of gametocyte development (0.29 $\log_2$(Cy5/Cy3)), corresponding to the lowest transcript abundance of GCN5 (-0.57 $\log_2$(Cy5/Cy3)).

In addition, the H3K56ac mark previously associated with trophozoite development (207), also peaks in abundance in stage III gametocytes (216). Interestingly, the genes typically regulated by this mark in yeast are involved in nucleosome packaging for DNA replication (312) and the mark is hypothesized to be acquired close to DNA replication during asexual *P. falciparum* development (211). The genes that correlate to the presence of this mark are then functionally related to DNA replication (DNA biosynthetic process, GO:0071897, *P*=0.028) and karyogamy (GO:0000741, *P*=0.019), which is significant as transcripts abundant during intermediate development are associated with stored gamete and sexual development transcripts (134).

As observed in Coetzee *et al.* (216), the lack of the activating marks H3K9ac and H3K14ac is concurrent with an increase in the silencing marks H3K9me3, and H3K36me2/3. The deposition of acetylation and methylation marks on specific histone residues are typically antagonistic, resulting in anticorrelated expression (r^2=-0.55) of SET3 (H3K9 methylation) with GCN5 (H3K9ac) and the corresponding abundance *vs*. absence of these marks during gametocyte development. SET3 is predicted to be translationally repressed, (134) but has been detected in stage II and V gametocytes (313). The remaining SET methyl transferases with known targets were also well correlated with the deposition of their marks throughout development (Figure 3.6B) with the exception of SET7, which is translationally repressed in gametocytes (134).

The H3K36me3 and H3K9me3 marks are specifically associated with virulence gene silencing in asexual parasites (214,215) and decreased transcripts associated with these marks included exported proteins as well as most *rifins* and *stevors*. Among the 15 transcripts that increase in abundance despite the presence of H3K9me3 were 5 *rifins (pf3d7_0101900, pf3d7_0115200, pf3d7_0324400, pf3d7_0400700, pf3d7_1479700)* and a PfEMP1 (*var* gene *(pf3d7_0712900)*. This would further support previous hypotheses that rifins could mediate gametocyte sequestration during the immature

stages (224,314). H3K36me3, however, is abundant during the intermediate sequestering stages of gametocytes and correlated with decreased abundance of the Ser repeat antigens (*sera*) 3,5,6,7 *(pf3d7_0207800, pf3d7_0207600, pf3d7_0207500, pf3d7_0207400)* involved in regulation of the immune response (GO:0050776, *P*=0.00095), that increase in abundance when the mark is absent, in the circulating gametocyte stages. The dynamic expression of genes associated with these epigenetic marks suggests that, as in asexual parasites, these marks could modulate circulation and sequestration dynamics in gametocytes.

3.3.5 ApiAP2 transcription factors express at, and regulate genes distinct to, specific intervals during gametocytogenesis

ApiAP2 transcription factors play an essential role in the differentiation of numerous life cycle stages (53,219,220,223,291,315). As the only characterized transcription factor family in *P. falciparum,* the expression and regulatory capacity of the ApiAP2 transcription factor were investigated in detail (Figure 3.7).

Of the 27 genes investigated, 13 genes encoding ApiAP2 transcription factors were increased in transcript abundance during gametocyte development (Figure 3.7A). AP2-G was increased in abundance during the pre-gametocytic stage of development, while 5 transcription factors *(pf3d7_1408200, pf3d7_1222400, pf3d7_1317200, pf3d7_0934400, pf3d7_0611200)* were increased at a discrete interval between stage I and III of development. Of the other 7 transcription factors, AP2-O *(pf3d7_1143100)* was increased in abundance during stages III-V of development but is translationally repressed (176), and the 6 remaining transcription factors *(pf3d7_0516800, pf3d7_0404100, pf3d7_1350900, pf3d7_1449500, pf3d7_0802100, pf3d7_1429200)* were increased in abundance from stage I to V of development.

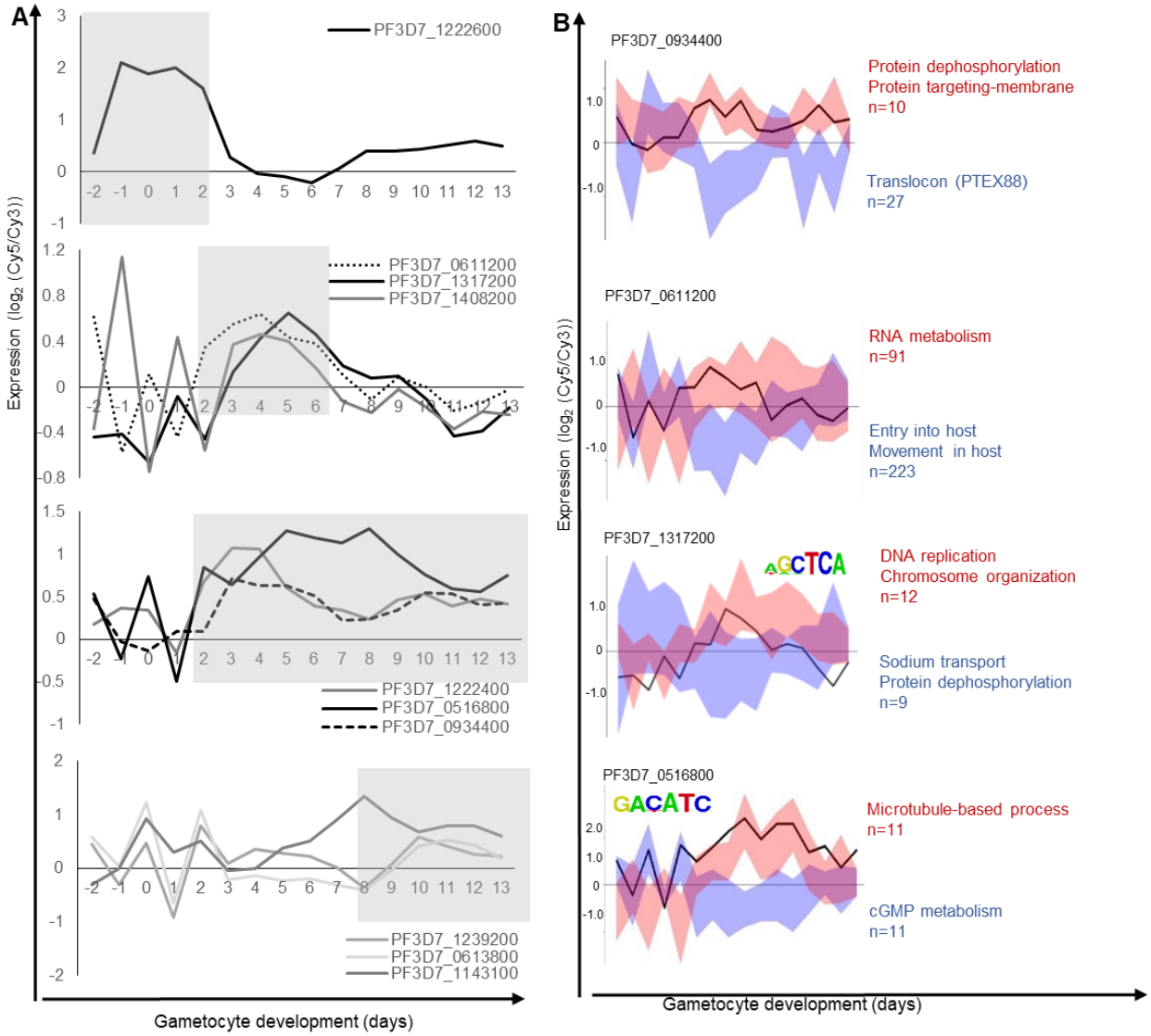

C

5' Motif	p-value	z-score	Enrichment
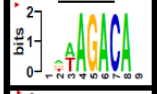	<1e-20	206.5	+ (n=539)
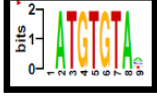	<1e-20	85.8	+ (n=577)

Figure 3.7: ApiAP2 transcription factors act as regulatory elements during gametocytogenesis. A) ApiAP2 transcription factors were evaluated for their expression **B)** regulatory activity throughout gametocyte development (black lines). For AP2-G (PF3D7_1222600) target genes were sourced from available functional data (53) while the rest of the transcription factors genes containing the TFBS indicated (142) or the total transcriptome were probed as target genes using GRENITS. The targets of each transcription factor are shown by shaded ribbons, with correlated transcripts indicated in red and anticorrelated transcripts indicated in blue. Generic functional terms describing enriched gene ontology terms are indicated for each transcription factor. **C)** The 2429 genes expressed during gametocytogenesis contained regulatory 5' motifs assessed by FIRE (316).

These 13 transcription factors were probed against the entire gametocyte transcriptome for regulation by coexpression using GRENITS (254). Of the 13 transcription factors, 4 *(pf3d7_1222600, pf3d7_0934400, pf3d7_0611200, pf3d7_0516800)* were determined to regulate >10 transcripts above probability of 0.7 and were used for subsequent analysis

(Figure 3.7B). *Pf3d7_1317200* was also included as its loss of activity has been shown to ablate gametocytogenesis (291). These 5 transcription factors were then subject to another round of coexpression analysis to determine their specific targets, with the exception of AP2-G, for which targets had been identified previously (53). The two transcription factors with known transcription factor binding sites (TFBS), *pf3d7_1317200* and *pf3d7_0516800* (142) were tested for regulation against genes containing their binding sites, while the other transcription factors, *pf3d7_0934400* and *pf3d7_0611200* were tested against the entire transcriptome. The number of probability links per threshold were used to guide a threshold cut off for each transcription factor's target genes (Appendix file 8).

The targets of AP2-G (53), peaked in transcript abundance directly following AP2-G peak abundance, coinciding with stage I of gametocyte development. Directly following AP2-G peak transcript abundance, *pf3d7_0611200* and *pf3d7_0934400* peak in abundance between day 3 and 6 (stage I-III) of development. These transcription factors each regulated 314 and 37 genes with a probability above 0.6 respectively. Of the 314 putative target genes of *pf3d7_0611200*, 223 were decreased in abundance following the peak abundance of *pf3d7_0611200*. The same transcripts increased in abundance following the decrease of abundance of the transcription factor (stage IV-V of development). These target transcripts included 12 rhoptry or merozoite surface proteins as well as a *var* gene *(pf3d7_0701000)* and were enriched for genes involved in host invasion (GO:0044409: entry into host, P=2.97e^{-12}). The 19 genes that were increased in abundance during the peak of the transcription factor were enriched for RNA metabolism (GO:0016070: RNA metabolic process, P=9.89e^{-7}).

The putative target genes of *pf3d7_0934400* were also biased towards transcripts that decrease in abundance, with 10/37 transcripts increased in abundance during the increased abundance of the transcription factor. These genes were enriched for protein targeting to the membrane (GO:0006612, P=0.036) and protein dephosphorylation (GO:0006470, P=0.0049). The 27 transcripts that were decreased in abundance are involved in protein translocation (GO:0044053, P=0.036) presumably through the translocon as PTEX88 (*pf3d7_1105600*) was among the targets.

As gametocytes develop into stage II-III, *pf3d7_1317200*, an ApiAP2 family member also previously associated with gametocyte developmental regulation (24), peaks in transcript

abundance. From coexpression analysis of genes containing the TFBS of *pf3d7_1317200*, 21 genes were putatively regulated by *pf3d7_1317200* during gametocyte development. The targets that were increased in abundance during *pf3d7_1317200* peak abundance (12/21) were enriched for genes involved in cell cycle processes, including DNA replication (GO:0044786, *P*=0.0061), chromosome organization (GO:0051276 *P*=0.0046) and histone methylation (GO:0034968, *P*=0.015). These 12 genes included *orc5 (pf3d7_0215800)*, which binds to the origin of DNA replication, a structural maintenance of chromosome protein *(pf3d7_1130700)* and a WD-repeat protein *(pf3d7_1347000)* that is involved in histone methylation. The decreased genes mostly lacked functional annotation, with the exception of a sodium/hydrogen antiporter *(pf3d7_1303500)*.

The last ApiAP2 transcription factor, *pf3d7_0516800*, is increased in abundance throughout development but peaks at stage IV (day 8-9) of development and was predicted to regulate 22 target genes that contained its TFBS (probability>0.6) (Figure 3.7B). Of these targets, 11 were increased during the peak abundance of the transcription factor, involved in microtubule based movement (GO:0007018, *P*=0.021) and 11 were decreased and enriched for cGMP biosynthesis (GO:0006182, *P*=0.0038). Taken together, this data supports the involvement of successive expression of ApiAP2 transcription factors in a regulatory cascade during gametocyte development, as has been proposed for *P. berghei* gametocytes (222).

The expressed ApiAP2 transcription factors far from explain the complement of 2429 genes that showed increased abundance during gametocyte development. In order to identify additional *cis*-regulatory elements specific to genes involved in gametocytogenesis, the 2429 genes were probed for enriched 5’ and 3’ regulatory motifs (Figure 3.7C). Two highly conserved motifs were overrepresented, 5’AGACA and 5’ATGTGTA but were not matched to any known *trans*-acting factors (139,155). Interestingly, the first motif, 5’AGACA, found in 539 of the genes, was also enriched in genes preferentially transcribed in parasites committed to sexual development (141,317). The second enriched motif, 5’ATGTGTA has been correlated to genes involved in DNA replication (316). The absence of associated trans-acting transcriptional regulators for these motifs prompts further investigation into their functional regulation.

3.4 DISCUSSION

This chapter reports a high-resolution, complete transcriptome of malaria parasites during sexual commitment and development. The transcriptome can prove a valuable resource for the interrogation of the function of gene products and possible mechanisms of regulation important for gametocytogenesis in *P. falciparum.* We show that gametocytogenesis in *P. falciparum* is a well-controlled process involving hierarchical activation of regulatory processes that mediate development during stage-transition, ultimately resulting in a parasite poised for transmission.

The data afford a detailed interrogation of the transcriptome of gametocytes during every day of their development. The results of the bifurcation towards continuation of asexual development or induction of gametocytogenesis, which is difficult to trace morphologically (59), was observed at the onset of gametocyte development between days 2 and 3 (stage I-III gametocytes). The transcriptional divergence between gametocytes and asexual parasites is further evident in the presence of a cluster of 589 genes exclusively enriched in gametocytogenesis, including 24 genes that have not previously been identified as gametocyte markers. Early-stage gametocytes can therefore not simply be described as 'similar' to trophozoite stage asexual parasites (43,49,293); rather the transcripts increased from commitment to gametocytogenesis start a cascade of closely timed transcription with ~45% of the total transcriptome increased in transcript abundance during gametocyte development.

Stage-specific gene expression is a well-studied hallmark of malaria parasites, the so-called 'just-in-time' expression of genes when needed in specific asexual developmental stages (43,128). The high-resolution gametocyte transcriptome indicates that although the majority of the transcriptome is in hiatus and not associated with such stage-specific expression, a significant gametocyte-specific profile is associated with distinct phases of transcription during gametocyte development. These observations emphasize that stage-specific gene expression is an essential mechanism of regulation of gene expression in *Plasmodium* spp. and particularly true for the extended and morphologically diverse gametocyte development of *P. falciparum* parasites. These patterns also show association with sex-specific transcription, begging the question what the significance is of this apparent delay between male-specific and female-specific genes being transcribed. This timed transcriptional program also highlights the need of annotation of genes implicated in sexual development. Of particular interest for further functional

characterization are the two conserved unknown proteins that are possible regulators of gene expression, PF3D7_1143500, implicated in regulation of chromatin condensation and PF3D7_0603600 as possible transcription factor.

The stage V gametocyte is shown to be remarkably different from the preceding stage IV gametocyte, decreasing the expression of transcripts associated with all enriched processes apart from those geared towards transmission. It is thus questionable whether analyzing gametocytocidal compounds against a mixed stage IV and V population is valid when, on a molecular level, these stages are clearly differentiated from each other. The mature gametocytes also lose their susceptibility to most schizonticides (318), but seem to share increased abundance of Ca^{2+} and cAMP signaling machinery with asexual development or commitment (319). This leads us to hypothesize that the signaling machinery encoded at these developmental crossroads form the lynchpin underlying the parasite's extraordinary ability to switch between its diverse life cycle stages, as per their involvement in transitioning other key points in the life cycle (70,127,320).

We identified several possible regulatory molecules with potential involvement in governing the timed transcriptional program of gametocytogenesis. The parasite expresses genes to control the transcriptional landscape of gametocytogenesis, epigenetic modifiers, particularly highly expressed methylators (SETs), specific ApiAP2 transcription factors and genes involved in mRNA decay. These molecules contribute to expressing genes needed for the parasite's differentiation and the decreasing expression of genes needed for cellular division– possibly keeping the parasite in its non-replicating state. The role of H3K36me3 in maintaining transcriptional silencing of genes during the sequestered stages is intriguing, as well as the apparent role of transcript stabilization during circulating parasite stages. The genes under the control of these molecular mechanisms could be of interest in understanding sequestration and circulation dynamics in gametocytogenesis.

We also add to data on the transcriptional regulation in *P. falciparum* by the ApiAP2 transcription factor family downstream of AP2-G, affirming the presence of a hierarchical transcription factor cascade enabling passage through gametocytogenesis as postulated for *P. berghei* (222). We also contribute additional molecular candidates for involvement in this cascade adding to previous work suggesting additional ApiAP2s regulate gametocytogenesis (291). However, the presence of conserved 5' regulatory motifs in

~34% of gametocyte genes without an associated modulator, reaffirms the need for probing into additional molecular regulators.

The complete high-resolution transcriptome profile of *P. falciparum* gametocytes offers a complete molecular landscape of parasite differentiation. We identify putative epigenetic and ApiAP2 transcription factors as hierarchically expressed regulators facilitating a timed transcriptional program that prepares the parasite for transmission. The profile provides molecular identity to differences and similarities in asexual and sexual development that can be exploitable for pharmaceutical intervention. Finally, the stage-specific events that complicate transmission-blocking drug discovery are highlighted, 1) the changing functional enrichment of developing gametocytes, 2) the metabolic and transcriptional quiescence of mature gametocytes, 3) the presence of gene products that are non-essential for gametocyte development and are only stored for use during gametogenesis and 4) the sex-specific transcription and translation of a large proportion of genes involved in gametocytogenesis.

In the following chapter, we attempt to evaluate the functional outcomes of the different gene expression profiles associated with asexual proliferation and sexual differentiation, as measured on the phenotypic level using a novel platform that enables real-time metabolic profiling.

Chapter 4

The phenotypic consequences of proliferation/differentiation decisions of the malaria parasite

4.1 INTRODUCTION

P. falciparum parasites undergo extensive transcriptional remodeling between their intraerythrocytic life cycle stages, leading to substantial divergence in energy metabolism between the asexual and sexual stages. The most striking difference in metabolism is a pronounced reliance on anaerobic glycolysis (75,76) in asexual stages versus an increased dependence on the TCA in sexual stages (37,50,75,76). This metabolic adaptation is postulated to be either a result of the different biological environments these parasites inhabit (37,76) or a survival strategy to accommodate the different energy requirements of the transmissible vs pathogenic stages of development (50,75,76,288,321).

Early asexual developmental stages are comparatively metabolically inactive, preventing detection of the parasite by the host immune system while the parasite circulates within the erythrocyte in the bloodstream (32). Energy requirement is substantially increased during the mature asexual stages (from ~15 hpi onwards) and infected erythrocytes are sequestered in the nutrient-rich microvasculature to prevent their clearance by the spleen (322). Despite the presence of oxygen in the circulation and microvasculature, asexual parasites rely heavily on anaerobic fermentative glycolysis for energy (34,323) and the pentose phosphate pathway for maintaining redox status (324,325). The rapid metabolism in these stages of parasite development thus produces mass amounts of lactic acid that gets exported from the cell (34). This dependence on anaerobic fermentative glycolysis is also seen in rapidly proliferating *S. cerevisiae,* wherein the yeast cells forego mitochondrial oxidation for the rapid energy production needed for the biomass expansion necessary to complete asexual replication (75).

The parasites that are committed to gametocytogenesis, in contrast, sequester in the host bone marrow where they experience reduced vascular flow, preventing effective clearance of excessive cellular waste produced during rapid glycolysis (326). These parasite remain in this environment throughout the immature stages (stage I-IV) of

gametocyte development (61,62). In these stages, the glycolytic end-products shift from lactic acid to acetate that preferentially enters the energy-efficient TCA cycle, presumably to accumulate energy for development in the mosquito and to accommodate the lengthy (~14 day) gametocyte maturation process (37,50). The early gametocyte stages also digest host hemoglobin similar to asexual parasites (50), but late gametocyte stages (IV-V) do not, resulting in disparate activity of drugs targeting parasite heme metabolism between late-stage gametocytes and asexual parasites (327,328). During the transition to stage V gametocytes, the gametocytes become more metabolically latent and re-enter the circulation as mature gametocytes (64). The late gametocyte stages also have increased metabolism of fatty acids compared to the asexual stages, typical of more quiescent organisms (50,262).

Previous metabolic studies have elucidated some preferred pathways and substrates for energy metabolism during proliferation as opposed to differentiation, but there are some limitations inherent in the techniques used. Isotope incorporation studies (37,329), while assaying the activity of a pathway in real time, are only useful to evaluate a single enzyme or pathway per experiment, requiring prior knowledge of the pathways existing in the organism. This is problematic for *P. falciparum* parasites, in which many metabolic enzymes are still unannotated (330). Conversely, cellular metabolomic analyses (35,50), whilst providing quantitative data on most metabolites, provide a static picture of the result of all possible metabolic pathways in a cell at a given time point. This makes it difficult to discern intermediate metabolites from endpoint metabolites and substrates (50) and extricate transport processes from metabolism (332). Phenomics systems described sets of biochemical and physical traits in an organism. Here, the term is used for metabolic analyses aiming to evaluate all carbon and nitrogen substrates that can be metabolized by live eukaryotic cells simultaneously over time, producing kinetic measurements of metabolism.

Here, phenomics evaluation was performed, in real-time, to highlight the phenotypic consequences of the transcriptional regulation observed in parasites during asexual and sexual development. Simultaneous quantitative and qualitative metabolic evaluation of a range of carbon and nitrogen substrates allowed an understanding of specific metabolic profiles associated with the rapidly metabolizing and dividing mature asexual parasites, the slowly differentiating immature gametocytes and circulating, metabolically latent mature gametocytes.

4.2 METHODS

4.2.1 Cell culture and preparation

For evaluation of asexual parasite metabolism, intraerythrocytic *P. falciparum* NF54 parasites (NF54-*pfs16*-GFP-Luc (295)) were cultured in human erythrocytes from a single donor (blood group O^+) and maintained as described in chapter 2, section 2.2.1. Asexual parasite populations used for phenotypic evaluations corresponded to 30-36 hpi trophozoite-schizont infected erythrocytes (referred to as trophozoites). Gametocytogenesis was induced as described in chapter 3, section 3.2.1 (243). These cultures were maintained until harvesting on day 5 for early-stage (I-III, referred to as EG), and day 10 for late-stage (IV-V, LG) gametocyte analysis. All cultures were monitored with Giemsa-stained thin smear microscopy.

P. falciparum infected erythrocytes (trophozoites, EG, LG) were enriched from uninfected erythrocytes to >90% parasitemia/gametocytemia using magnetic separation (333,334). CS columns (Miltenyi Biotec, Germany) were used with a VarioMACS separator to purify infected erythrocytes (334) and EG/LG were isolated using LS columns mounted on a MidiMACS separator (110). The different parasite populations were washed 3x with 1X PBS (37°C) and resuspended in inoculation fluid medium 2 (IFM2, a proprietary RPMI-based medium lacking carbon and nitrogen substrates, Biolog Inc., USA) supplemented with 24 µg/ml gentamicin ($IFM2_g$). Cells were enumerated on a Nieubauer-improved Bright Line hemocytometer (Weber, England) before adjusting the cell number to final concentrations as stated below.

4.2.2 Optimization of Biolog Phenotype Microarray™ assay conditions

The Biolog Phenotype Microarray™ system was used to evaluate carbon and nitrogen substrate use. Firstly, the cell number per well and the appropriate redox dye mix (MA or MB, proprietary composition, Biolog Inc., USA) for each parasite population were optimized by determining the best signal-to-background (S/B) and signal-to-noise (S/N) ratios (335). While both redox dye mixes contain a tetrazolium based dye that is reduced to soluble purple formazan by NADH produced in actively metabolizing cells, the specific electron transfer reagent that transfers electrons from intracellular NADH to the extracellular tetrazolium differs between the two dyes (335). All parasite populations (trophozoites, EG, LG) were suspended in triplicate in $IFM2_g$ alone, to observe background levels of formazan production or $IFM2_g$ supplemented with 11 mM glucose ($IFM2_{g/gluc}$) as positive control for NADH production. The latter contained the same

concentration of glucose typically used to supplement RPMI-1640 for routine intraerythrocytic *P. falciparum* culturing *in vitro.*

Optimal cell number was determined with serial dilution from 160000 cells per well to 5000 cells per well in $IFM2_{g/gluc}$. To ensure that any remaining intracellular energy sources were depleted prior to measuring the energy production from external substrates, all parasites were incubated for 1 h at 37°C before adding the redox dye mix (1:5 v/v dye to cell suspension). The kinetic production of formazan was measured every 15 min under hypoxic conditions produced by the candle-jar method (241), in sealed plates (Greiner multiwell plate sealers, Sigma Aldrich, USA) in the Omnilog™ PM system (Biolog Inc., USA). Formazan production results in a purple color change, which is quantified using the Biolog PMM Kinetic Analysis Software v1.0 by converting pixel color intensity to a kinetic parameter termed “average height of color development” by the proprietor (here referred to as Omnilog values).

To determine the length of time the trophozoites can survive the assay conditions, an independent assessment of metabolic activity and viability was performed by using the parasite lactate dehydrogenase (pLDH) assay (336). The enriched trophozoites were seeded at 40000 cells/well in 50 µl $IFM2_g$, $IFM2_{g/gluc}$ or culture medium (RPMI-1640 supplemented as described in chapter 2, section 2.2.1) and kept at 37°C under hypoxic conditions. Samples were removed after 0, 3, 6, 9, 12 and 24 h of incubation and stored at -20˚C. Following the experiment, 100 µl Malstat reagent (0.21% v/v Triton-100, 222 mM L-(+)-lactic acid; 54.5 mM Tris; 0.166 mM 3-acetylpyridine adenine dinucleotide (APAD; Sigma-Aldrich, USA); adjusted to pH 9 with 1 M NaOH) and 25 µl PES/NBT (1.96 mM nitro blue tetrazoliumchloride (NBT); 0.239 mM phenazine ethosulphate (PES)) were added to each parasite sample, incubated for 30 min at 22˚C and color development was measured at 600 nm using the absorbance module of a GloMax®-Multi Detection System (Promega, USA).

4.2.3 Phenotype microarray analysis

The Biolog Phenotype Microarray™ system was used to simultaneously measure carbon and nitrogen substrate use by intraerythrocytic *P. falciparum* parasite stages in $IFM2_g$ and using redox dye MA. Cells (trophozoites, 10000 cells/well; or EG, LG, 40000 cells/well) in $IFM2_g$ were seeded into Biolog Inc. Phenotype Microarray™ PMM1-4 96-well plates (full list of substrates in Appendix file 9) and incubated for 1 h at 37°C to ensure depletion

of intracellular substrates (337). Following incubation, the redox dye MA was added (1:5 v/v dye to cell suspension) and the plates sealed under hypoxic conditions. Real-time color development was measured every 15 min over 12 h at 37°C in the Omnilog™ PM system described as above.

4.2.4 Data analysis

Initial data analysis was performed using the Biolog Omnilog PM Kinetic software™ (beta version) to extract the average height of color development parameter (Omnilog values). In all experiments, results from wells containing D-palatinose, D-turanose, D-tagatose and L-sorbose were excluded as these are reducing sugars that were consistently associated with abiotic color development (337). Prior to further analysis, an average of the Omnilog values in the negative control wells (A01-A03), containing no metabolic substrates, were subtracted from every other well in a specific plate. Each individual plate corresponding to PMM1-4 plates were normalized between biological repeats as described in Vehkala *et al.* (338) in the OPM R-package (339). The source code and available script (338) were modified for use with 1) updated versions of R (3.3.2 and onwards), 2) use with mammalian PMM plates and 3) further analysis of normalized data. These analyses included calculating statistical growth parameters, including slope (rate), area under curve (AUC), lag in signal production and maximum signal by using available functions in the Grofit package in R (340). All other data analysis, visualization and manipulation were performed in Microsoft Office excel 2016 or using the ggplot2 package in R.

4.3 RESULTS

4.3.1 Suitability of the Biolog Phenotype microarray system for use with intraerythrocytic *P. falciparum* parasites

The Omnilog™ PM system uses a specialized incubator with attached camera that converts the formazan color intensity resulting from the presence of NADH, detected in real-time, to a kinetic parameter in the Biolog PM software reported as Omnilog values. This system consists of 96-well plates pre-loaded with carbon energy sources (plate PMM1) and nitrogen substrates, including single amino acids and di-peptides (PMM2-4), that, if metabolized, result in a quantifiable color production through tetrazolium reduction to formazan. The kinetic measurements of color production from live cells in a minimal medium ($IFM2_g$) are used to evaluate the ability of these cells to produce energy from multiple different substrates. To assess if the rapid metabolism of trophozoites can be accommodated in the minimal media used for the phenotypic measurements ($IFM2_g$), a pLDH assay was first performed on these parasites to evaluate metabolic activity under conditions mimicking those that would be available in the Biolog phenotype microarray experiment (Figure 4.1).

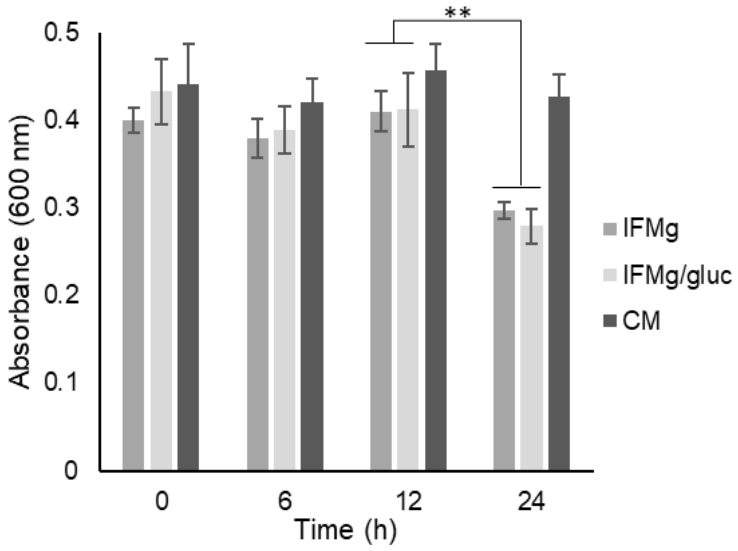

Figure 4.1: Comparative metabolic viability of *P. falciparum* trophozoites in minimal and supplemented media. Intraerythrocytic NF54-*pfs16*-GFP-Luc parasites were seeded at 40000 cells/well into $IFM2_g$, $IFM2_{g/gluc}$ or culture medium (CM) respectively before assaying the activity of parasite lactate dehydrogenase as a proxy for metabolic viability of the enriched trophozoites, data are from n=3 biological repeats in technical triplicate, ±SE. Significance was determined using a student's t-test (**=*P*<0.01).

Trophozoites were viable in $IFM2_g$ and $IFM2_{gluc}$ at comparable levels (*P*>0.05) to the metabolic activity determined with the pLDH assay in culture medium, for a period of at least 12 h (Figure 4.1). However, longer incubation periods (24 h) resulted in significant (n=3, *P*<0.01) 32.2% reduction in pLDH activity between the 12 and 24 h time points in the $IFM2_{g/gluc}$ medium, and similarly 27.5% decrease in $IFM2_g$ (Figure 4.1). This was not

observed for parasites evaluated in normal culture media. This indicated that parasites can be evaluated in the minimal media in the Biolog system, if the evaluation is done within 12 h.

The Biolog Phenotype Microarray™ system was subsequently applied to study carbon and nitrogen metabolism of trophozoites, early-stage gametocytes (EG) and late-stage gametocytes (LG) with each of these populations (Figure 4.2).

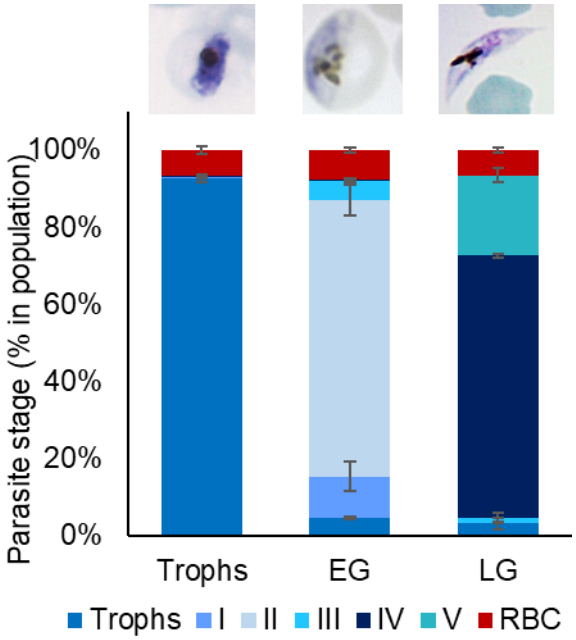

Figure 4.2: Evaluation of parasite populations included in intraerythrocytic *P. falciparum* parasite phenome analysis. The composition of *P. falciparum* NF54-*pfs16*-GFP-Luc parasite populations used in each phenotype microarray experiment were determined using Giemsa-stained microscopy, counting at least 100 parasitized RBC per sample with representative parasites shown above graph. The key shows uninfected erythrocytes (RBC), trophozoites (Trophs) and gametocyte stages I-V.

Enumeration of parasite populations showed that for all parasite populations counted, RBC made up <8% of the population (Figure 4.2). The core population of the trophozoite samples showed a 92.6±0.9% enrichment of trophozoite-stage parasites. The EG samples was enriched for stage I-III gametocytes at 87.4±0.5% with less than 5% (4.6±0.4%) asexual contamination. The LG samples contained 90.2±2.0% stage IV-V gametocytes with less than 5% contamination by asexual parasites or early-stage (III) gametocytes (3.2±1.4% and 1.6±1.1% respectively).

The Biolog Phenotype Microarray™ system was subsequently optimized for use with trophozoites, early-stage gametocytes and late-stage gametocytes (Figure 4.3). Optimization variables included the Biolog redox dye mixture (MA or MB) and cell number

to evaluate the highest S/B ratio between substrate replete $IFM2_{g/gluc}$ (positive control for NADH production) and substrate depleted $IFM2_g$ (negative control for NADH production).

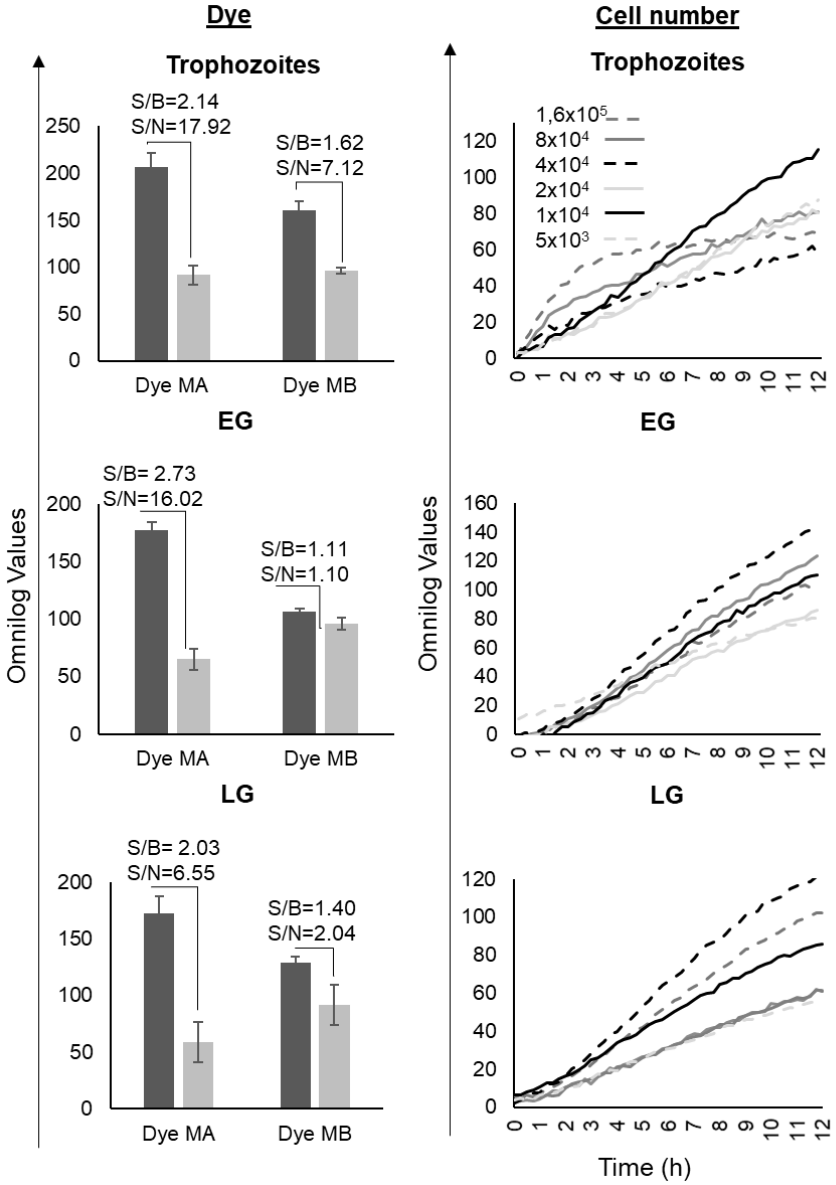

Figure 4.3: Optimization of the Biolog Phenotype Microarray system™ for use with trophozoites, early-stage and late-stage gametocytes. For each parasite population (Trophozoites, EG=early-stage gametocytes, LG=late-stage gametocytes) the available redox dyes MA and MB were tested according to the manufacturer's instructions at 37˚C using 20 000 cells/well for color production in $IFM2_{g/gluc}$ (signal, dark grey) and $IFM2_g$ (background, light grey). Optimization experiments were conducted n=1 in technical triplicate and are shown ±SD with S/B and S//N calculated after 12 h incubation for each condition. Cell numbers between 160000 and 5000 were tested for the best signal produced ($IFM2_{g/gluc}$ – $IFM2_g$) in dye MA for each parasite population and the highest color production used for further experiments.

While both dye MA and MB resulted in increased signal for $IFM2_{g/gluc}$ compared to $IFM2_g$, dye MA consistently produced greater S/B (2.03-2.73) and S/N (6.55-17.92) ratios at endpoint (12 h) than dye MB (S/B=1.11-1.62, S/N=1.10-7.12) in all parasite populations tested (20000 cells/well) and was therefore used for further experiments (Figure 4.3A). For rapidly metabolizing trophozoites, the highest signal of 148 Omnilog values was obtained at 10000 cells/well (Figure 4.3B), evident already at 6 h onwards. The highest

concentrations of cells, 160000 cells/well, resulted in Omnilog values plateauing around 3 h, despite a rapidly increased color development at the start of the experiment (0-3 h). For the gametocytes, the increase in color development was gradual for all cell numbers tested, but 40000 cells showed increased signal from 3-4 h onwards for both early- and late-stage gametocytes, with maximal endpoint values of 142 and 123, respectively. Consequently, the phenomics experiments were conducted using 40000 cells/well of early and late-stage gametocytes and 10 000 cells/well trophozoites.

4.3.2 Translating signal produced from the Biolog Phenotype microarray system to informative parameters describing the metabolism of intraerythrocytic *P. falciparum* parasites

The Biolog Phenotype Microarray™ system (337,341) colorimetrically measures formazan production every 15 min, enabling kinetic assessment of metabolism. This measurement allows determination of statistical curve parameters, with area under curve (AUC) used as a metric of total use of a substrate while slope, max and lag give an indication of rate, magnitude and delay before metabolism respectively (Figure 4.4).

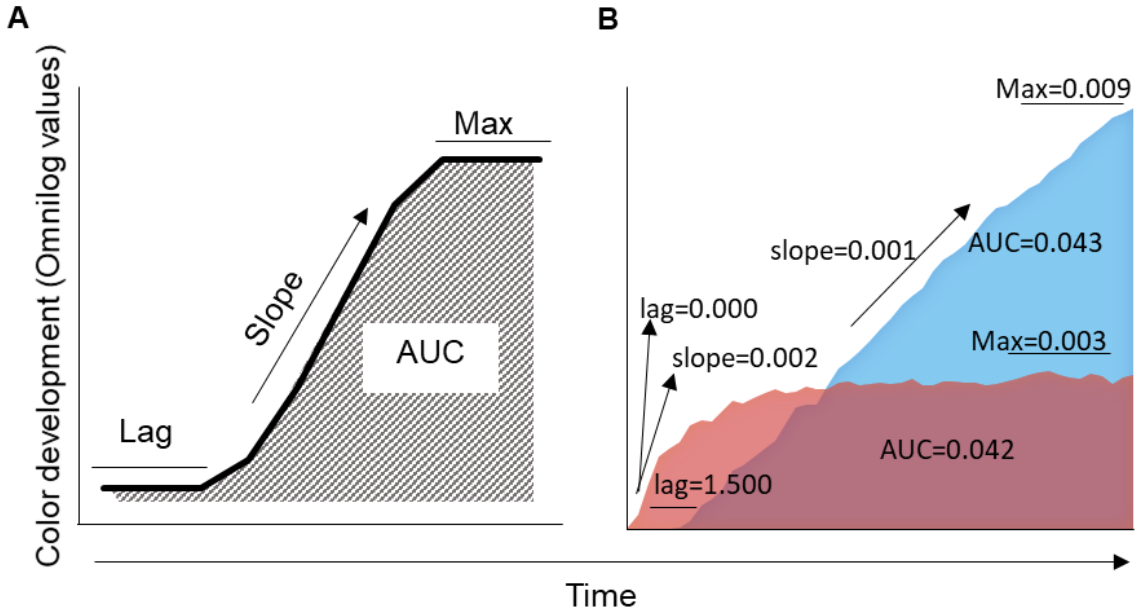

Figure 4.4: Principle of Biolog Phenotype Microarray™ system for use with *P. falciparum* infected human erythrocytes. (A) The degree of color development measured at 15 min intervals over 12 h using the Omnilog™ PM system is quantified as Omnilog values resulting in kinetic data that can be used to determine curve parameters such as lag, slope/rate, max and area under curve (AUC). **(B)** AUC values assess cumulative metabolism, but similar values can result from different slope, lag and max values as shown in curves for two substrates metabolized in trophozoites.

The Biolog Phenotype Microarray system was subsequently used to measure the global carbon and nitrogen metabolism of trophozoites, early-stage and late-stage gametocytes. Parasites were exposed to substrates on the Biolog Mammalian PPM1-4 plates, and only

wells that produced a signal of >0.0005 Omnilog values per cell in at least 2 biological repeats were included in analysis of the kinetic parameters of metabolism including AUC, slope, max and lag. While AUC gives an indication of total metabolism (Figure 4.4A), kinetic parameters like maximum color development (Max), rate (slope) and delay (lag) all contribute towards the cumulative profile of substrate use (Figure 4.4B), resulting in, for example, similar AUC values (0.042 and 0.043 Omnilog values*total h) for substrates with far different maximum color development (0.003 and 0.009 Omnilog values), slope (0.002 and 0.001 Omnilog values/h) and lag (0.000 and 1.500 h) values. These parameters were then used to describe metabolism of each substrate.

4.3.3 Assessing total parasite metabolism of carbon and nitrogen substrates using phenotypic microarrays

As an indication of total metabolism of each substrate in each parasite population, the AUC was first evaluated (Figure 4.5).

A striking difference in overall metabolism was observed between the different parasite populations (Figure 4.5A). Actively proliferating trophozoites were highly metabolically active as evident in AUC values of >0.02 Omnilog values*total h for 80% of the substrates tested, while the AUCs in early-stage and late-stage gametocytes were considerably lower. The overall metabolism was further decreased in late-stage gametocytes with an interquartile range (IQR) of 0.0043-0.0098 Omnilog values*total h compared to the early stages (IQR=0.0065-0.013 Omnilog values*total h). The number of substrates used by each parasite population also varied (Figure 4.5B), with trophozoites using the least number of substrates (10) and this consisting mostly of monosaccharides (4) and dipeptides (4). Comparatively, late-stage gametocytes used the highest number of substrates (16), mostly comprised of dipeptides (7). The trophozoites highly metabolize a few substrates, while late-stage gametocytes were diverse in their nutrient consumption but metabolize most substrates to a lesser extent, consistent with the different energy requirements during proliferation compared to differentiation.

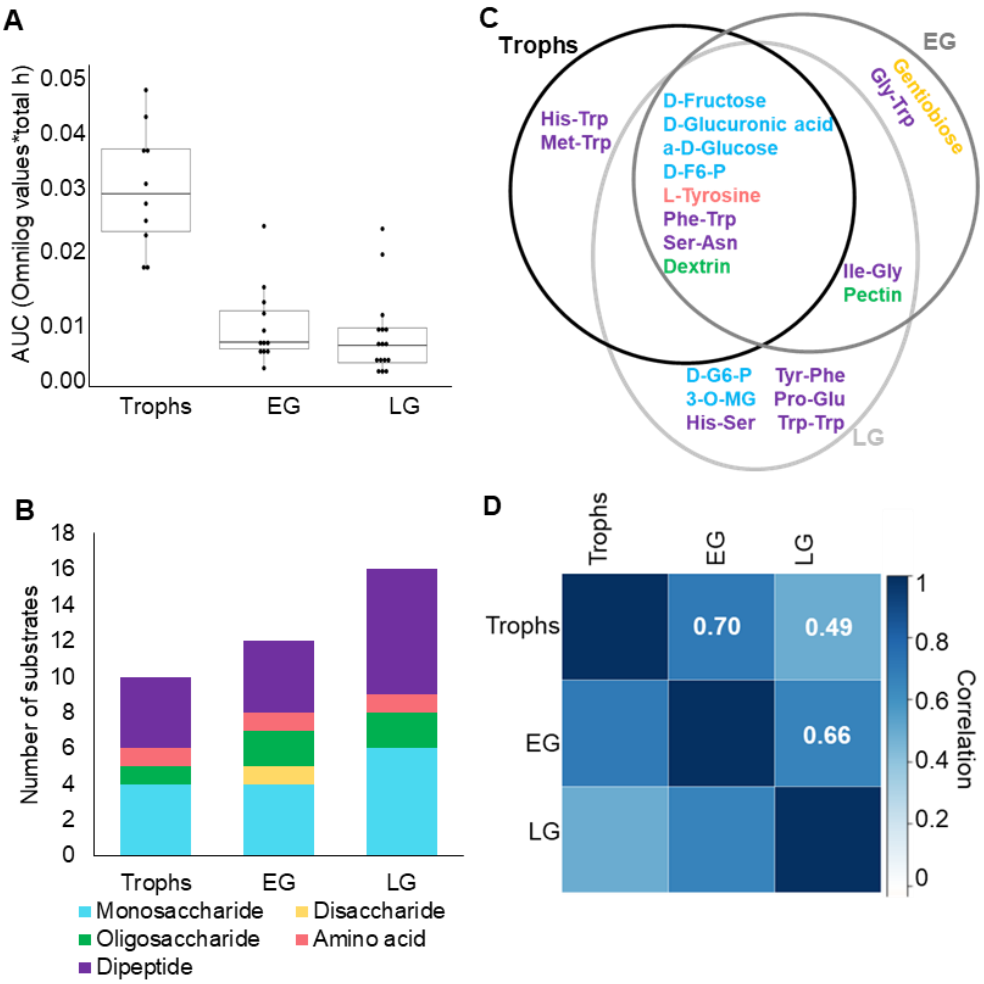

Figure 4.5: Total substrate use during intraerythrocytic *P. falciparum* parasite carbon and nitrogen metabolism for each parasite population. Parasite populations were incubated over 12 h at 37˚C in the Biolog Omnilog incubator, with colorimetric measurements taken every 15 min. **(A)** Distribution of AUC values for substrates metabolized by each parasite population, corrected for cell number used in each assay, shown per cell. **(B)** Number and type of substrates used by asexual and sexual stage parasites. **(C)** Substrates metabolized by each parasite population, colored according to type of substrate with key shown in B. **(D)** Pearson correlations of all curve parameters for substrates metabolized by trophozoites (trophs), EG and LG respectively with darker shades corresponding to stronger correlations.

In total, 20 unique substrates were metabolized by the different parasite populations (Figure 4.5C), with the metabolism of monosaccharides shared between all three parasite populations. This includes metabolism of D-fructose, D-fructose-6-phosphate (D-F6-P) and α-D-glucose (342) and D-glucuronic acid, that is metabolized to pentose phosphate pathway intermediates in mammalian cells (343) (Figure 4.5C). Few other carbon substrates were metabolized; the parasites metabolized dextrin, a short α-D-glucose polymer and both the early- and late-stage gametocytes metabolized pectin, a variable length and composition plant oligosaccharide (344). Only early-stage gametocytes were able to metabolize the disaccharide gentiobiose (β-1,6 linked D-glucose), while the late-stage gametocytes produced signal for glucose-6-phosphate and metabolically inert 3-O-methylglucose (345).

Of the nitrogen-containing substrates, Tyr produced a signal in all parasite populations, consistent with the reduction reported in proliferation if Tyr is excluded from asexual parasite medium (342) and consumption of Tyr from growth medium during gametocytogenesis (50). Arg or Lys did not produce a positive signal in any of the parasite populations. Interestingly, the iRBC is permeable to almost all amino acids and dipeptides (346) with the exception of Lys and Arg (342). In accordance, no dipeptides containing these amino acids were metabolized by any of the parasite populations. From the dipeptide substrates, all parasite populations metabolized Ser-Asn and Phe-Trp, while late-stage gametocytes and early-stage gametocytes shared metabolism of Ile-Gly, consistent with the ability of gametocytes to use Ile from culture medium (50). Increased levels of intracellular Asn has been previously associated with asexual parasite infections (331), but the metabolic pathways that Asn, Phe, Trp or Ser could participate in are unexplored. Trophozoites uniquely metabolized two Trp containing dipeptides, Met-Trp and His-Trp, consistent with an increase of Trp transport following infection (347) and a reduction in growth of parasites in medium lacking Met or His (342). The increased number of dipeptides metabolized in late-stage gametocytes, including 4 that were unique (His-Ser, Pro-Glu, Tyr-Phe, Trp-Trp), is not completely unexpected, as the predominant source of amino acids for the intraerythrocytic parasites, hemoglobin, is depleted by late-stage development (318).

The substantial differences in metabolized substrates described here confirmed the divergence in differentiating gametocyte and proliferating parasite metabolic requirements (Figure 4.5D). Early-stage gametocytes and trophozoites that share similar metabolic requirements (318) showed highly correlated total metabolic profiles (r^2=0.7). While the differences in the metabolic requirements between late gametocytes and trophozoites resulted in a reduced correlation between their metabolic profiles (r^2=0.49), early and late-stage gametocytes correlated well (r^2=0.66) confirming that the early-stage gametocytes were already differentiating from asexual metabolism and that the metabolic differences became more pronounced as the gametocytes matured.

4.3.4 Rate and magnitude of carbon and nitrogen substrate metabolism in *P. falciparum* parasites

Following the qualitative analysis of the global metabolic profiles (indicated by AUC) for carbon and nitrogen substrate metabolism for each parasite population, the remaining curve parameters (slope, maximum and lag) were analyzed for the maximum and kinetics

of substrate use to quantify the different metabolic profiles of the parasite populations (Figure 4.6 and Figure 4.7).

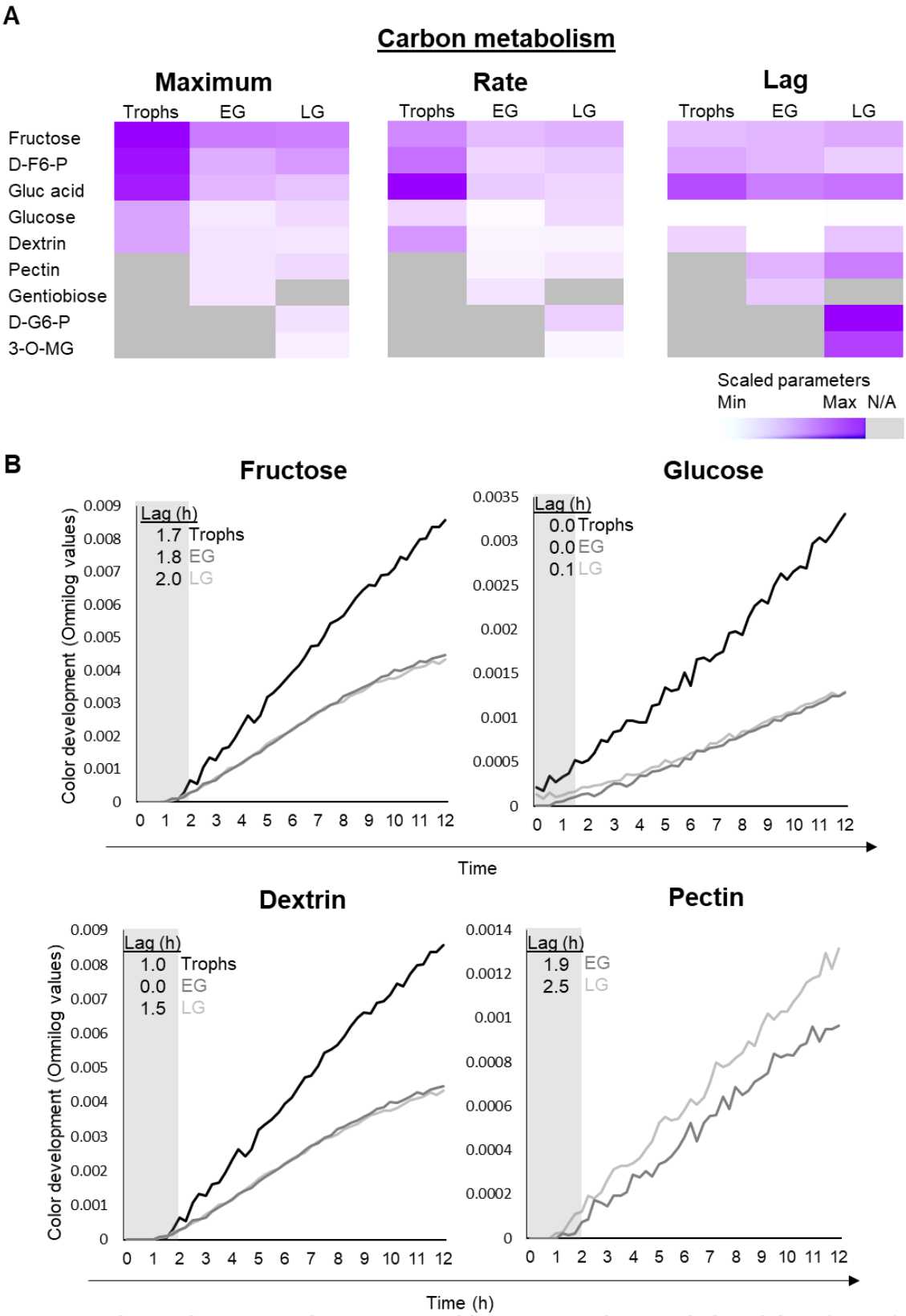

Figure 4.6: Carbon substrate maximum, rate and lag per parasite population. (A) Carbon substrates were evaluated in terms of their maximum color development, rate (slope) and delay before metabolism (lag). Heatmaps were scaled such that the highest value for each parameter is most colored, fading to the least colored for lowest values. Abbreviations: D-fructose-6-phosphate, D-F6-P; 3-O-methyl glucose, 3-O-MG; D-glucose-6-phosphate, D-G6-P; Gluc acid, D-glucuronic acid. **(B)** Substrate profile for select substrates metabolized in each parasite population colored per legend.

The parasites highly metabolized D-fructose, D-F6-P and D-glucuronic acid in particular (Figure 4.6A). Interestingly, there was a notable lag before these substrates began to generate positive signal, which might indicate the time required for transport of these metabolites, having to cross three membranes (32) to be metabolized. Of the 3 substrates, glucuronic acid showed the longest lag periods which could be due to delayed transport or multiple metabolic modifications that need to be made before energy is produced from this substrate.

Glucose was metabolized at much lower levels than fructose, albeit without any notable delay before metabolism (Figure 4.6B), a surprising result given that glucose is the major substrate for energy metabolism in the parasite (32,37), although the concentrations of the metabolites are unknown. As would be expected, the oligosaccharides (dextrin, pectin) that were metabolized were used slowly and at low levels (Figure 4.6B) with the exception of dextrin in early gametocytes that did not show a notable lag before color production. The late-stage gametocytes also produced signal for unusual glucose monosaccharides, D-glucose-6-phosphate (D-G6-P) and 3-O-methyl glucose (3-O-MG) after exceptionally long lag periods (>4 h) at low levels, suggesting that these signals may be a false positive result. The nitrogen substrates also revealed interesting dynamics of metabolism (Figure 4.7).

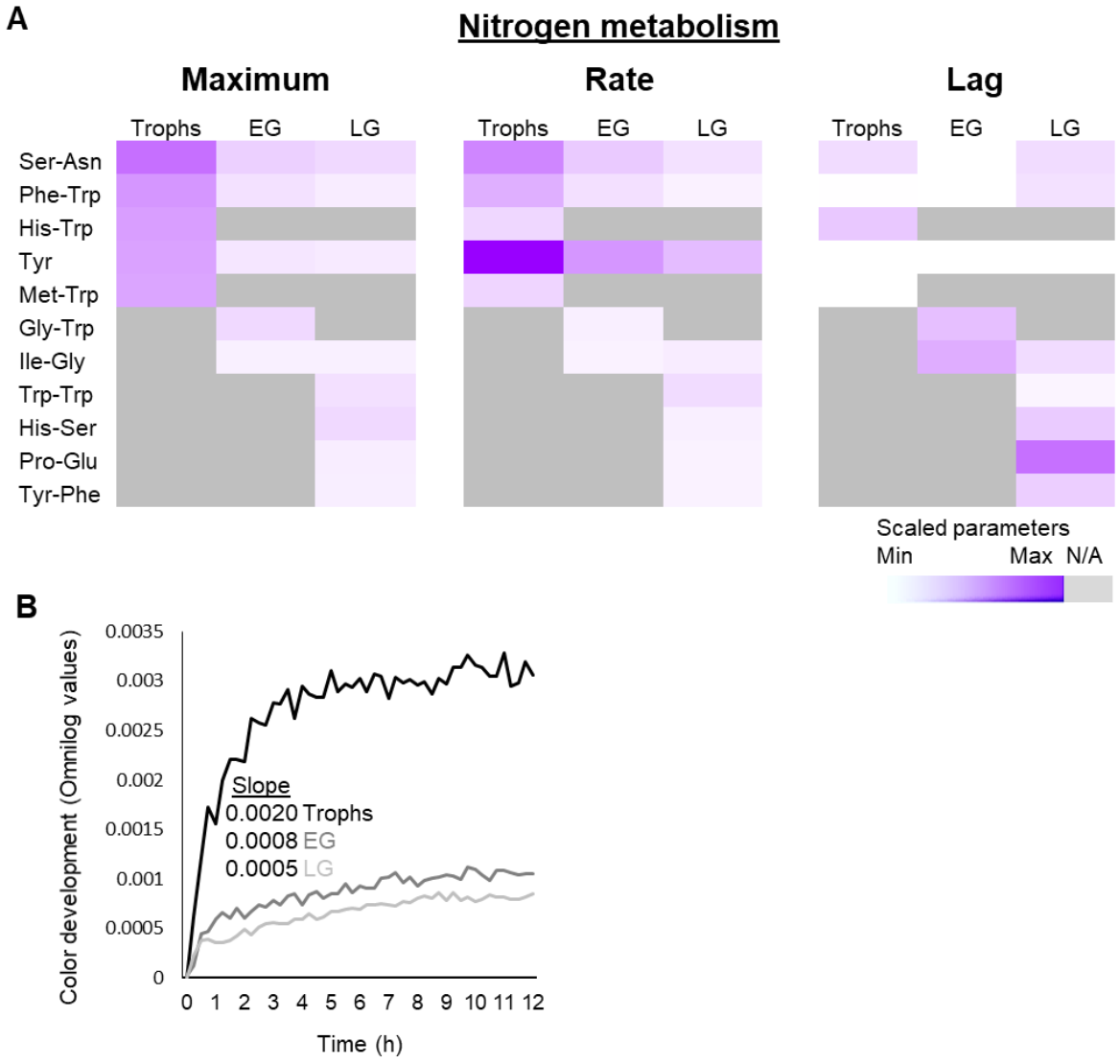

Figure 4.7: Nitrogen substrate maximum, rate and lag per parasite population. (A) Nitrogen substrates were evaluated in terms of their maximum color development, rate (slope) and delay before metabolism (lag). Heatmaps were scaled such that the highest value for each parameter is most colored, fading to the least colored for lowest values. **(B)** Substrate profile for Tyr metabolism in each parasite population colored per legend.

Of the nitrogen substrates, Tyr was metabolized most rapidly in all of the parasite populations (Figure 4.7A&B). Although both sexual and asexual stage parasites consume the amino acid from culture medium (50,342), the kinetics of this process is unknown and can potentially be investigated further. Interestingly, all substrates metabolized by late-stage gametocytes with the exception of Tyr and glucose were only metabolized after lag periods, consistent with decreased metabolism in these stages (37). It is also striking that although several substrates seemed to be metabolized at similar rates in early-stage and late-stage gametocytes, the maximum values remained low and delays were more pronounced in late-stage gametocytes, suggesting the low overall metabolism in late-stages is due to delays and low levels of metabolism, more than the rate of the reactions. The comparatively low levels of metabolism of dipeptides in all parasite populations also

confirms that they cannot replace monosaccharides as energy sources for the parasite but form supplemental nutrient requirements.

4.3 DISCUSSION

The phenome of intraerythrocytic *P. falciparum* parasites provides a global view of carbon and nitrogen metabolism during both the sexual and asexual stages of development and allows functional evaluation of the transcriptional control described in the previous chapters. This technique has both advantages and shortcomings compared to traditional metabolomics techniques, which if applied correctly, can contribute valuable information about parasite biology.

Metabolomics techniques allow the study of the structure of products produced by a specific chemical pathway, giving clues as to which pathways preferentially use a specific substrate (37). The caveat of phenomic evaluation would be the inability to identify the specific metabolic pathway which consumes a specific substrate; here for example, glucose is consumed in all parasite populations, but the preference for entry into the TCA or anaerobic glycolysis cannot be differentiated using this platform. The phenomics technique also relies on both effective transport and metabolism to produce a positive signal, but the two parameters cannot be extricated, rather the assay returns an end result of both processes. The advantage of using phenomics in this context is the simultaneous assay of multiple substrates without the need for extraction of specific metabolic end products (50,331) or assay of recombinant enzymes (348,349), but rather generating information *in situ* as observed in culture. These phenotype microarrays thus provide a usage metric for all assayed substrates, with the potential of identifying novel or interesting substrates that can then be studied individually regarding their transport, metabolic pathways and products of their metabolism.

The global phenomic profile of trophozoite-stage parasites and early gametocytes closely resembled one another consistent with their previous metabolic characterization (37,50). However, there was clearly some metabolic divergence evident from early sexual differentiation, consistent with the transcriptional patterns observed in chapter 3. This suggests that the Biolog Phenotype Microarray™ system could be useful in *P. falciparum* as a global typing tool, similar to its use in the identification of prokaryotic bacterial species (350).

An unexpected feature of the phenomic profile was the higher metabolism of fructose compared to glucose. This result could be due to suboptimal concentrations of glucose used in the commercially available Biolog Phenotype Microarray™ PMM1-4 plates. The

proprietary concentration of glucose used in the Biolog Phenotype Microarrays™ mostly preclude speculation on this basis, but the optimal glucose concentration used in the optimization experiments did result in substantially higher signal in the parasite populations than in any of the phenomic plate measurements. The parasite's decreased glucose metabolism could also be due to isoleucine starvation (85), as glucose supplementation alone is not sufficient to support growth of asexual intraerythrocytic parasites and a significant deviation between starved and Ile-fed samples is observed by 6 h post-starvation (85). The results of the parasite lactate dehydrogenase assay however, show comparative viability between supplemented culture medium and $IFM2_{g/gluc}$ for the 12 h assay measurement. This observation rather supports the hypothesis of glucose metabolism signal in this assay being concentration dependent with sub-optimal levels in the plates, consistent with glucose transport in the *P. falciparum* infected erythrocyte being mediated by equilibrative rather than active transport (345). However, an interesting observation is the high metabolism of fructose, which was previously shown as the only monosaccharide substrate to yield similar asexual parasite growth rates to glucose *in vitro* (351).

Within the phenomic profiles, the most distinguishing feature was the increase in dipeptide metabolism in late gametocytes stages. Although most amino acids are transported into asexual parasites, the parasite's metabolic requirements for amino acids are mostly met by heme metabolism, with only exogenous Ile needed to sustain intraerythrocytic development (352). In addition, the parasite lacks the gluconeogenic pathway (81) and in accordance, gluconeogenic substrates Gln and Ala were absent from any of the metabolized dipeptides. This is consistent with very few dipeptides metabolized in trophozoites and early-stage gametocytes, where the erythrocyte can still supply hemoglobin for degradation (33). The majority of dipeptides that were metabolized by the stage IV-V late gametocyte population used contained Ile, Phe, Tyr or Glu, that can all either enter the TCA cycle or generate redox potential by conversion to 2-oxoglutarate, reducing $NADP^+$ or NAD^+ (353), suggesting a possible mechanism for the metabolism of these peptides. The mature gametocyte stages are believed to be mostly metabolically latent (50), which could be a result of evolutionary adaptation to evade the immune system while circulating in the blood stream (59) until transmission. Here, we see that at the very least that slow, delayed levels of metabolic activity are observed in late-stage gametocytes compared to the other populations, with a diversification of amino acid metabolism unique to these stages. These possible mechanisms of amino acid

metabolism in the late-stage gametocyte resulting in energy metabolism or redox potential generation represent novel findings that should be investigated further.

An important aspect of late-stage gametocyte metabolism not observed using the phenomics platform was the increased consumption of lipid moieties observed previously (50) and discussed in chapter 3. This is potentially due to the specific lipid substrates the gametocyte typically consumes; it was shown that gametocytes do not preferentially consume carboxylic acid forms of lipids and rather take up neutral lipid moieties (50) that are not present on the PMM1-4 plates (all lipid moieties in the PMM1 plate are carboxylic forms, Appendix file 9). Alternatively, the lack of metabolism could be a result of lipid moieties not being used for energy metabolism and NADH production but rather stored to provide energy for gametogenesis in the mosquito (75,321), also supported by increased reliance on fatty acid synthesis (rather than degradation) in the sexual stages of development (354).

The phenomic characterization of asexual and sexual life cycle stages of the parasite highlight the metabolic adaptations of these parasites. The similar lifestyles of actively metabolizing early gametocytes and mature asexual stages, both sequestered away from circulation with access to glucose are reflected in the similarity of their phenomic profiles. The gametocyte stages, that preferentially make use of the more energy-efficient but slower TCA cycle for ATP production (37,75) needed a higher number of cells to generate signal comparable to the voracious trophozoites. The late stages of gametocytogenesis showed further metabolic adaptation to their hemoglobin-depleted environment, metabolizing more exogenous dipeptides than the other stages of development. Together, these results confirm the divergence in metabolic profile observed between life cycle stages of *P. falciparum* parasites (321), emphasizing their role in the parasite's ability to survive in different host environments as a direct consequence of the differential control of gene expression investigated in the preceding chapters.

Chapter 5
Concluding discussion

The *P. falciparum* parasitic infection in human erythrocytes consists of extremely heterogenous parasite populations in various stages of development. The asexually proliferating parasites are characterized by a tightly regulated transcriptome (128) that gets translated "just-in-time" to fulfil their biological functions (355). *P. falciparum* gametocytes undergo their lengthy development following the epigenetic activation of AP2-G (53–55), initiating a transcriptional cascade (129) that leaves the mature stage of these parasites metabolically less active (88), poised for activation and ready to transmit to a feeding mosquito. This previous understanding grossly oversimplifies the extraordinarily complex, orchestrated cascade of events resulting from a binary decision each schizont population undergoes: proliferate or differentiate?

Building a solid knowledge base of both the regulation and consequences of this decision enables progress in intelligent development of antimalarial compounds (87,288); understanding the effect of antimalarials on different stages of development and their disparate drug sensitivity profiles (88,318). This study set out to dissect the key role players enabling parasites to replicate their DNA, an essential step in proliferation, and complete gametocyte development to better understand how the parasite's molecular landscape is shaped and sculpted following bifurcation in the parasite's life cycle decision. In keeping with our hypothesis, the parasite was shown to possess unique regulatory mechanisms that enable it to completely alter its molecular make up in order to complete entirely different biological processes within erythrocytes.

During the IDC, the parasite's characteristic transcriptome is shaped by epigenetic regulation (207,213) and (presumably) activity of specific ApiAP2 transcription factors (142,151), with a degree of post-transcriptional control implied (141,293) by stabilizing factors like ALBA1 (170,356) and finally the activity of many of the parasite's proteins heavily reliant on post-translational modification (188,201,203,357). Despite these expansive control mechanisms, the cell cycle of the parasite was previously hypothesized to be poorly controlled and lacking in cell cycle checkpoints (46,97). Arguably, the unique

situation of asynchronous nuclear division within schizont populations, although fascinating, limits the ability to study the molecular regulation of the transition between the respective phases of the cell cycle. In order to accurately study these transitions, effective, absolute synchronization of the parasite population to a single point in the cell cycle would be key to observe the events surrounding this progression. Thus, rather than the cell cycle being poorly controlled, the tools to study the cell cycle in *P. falciparum* were not available.

In chapter 2, we deprived asexual parasites of polyamines as mitogenic substrates for macromolecular synthesis (268,270) very early in their development, preventing nuclear division in almost the total parasite population. Within this body of work, several lines of evidence suggest that the parasites do possess a boundary before DNA synthesis resembling a mammalian G_1/S checkpoint. The first line of evidence is the entry into a quiescent state of G_1/G_0 arrest associated with altered expression of signaling molecules (*pk2*) to prevent the entry of a proliferative state it would not be able to complete and/or stay poised for sensing signals to re-start proliferation. The reversible application of transcriptional control (*sap18*, *myb1*) (141), to alternatively keep the parasite in an arrested state or re-initiate the cell cycle also supports a cell cycle control point at the G_1/S boundary. Finally, the parasite progresses rapidly into S phase after the block in proliferation is lifted, bringing into focus a clear cascade of molecular events that preface nuclear division. The re-initiation of the cell cycle would seem to first require mobilization of signaling molecules and transcriptional regulators before functional regulators (CDKs i.e. PK5) of DNA replication machinery (104,358) to support the multiple nuclear divisions of the parasite. This finding significantly impacts cell cycle research in the parasite, with the seemingly uncontrolled nuclear division in the parasite only occurring following a controlled cellular decision, based on the presence of growth factors and/or mitogens in the extracellular environment. It would be very tempting to speculate that this point in development could also be where the parasite's developmental fate bifurcates, where the controlled decision to proliferate can also be translated into differentiation.

Thus far, major genetic regulators of gametocytogenesis have been identified for the process of commitment, Hda2, HP1 and AP2-G (53–55) as well as extracellular environments that increase likelihood of gametocyte induction (110). Following commitment, many of the events regulating the extended differentiation in *P. falciparum* were obscured. It has been postulated that AP2-G initiates a cascade of expression

allowing entry into gametocytogenesis (53) and that a second transcription factor, PF3D7_1317200, acts downstream as a regulator (291), but further in-depth analysis had been lacking.

We contribute a complete, high-resolution transcriptomics dataset of gametocytogenesis, adding greater detail to previous metabolic datasets (49) and providing temporal context to the expression of previously identified gametocyte markers (292,359,360). The data contribute candidates for probing sexual differentiation related genes that result in male and female development and show that the later stages (III-IV), express genes that are essential for gametogenesis. This observation has intriguing implications on researching sexual development. If the later stages of gametocytes are mostly concerned with storage of gamete transcripts and proteins, transcriptomic analyses alone would not necessarily provide a complete view of regulation or molecular profile in these stages, but implies that functional validation is needed for conclusions to be made about specific molecular requirements for sexual development. It is possible that targeting proteins expressed in late stages of gametocytogenesis would not necessarily result in killing of the gametocytes, but possibly prevent gametogenesis in the mosquito, still effectively preventing transmission.

However, the study did confirm the validity of targeting ion homeostasis and post-translational protein modification (88) in both asexual and late gametocyte stage populations, as Ca^{2+} and cAMP signaling kinases were expressed in both populations. Signaling events are key in the parasite's complex life cycle, with second messenger signaling transductors (primarily CDPKs) allowing transition to microgametogenesis, oocyst development and cytokinesis in the asexually replicating parasites (108). Certainly, the parasite would have to evolve in tight concert with its two hosts to survive, as defects at any of the key transition points could leave the parasite unable to adapt its intracellular composition to its new extracellular environments. This ties in to postulations about the reproductive fitness of intraerythrocytic parasites, where the extraneous signals like high parasitemia and increased waste products can modulate the drive to differentiate sexually, to propagate the species (75). Genetic modification also affects conversion rate (55), suggesting that genetic fitness for reproduction is also a key factor in commitment to gametocytogenesis (74). The ablation of the activity of key genes in commitment, for example AP2-G in the F12 gametocyte-less strain also emphasizes that environmental signaling alone is not sufficient in forcing the decision to differentiate. Rather,

environmental signaling could induce gametocytogenesis in reproductively fit genetic progeny, consistent with complete conversion of progeny from a single schizont.

An open question about both the proliferation and differentiation decisions are how exactly the signal transduction ties into the transcriptional regulation that shapes the molecular landscape of each event (Figure 5.1). Hypothetically, specific extracellular signals can be translated to intracellular second messenger cascades, that can phosphorylate specific transcription factors (201), regulating their transcriptional activity (122). This paints a picture of a single transcriptional regulator as gatekeeper allowing transition through specific phases of development, reinforced by functional characterization of AP2-G (53), AP2-I (140), MYB1 (152) and the hierarchical expression of ApiAP2 transcription factors during *P. falciparum* gametocyte development. Alternatively, the signals influencing developmental fates of the parasite can also be translated to the epigenome, consistent with epigenetic regulation of AP2-G (55,361), the dynamic epigenetic landscape during intraerythrocytic development (207) and observed influence of epigenetic marks on the gametocyte transcriptome. The latter hypothesis would imply tighter association between epigenetic control and transcription factors than has been observed to date, but akin to what was observed for AP2-G.

The observations on the phenomic profiles of asexual parasites and gametocytes was not able to capture some nuanced aspects of divergence in metabolism, including the switch from anaerobic glycolysis to oxidative metabolism (37,50) also described in chapter 3. However, the decreased transcript abundance of genes involved in hemoglobin digestion observed in the gametocyte transcriptome did translate to the late stage gametocyte phenome as an increased requirement for nitrogen sources. This requirement was not observed in the early-stage gametocytes, supporting previous observations that metabolically, trophozoites and early-stage gametocytes are similar, despite the substantial divergence in their transcriptomes. The lack of metabolism of lipid moieties in the gametocytes, despite the increased transcript abundance of enzymes involved in these pathways is also potentially significant. Although the fatty acid metabolic pathways are required in the parasite apicoplast for mosquito-stage development, lipid metabolism for energy production in gametocytes has not been observed. This discrepancy in transcriptional regulation and ultimate function, besides possibly being a result of the preferred lipid substrates not being included in the tested carbon substrates,

could be due to additional levels of regulation following transcription, as described in chapter 1.

In conclusion, we contribute valuable information on developmental decisions that are intrinsic to the continued survival of the *P. falciparum* parasite (Figure 5.1). We hypothesize that the parasite fulfils its complex biological functions by incorporating environmental signals into exquisite transcriptional control. We highlight the existence of a G_1/S transition check that is key in completing asexual parasite development, with functional studies on molecular role players highlighted in this process, CDPK4, SAP18, PF3D7_1112100, currently underway. We show a planned transcriptional program with stage-specific gene expression underlying prolonged gametocyte development in *P. falciparum* and identify possible transcriptional (Api_1317200, Api_0516800, Api_0934400, Api_0611200) and epigenetic regulation (H3K9me3, H3K36me3) that can be investigated in further studies. Finally, we prove that biologically relevant divergence exists in amino acid metabolism and metabolic rates of monosaccharide metabolism between sexual and asexual development and provide a system that has the potential to be optimized further for metabolic assaying of differential metabolic profiles of the parasite during stages of asexual and sexual development.

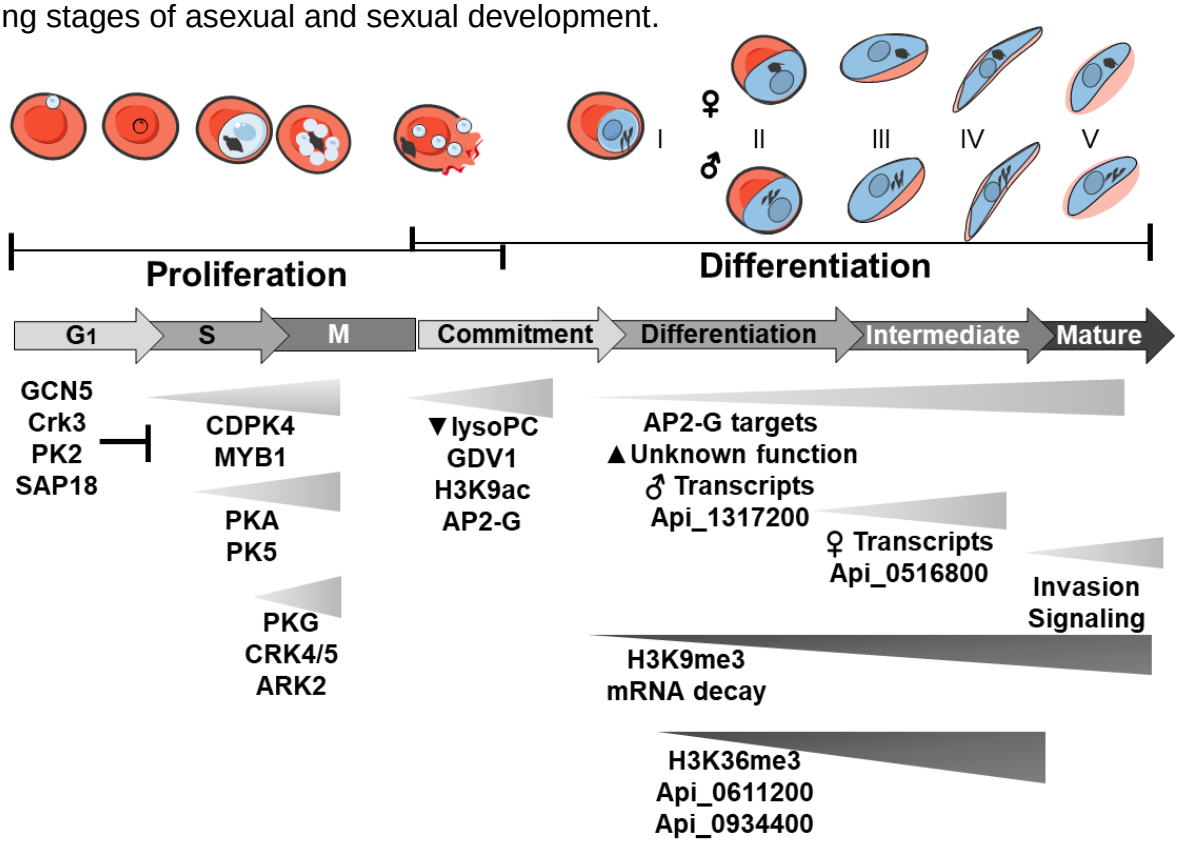

Figure 5.1: Molecular model of regulatory modules that shape the proliferative and differentiating stages of parasite development. Dark blocks show negative regulators of transcriptional abundance while light blocks show positive regulators of the parasite's progression through the respective life cycle stages.

6. References

1. World Health Organisation. World Malaria Report 2017. 2017.
2. Rabinovich RN, Drakeley C, Djimde AA, Hall BF, Hay SI, Hemingway J, et al. malERA: An updated research agenda for malaria elimination and eradication. PLoS Medicine. 2017.
3. Roll Back Malaria. The Global Malaria Action Plan. 2008.
4. malERA Group. A research agenda for malaria eradication: health systems and operational research. PLoS Med. 2011 Jan;8(1):e1000397.
5. Mwangangi JM, Mbogo CM, Orindi BO, Muturi EJ, Midega JT, Nzovu J, et al. Shifts in malaria vector species composition and transmission dynamics along the Kenyan coast over the past 20 years. Malar J [Internet]. 2013;12(1):13. Available from: http://malariajournal.biomedcentral.com/articles/10.1186/1475-2875-12-13
6. Killeen GF. Characterizing, controlling and eliminating residual malaria transmission. Malar J [Internet]. 2014;13(1):330. Available from: http://malariajournal.biomedcentral.com/articles/10.1186/1475-2875-13-330
7. Raghavendra K, Barik TK, Reddy BPN, Sharma P, Dash AP. Malaria vector control : from past to future. Parasitol Res. 2011;108:757–79.
8. Birkholtz L-M, Bornman R, Focke W, Mutero C, de Jager C. Sustainable malaria control: transdisciplinary approaches for translational applications. Malar J. 2012 Jan;11:1–11.
9. Kelly-hope L, Ranson H, Hemingway J. Lessons from the past : managing insecticide resistance in malaria control and eradication programmes. Lancet Infect Dis. 2008;8(June):387–9.
10. Naqqash MN, Gökçe A, Bakhsh A, Salim M. Insecticide resistance and its molecular basis in urban insect pests. Parasitol Res [Internet]. 2016 Apr;115(4):1363–73. Available from: https://doi.org/10.1007/s00436-015-4898-9
11. RTS/S Clinical Trials Partnership. Efficacy and safety of RTS,S/AS01 malaria vaccine with or without a booster dose in infants and children in Africa: final results of a phase 3, individually randomised, controlled trial [Internet]. The Lancet. 2015. Available from: http://linkinghub.elsevier.com/retrieve/pii/S0140673615607218
12. Ménard R. The journey of the malaria sporozoite through its hosts: two parasite proteins lead the way. Microbes Infect. 2000;2(6):633–42.
13. Menard R, Sultan AA, Cortes C, Altszuler R, van Dijk MR, Janse CJ, et al. Circumsporozoite protein is required for development of malaria sporozoites in mosquitoes. Nature [Internet]. 1997 Jan 23;385(6614):336–40. Available from: http://dx.doi.org/10.1038/385336a0
14. Gosling R, von Seidlein L. The Future of the RTS,S/AS01 Malaria Vaccine: An Alternative Development Plan. PLoS Med. 2016;13(4):1–6.
15. Burrows JN, Chibale K, Wells TNC. The State of the Art in Anti-Malarial Drug Discovery and Development. Curr Top Med Chem. 2011;11:1226–54.
16. Khan S, Ferguson E. A brief history of malaria chemotherapy. J R Coll Physicians Edinb. 2010;40:172–7.
17. Brown GD. The Biosynthesis of Artemisinin (Qinghaosu) and the Phytochemistry of Artemisia annua L. (Qinghao). Molecules. 2010;15:7603–98.
18. Muller IB, Hyde JE. Antimalarial drugs: modes of action and mechanisms of parasite resistance. Future Microbiol. 2010;5(12):1857–73.
19. Xie SC, Dogovski C, Hanssen E, Chiu F, Yang T, Crespo MP, et al. Haemoglobin degradation underpins the sensitivity of early ring stage Plasmodium falciparum to artemisinins. J Cell Sci. 2016;129:406–16.
20. Ismail HM, Barton V, Phanchana M, Charoensutthivarakul S, Wong MHL, Hemingway J, et al. Artemisinin activity-based probes identify multiple molecular targets within the asexual stage of the malaria parasites Plasmodium falciparum 3D7. PNAS. 2016;113(8):2080–5.
21. World Health Organisation. Guidelines for the treatment of malaria (3rd Edition). 2015. 1-316 p.
22. Dondorp AM, Nosten F, Yi P, Das D, Phyo AP, Tarning J, et al. Artemisinin Resistance in Plasmodium falciparum Malaria. N Engl J Med. 2009;361:455–67.
23. Lu F, Culleton R, Zhang M, Ramaprasad A, Seidlein L von, Zhou H, et al. Emergence of Indigenous Artemisinin-Resistant Plasmodium falciparum in Africa. N Engl J Med. 2017;1–3.
24. Burrows JN, van Huijsduijnen RH, Möhrle JJ, Oeuvray C, Wells TNC. Designing the next generation of medicines for malaria control and eradication. Malar J. 2013;12(1):187.
25. Burrows JN, Duparc S, Gutteridge WE, Hooft van Huijsduijnen R, Kaszubska W, Macintyre F, et al. New developments in anti-malarial target candidate and product profiles. Malar J [Internet]. BioMed Central; 2017;16(1):26. Available from: http://malariajournal.biomedcentral.com/articles/10.1186/s12936-016-1675-x
26. Bushell E, Gomes AR, Sanderson T, Anar B, Girling G, Herd C, et al. Functional Profiling of a Plasmodium Genome Reveals an Abundance of Essential Genes. Cell. Elsevier Inc.;

2017;170(2):260–272.e8.
27. Cowell AN, Istvan ES, Lukens AK, Maria G. Gomez-lorenzo, Vanaerschot M, Sakata-Kato T, et al. Mapping the malaria parasite druggable genome by using in vitro evolution and chemogenomics. Science (80-). 2018;II(January):1–36.
28. Price RN, Douglas NM, Anstey NM. New developments in Plasmodium vivax malaria : severe disease and the rise of chloroquine resistance. Curr Opin Infect Dis. 2009;22:430–5.
29. Naing C, Whittaker MA, Wai VN, Mak JW. Is Plasmodium vivax Malaria a Severe Malaria ?: A Systematic Review and Meta-Analysis. PLoS Negl Trop Dis. 2014;8(8):1–11.
30. Howes RE, Battle KE, Mendis KN, Smith DL, Cibulskis RE, Baird JK, et al. Global epidemiology of Plasmodium vivax. Am J Trop Med Hyg. 2016;95(Suppl 6):15–34.
31. Risco-Castillo V, Topçu S, Marinach C, Manzoni G, Bigorgne AE, Briquet S, et al. Malaria sporozoites traverse host cells within transient vacuoles. Cell Host Microbe. 2015;18(5):593–603.
32. Kirk K. Membrane Transport in the Malaria-Infected Erythrocyte. Physiol Rev. 2001;81(2):495–537.
33. Hanssen E, Knoechel C, Dearnley M, Dixon MWA, Le Gros M, Larabell C, et al. Soft X-ray microscopy analysis of cell volume and hemoglobin content in erythrocytes infected with asexual and sexual stages of Plasmodium falciparum. J Struct Biol [Internet]. Elsevier Inc.; 2012;177(2):224–32. Available from: http://dx.doi.org/10.1016/j.jsb.2011.09.003
34. Teng R, Junankar PR, Bubb WA, Rae C, Mercier P, Kirk K. Metabolite profiling of the intraerythrocytic malaria parasite Plasmodium falciparum by H NMR spectroscopy. NMR Biomed. 2009;22:292–302.
35. Tilley L, Dixon MWA, Kirk K. The Plasmodium falciparum-infected red blood cell. Int J Biochem Cell Biol. Elsevier Ltd; 2011;43(6):839–42.
36. Baumeister S, Winterberg M, Przyborski JM, Lingelbach K. The malaria parasite Plasmodium falciparum: cell biological peculiarities and nutritional consequences. Protoplasma. 2010 Apr;240(1–4):3–12.
37. Macrae JI, Dixon MWA, Dearnley MK, Chua HH, Chambers JM, Kenny S, et al. Mitochondrial metabolism of sexual and asexual blood stages of the malaria parasite Plasmodium falciparum. BMC Biol. 2013;11:67–76.
38. Lang-Unnasch N, Murphy a D. Metabolic changes of the malaria parasite during the transition from the human to the mosquito host. Annu Rev Microbiol. 1998 Jan;52:561–90.
39. Ke H, Lewis IA, Morrisey JM, Mclean KJ, Suresh M, Painter HJ, et al. Genetic Investigation of Tricarboxylic Acid Metabolism During the Plasmodium falciparum Lifecycle. Cell Rep. 2016;11(1):164–74.
40. Roth Jr. E. Plasmodium falciparum carbohydrate metabolism: A connection between host cell and parasite. Blood Cells. 1990;16(2–3):453–60.
41. Chulay JD, Haynes JD, Diggs CL. Plasmodium falciparum: Assessment of in vitro growth by [3H]hypoxanthine incorporation. Exp Parasitol. 1983;55(1):138–46.
42. Inselburg J, Banyal H. SYNTHESIS OF DNA DURING THE ASEXUAL CYCLE OF PLASMODIUM. Biochem Parasitol. 1984;10(1):79–87.
43. Hall N, Karras M, Raine J, Carlton J, Kooij T, Berriman M, et al. A comprehensive survey of the Plasmodium life cycle by genomic, transcriptomic, and proteomic analyses. Science. 2005 Jan 7;307(5706):82–6.
44. Bannister L, Hopkins J, Fowler R, Krishna S, Mitchell G. A brief illustrated guide to the ultrastructure of Plasmodium falciparum asexual blood stages. Parasitol Today. 2000;16(10):427–33.
45. Van Dooren GG, Marti M, Tonkin CJ, Stimmler LM, Cowman AF, Mcfadden GI. Development of the endoplasmic reticulum , mitochondrion and apicoplast during the asexual life cycle of Plasmodium falciparum. Mol Microbiol. 2005;57:405–19.
46. Arnot DE, Ronander E, Bengtsson DC. The progression of the intra-erythrocytic cell cycle of Plasmodium falciparum and the role of the centriolar plaques in asynchronous mitotic division during schizogony. Int J Parasitol. Australian Society for Parasitology Inc.; 2011;41(1):71–80.
47. Stanojcic S, Kuk N, Ullah I, Sterkers Y, Merrick CJ. Single-molecule analysis reveals that DNA replication dynamics vary across the course of schizogony in the malaria parasite Plasmodium falciparum. Sci Rep [Internet]. Springer US; 2017;(March):1–12. Available from: http://dx.doi.org/10.1038/s41598-017-04407-z
48. Talman AM, Domarle O, McKenzie FE, Ariey F, Robert V. Gametocytogenesis: the puberty of Plasmodium falciparum. Malar J. 2004;3:1–14.
49. Young JA, Fivelman QL, Blair PL, De P, Le KG, Zhou Y, et al. The Plasmodium falciparum sexual development transcriptome : A microarray analysis using ontology-based pattern identification. Mol Biochem Parasitol. 2005;143:67–79.
50. Lamour SD, Straschil U, Saric J, Delves MJ. Changes in metabolic phenotypes of Plasmodium

falciparum in vitro cultures during gametocyte development. Malar J. 2014;13(468):1–10.
51. Kaushal DC, Carter R, Miller LH, Krishna G. Gametocytogenesis by malaria parasites in continuous culture. [Internet]. Nature. 1980. p. 490–2. Available from: http://www.ncbi.nlm.nih.gov/pubmed/6250067
52. Brancucci NMB, Gerdt JP, Wang CQ, De Niz M, Philip N, Adapa SR, et al. Lysophosphatidylcholine Regulates Sexual Stage Differentiation in the Human Malaria Parasite Plasmodium falciparum. Cell. 2017;171(7):1532–1544.e15.
53. Kafsack BFC, Rovira-Graells N, Clark TG, Bancells C, Crowley VM, Campino SG, et al. A transcriptional switch underlies commitment to sexual development in malaria parasites. Nature. 2014;507:248–54.
54. Coleman BI, Skillman KM, Jiang RHY, Childs LM, Altenhofen LM, Ganter M, et al. A Plasmodium falciparum Histone Deacetylase regulates antigenic variation and gametocyte conversion. Cell Host Microbe. 2014;16(2):177–86.
55. Brancucci NMB, Bertschi NL, Zhu L, Niederwieser I, Chin WH, Wampfler R, et al. Heterochromatin protein 1 secures survival and transmission of malaria parasites. Cell Host Microbe. 2014;16(2):165–76.
56. Filarsky M, Fraschka SA, Niederwieser I, Brancucci NMB, Carrington E, Carrió E, et al. GDV1 induces sexual commitment of malaria parasites by antagonizing HP1-dependent gene silencing. Science (80-). 2018;359:1259–63.
57. Inselburg J. Gametocyte formation by the progeny of single Plasmodium falciparum schizonts. J Parasitol. 1983;69(3):584–91.
58. Silvestrini F, Alano P, Williams JL. Commitment to the production of male and female gametocytes in the human malaria parasite Plasmodium falciparum. Parasitology. University of Pretoria; 2000;121(2000):465–71.
59. Hawking F, Wilson M, Gammage K. Evidence for cyclic development and short-lived maturity in the gametocytes of plasmodium falciparum. Trans R Soc Trop Med Hyg. 1971;65(5):549–59.
60. Alano P. Plasmodium falciparum gametocytes: Still many secrets of a hidden life. Mol Microbiol. 2007;66(2):291–302.
61. Pelle K, Oh K, Buchholz K, Narasimhan V, Joice R, Milner D, et al. Transcriptional profiling defines dynamics of parasite tissue sequestration during malaria infection. Genome Med. 2015;7(19):1–20.
62. Joice R, Nilsson SK, Montgomery J, Dankwa S, Morahan B, Seydel KB, et al. Plasmodium falciparum transmission stages accumulate in the human bone marrow. Sci Transl Med. 2014;6(244):1–16.
63. Meibalan E, Marti M. The biology of malaria transmission. Cold Spring Harb Perspect Med. 2016;7:1–15.
64. Dearnley M, Chu T, Zhang Y, Looker O, Huang C, Klonis N, et al. Reversible host cell remodeling underpins deformability changes in malaria parasite sexual blood stages. Proc Natl Acad Sci U S A. 2016;1–6.
65. Kuehn A, Pradel G. The coming-out of malaria gametocytes. J Biomed Biotechnol. 2010 Jan;2010:976827.
66. Sinden R. The cell biology of sexual development in Plasmodium. Parasitology. Cambridge, UK: Cambridge University Press; 1983;86(4):7–28.
67. Billker RESGAB, Fleck SL. Regulation of Infectivity of PIasmodium to the Mosquito Vector. Adv Parasitol. 1996;38:53–117.
68. Billker O, Shaw MK, Margos G, Sinden RE, O. Billker, M.K. Shaw, G. Marcos RES. The roles of temperature, pH and mosquito factors as triggers of male and female gametogenesis of Plasmodium berghei in vitro. Parasitology. 1997 Jul;115 (Pt 1:1–7.
69. Billker O, Lindo V, Panico M, Etienne AE, Paxton T, Dell A, et al. Identification of xanthurenic acid as the putative inducer of malaria development in the mosquito. Nature [Internet]. 1998 Mar 19;392(6673):289–92. Available from: http://dx.doi.org/10.1038/32667
70. Billker O, Dechamps S, Tewari R, Wenig G, Franke-Fayard B, Brinkmann V. Calcium and a calcium-dependent protein kinase regulate gamete formation and mosquito transmission in a malaria parasite. Cell. 2004 May 14;117(4):503–14.
71. Guerreiro A, Deligianni E, Santos JM, Silva PA, Louis C, Pain A, et al. Genome-wide RIP-Chip analysis of translational repressor-bound mRNAs in the Plasmodium gametocyte. Genome Biol [Internet]. 2014;15(11):493. Available from: http://genomebiology.biomedcentral.com/articles/10.1186/s13059-014-0493-0
72. Vlachou D, Schlegelmilch T, Runn E, Mendes A, Kafatos FC. The developmental migration of Plasmodium in mosquitoes. Curr Opin Genet Dev. 2006;16(4):384–91.
73. Suhrbier A, Janse C, Mons B, Fleck SL, Nicholas J, Davies CS, et al. The complete development in vitro of the vertebrate phase of the mammalian malarial parasite Plasmodium berghei. Trans R

Soc Trop Med Hyg. 1987;81(6):907–9.
74. Frontali C. Genome plasticity in Plasmodium. Genetica. 1994;91–100.
75. Salcedo-sora JE, Caamano-gutierrez E, Ward SA, Biagini GA. The proliferating cell hypothesis : a metabolic framework for Plasmodium growth and development. Trends Parasitol. 2014;30(4):170–5.
76. Jacot D, Waller RF, Soldati-Favre D, MacPherson DA, MacRae JI. Apicomplexan Energy Metabolism: Carbon Source Promiscuity and the Quiescence Hyperbole. Trends Parasitol [Internet]. Elsevier Ltd; 2016;32(1):56–70. Available from: http://dx.doi.org/10.1016/j.pt.2015.09.001
77. Cobbold SA, Vaughan AM, Lewis IA, Painter HJ, Camargo N, Perlman DH, et al. Kinetic Flux Profiling Elucidates Two Independent Acetyl-CoA Biosynthetic Pathways in Plasmodium falciparum. J Biol Chem. 2013;288(51):36338–50.
78. Oppenheim RD, Creek DJ, Macrae JI, Modrzynska KK, Pino P, Limenitakis J, et al. BCKDH : The Missing Link in Apicomplexan Mitochondrial Metabolism Is Required for Full Virulence of Toxoplasma gondii and Plasmodium berghei. PLoS Pathog. 2014;10(7):1–18.
79. Painter HJ, Morrisey JM, Vaidya AB, Plasmodium I. Mitochondrial Electron Transport Inhibition and Viability of Intraerythrocytic Plasmodium falciparum. Antimicrob Agents Chemother. 2010;54(12):5281–7.
80. Gardner MJ, Hall N, Fung E, White O, Berriman M, Hyman RW, et al. Genome sequence of the human malaria parasite Plasmodium falciparum. Nature. 2002;419:498–511.
81. Olszewski KL, Llinás M. Central carbon metabolism of Plasmodium parasites. Mol Biochem Parasitol. Elsevier B.V.; 2011;175(2):95–103.
82. Krugliak M, Zhang J, Ginsburg H. Intraerythrocytic Plasmodium falciparum utilizes only a fraction of the amino acids derived from the digestion of host cell cytosol for the biosynthesis of its proteins. Mol Biochem Parasitol. 2002;119(2):249–56.
83. Famin O, Ginsburg H. Differential effects of 4-aminoquinoline-containing antimalarial drugs on hemoglobin digestion in Plasmodium falciparum-infected erythrocytes. Biochem Pharmacol. 2002;63(3):393–8.
84. Divo AA, Geary TG, Davis NL, Jensen JB. Nutritional Requirements of Plasmodium falciparum in Culture. I. Exogenously Supplied Dialyzable Components Necessary for Continuous Growth. J Protozool. 1985;32(1):59–64.
85. Babbitt SE, Altenhofen L, Cobbold S a., Istvan ES, Fennell C, Doerig C, et al. PNAS Plus: Plasmodium falciparum responds to amino acid starvation by entering into a hibernatory state. Proc Natl Acad Sci. 2012;109(47).
86. van Schaijk BCL, Santha Kumar TR, Vos MW, Richman A, van Gemert GJ, Li T, et al. Type II fatty acid biosynthesis is essential for Plasmodium falciparum sporozoite development in the midgut of anopheles mosquitoes. Eukaryot Cell. 2014;13(5):550–9.
87. Delves MJ. Plasmodium cell biology should inform strategies used in the development of antimalarial transmission-blocking drugs. Future Med Chem. 2012 Dec;4(18):2251–63.
88. Plouffe DM, Wree M, Du AY, Meister S, Li F, Patra K, et al. High-Throughput Assay and Discovery of Small Molecules that Interrupt Malaria Transmission. Cell Host Microbe. 2016;19(1):114–26.
89. Leete T, Rubin H. Malaria and the Cell Cycle. Parasitol Today. 1996;12(11):442–4.
90. Patterson S, Robert C, Whittle C, Chakrabarti R, Doerig C, Chakrabarti D. Pre-replication complex organization in the atypical DNA replication cycle of Plasmodium falciparum : Characterization of the mini-chromosome maintenance (MCM) complex formation. Mol Biochem Parasitol. 2006;145:50–9.
91. Francia ME, Striepen B. Cell division in apicomplexan parasites. Nat Rev Microbiol [Internet]. Nature Publishing Group; 2014;12(2):125–36. Available from: http://dx.doi.org/10.1038/nrmicro3184
92. Lee LA, Orr-Weaver TL. Regulation of Cell Cycles in Drosophila Development: Intrinsic and Extrinsic Cues. Annu Rev Genet [Internet]. 2003;37(1):545–78. Available from: http://www.annualreviews.org/doi/10.1146/annurev.genet.37.110801.143149
93. Aikawa M. Parasitological review. Plasmodium: the fine structure of malarial parasites. Exp Parasitol. 1971;30(2):284–320.
94. Gerald N, Mahajan B, Kumar S. Mitosis in the Human Malaria Parasite Plasmodium falciparum. Eukaryot Cell. 2011;10(4):474–82.
95. Read M, Sherwin T, Holloway SP, Gull K, Hyde JE. Microtubular organization visualized by immunofluorescence microscopy during erythrocytic schizogony in Plasmodium falciparum and investigation of post-translational modifications of parasite tubulin. Parasitology. 1993;106(03):223–32.
96. Reilly HB, Wang H, Steuter JA, Marx AM, Ferdig MT. Quantitative dissection of clone-specific growth rates in cultured malaria parasites. Int J Parasitol. 2007;37(14):1599–607.

97. Naughton JA, Bell A. Studies on cell-cycle synchronization in the asexual erythrocytic stages of Plasmodium falciparum. Parasitology. 2007;331–7.
98. Ward P, Equinet L, Packer J, Doerig C. Protein kinases of the human malaria parasite Plasmodium falciparum : the kinome of a divergent eukaryote. BMC Genomics. 2004;5(79):1–19.
99. Doerig C, Endicott J, Chakrabarti D. Cyclin-dependent kinase homologues of Plasmodium falciparum. Int J Parasitol. 2002;32:1575–85.
100. Merckx A, le Roch K, Dorin D, Alano P, Gutierrez GJ, Nebreda AR, et al. Identification and Initial Characterization of Three Novel Cyclin-related Proteins of the Human Malaria Parasite Plasmodium falciparum. J Biol Chem. 2003;278(41):39839–50.
101. Aurrecoechea C, Brestelli J, Brunk BP, Dommer J, Fischer S, Gajria B, et al. PlasmoDB: A functional genomic database for malaria parasites. Nucleic Acids Res. 2009;37(SUPPL. 1):539–43.
102. Roques M, Wall RJ, Douglass AP. Plasmodium P-Type Cyclin CYC3 Modulates Endomitotic Growth during Oocyst Development in Mosquitoes. PLoS Pathog. 2015;1–29.
103. Morgan DO. CYCLIN-DEPENDENT KINASES : Engines , Clocks , and Microprocessors. Annu Rev Cell Dev Biol. 1997;13:261–91.
104. Le Roch K, Sestier C, Dorin D, Waters N, Kappes B, Chakrabarti D, et al. Activation of a *Plasmodium falciparum* cdc2-related kinase by heterologous p25 and cyclin H. J Biol Chem. 2000;275(12):8952–8.
105. Robbins JA, Absalon S, Streva VA, Dvorin JD. The Malaria Parasite Cyclin H Homolog PfCyc1 Is Required for Efficient Cytokinesis in Blood-Stage Plasmodium falciparum. MBio. 2017;8(3):1–12.
106. Sinden R, Smalley M. Gametocytogenesis of Plasmodium falciparum in vitro: the cell-cycle. Parasitology. 1979;79:277–96.
107. Janse CJ, Ponnudurai T, Lensen a H, Meuwissen JH, Ramesar J, Van der Ploeg M, et al. DNA synthesis in gametocytes of Plasmodium falciparum. Parasitology. 1988;96 (Pt 1):1–7.
108. Brochet M, Billker O. Calcium signalling in malaria parasites. Mol Microbiol. 2016;100(3):397–408.
109. Baker DA, Drought LG, Flueck C, Nofal SD, Patel A, Penzo M, et al. Cyclic nucleotide signalling in malaria parasites. Open Biol. 2017;7(170213):1–18.
110. Saliba KS, Jacobs-lorena M. Production of Plasmodium falciparum Gametocytes In Vitro. Methods Mol Biol [Internet]. 2013;923(9):17–25. Available from: http://link.springer.com/10.1007/978-1-62703-026-7
111. Trager W, Gill GS. Plasmodium falciparum gametocyte formation in vitro: its stimulation by phorbol diesters and by 8-bromo cyclic adenosine monophosphate. J Protozool. 1989;36(5):451–4.
112. Lepski G, Jannes CE, Nikkhah G, Bischofberger J. cAMP promotes the differentiation of neural progenitor cells in vitro via modulation of voltage-gated calcium channels. Front Cell Neurosci [Internet]. 2013;7(September):1–11. Available from: http://journal.frontiersin.org/article/10.3389/fncel.2013.00155/abstract
113. Petersen RK, Madsen L, Pedersen LM, Hallenborg P, Hagland H, Viste K, et al. Cyclic AMP (cAMP)-Mediated Stimulation of Adipocyte Differentiation Requires the Synergistic Action of Epac- and cAMP-Dependent Protein Kinase-Dependent Processes. Mol Cell Biol [Internet]. 2008;28(11):3804–16. Available from: http://mcb.asm.org/cgi/doi/10.1128/MCB.00709-07
114. Pandey R, Mohmmed A, Pierrot C, Khalife J, Malhotra P, Gupta D. Genome wide in silico analysis of Plasmodium falciparum phosphatome. BMC Genomics. 2014;15(1):1024.
115. Dorin D, Semblat J, Poullet P, Alano P, Goldring JPD, Whittle C, et al. PfPK7 , an atypical MEK-related protein kinase , reflects the absence of classical three-component MAPK pathways in the human malaria parasite Plasmodium falciparum. Mol Microbiol. 2005;55(1):184–96.
116. Koyama F, Ribeiro R, Garcia J, Azevedo M, Chakrabarti D, Garcia CRS. Ubiquitin Proteasome System and the atypical kinase PfPK7 are involved in melatonin signaling in Plasmodium falciparum. J Pineal Res. 2013;53(2):147–53.
117. Brochet M, Collins MO, Smith TK, Thompson E, Sebastian S, Volkmann K, et al. Phosphoinositide Metabolism Links cGMP-Dependent Protein Kinase G to Essential Ca 2 + Signals at Key Decision Points in the Life Cycle of Malaria Parasites. PLoS Biol. 2014;12(3):1–15.
118. Furuyama W, Enomoto M, Mossaad E, Kawai S, Mikoshiba K, Kawazu S. An interplay between 2 signaling pathways: Melatonin-cAMP and IP3–Ca2+ signaling pathways control intraerythrocytic development of the malaria parasite Plasmodium falciparum. Biochem Biophys Res Commun [Internet]. Elsevier Inc.; 2014;446(1):125–31. Available from: http://linkinghub.elsevier.com/retrieve/pii/S0006291X14003325
119. Lima WR, Tessarin-Almeida G, Rozanski A, Parreira KS, Moraes MS, Martins DC, et al. Signaling transcript profile of the asexual intraerythrocytic development cycle of Plasmodium falciparum induced by melatonin and cAMP. Genes Cancer [Internet]. 2016;7(9–10):323–39. Available from: http://www.ncbi.nlm.nih.gov/pubmed/28050233%0Ahttp://www.pubmedcentral.nih.gov/articlerender.fcgi?artid=PMC5115173

120. Zhao Y, Kappes B, Yang J, Franklin RM. Molecular cloning, stage-specific expression and cellular distribution of a putative protein kinase from Plasmodium falciparum. Eur J Biochem. 1992;207(1):305–13.
121. Billker O, Lourido S, Sibley LD. Calcium-dependent signaling and kinases in apicomplexan parasites. Cell Host Microbe [Internet]. Elsevier Inc.; 2009 Jun 18 [cited 2013 Mar 11];5(6):612–22. Available from: http://www.pubmedcentral.nih.gov/articlerender.fcgi?artid=2718762&tool=pmcentrez&rendertype=abstract
122. Carvalho TG, Morahan B, John von Freyend S, Boeuf P, Grau G, Garcia-Bustos J, et al. The ins and outs of phosphosignalling in Plasmodium: Parasite regulation and host cell manipulation. Mol Biochem Parasitol. Elsevier B.V.; 2016;208(1):2–15.
123. Kumar P, Tripathi A, Ranjan R, Halbert J, Gilberger T, Doerig C, et al. Regulation of Plasmodium falciparum development by calcium-dependent protein kinase 7 (PfCDPK7). J Biol Chem. 2014;289(29):20386–95.
124. Schulz P, Herde M, Romeis T. Calcium-Dependent Protein Kinases: Hubs in Plant Stress Signaling and Development. Plant Physiol [Internet]. 2013;163(2):523–30. Available from: http://www.plantphysiol.org/cgi/doi/10.1104/pp.113.222539
125. Bansal A, Singh S, More KR, Hans D, Nangalia K, Yogavel M, et al. Characterization of plasmodium falciparum calcium-dependent protein kinase 1 (PFCDPK1) and its role in microneme secretion during erythrocyte invasion. J Biol Chem. 2013;288(3):1590–602.
126. Dvorin JD, Martyn DC, Patel SD, Grimley JS, Collins R, Hopp CS, et al. A Plant-Like Kinase in Plasmodium falciparum Regulates Parasite Egress From Erythrocytes. Science (80-). 2011;328(5980):910–2.
127. Siden-Kiamos I, Ecker A, Nybäck S, Louis C, Sinden RE, Billker O. Plasmodium berghei calcium-dependent protein kinase 3 is required for ookinete gliding motility and mosquito midgut invasion. Mol Microbiol. 2006;60(6):1355–63.
128. Bozdech Z, Llinas M, Pulliam BL, Wong ED, Zhu J, Derisi JL. The Transcriptome of the Intraerythrocytic Developmental Cycle of Plasmodium falciparum. PLoS Biol. 2003;1(1):85–100.
129. Poran A, Nötzel C, Aly O, Mencia-Trinchant N, Harris CT, Guzman ML, et al. Single-cell RNA sequencing reveals a signature of sexual commitment in malaria parasites. Nature [Internet]. Nature Publishing Group; 2017;1–22. Available from: http://www.nature.com/doifinder/10.1038/nature24280
130. Aravind L, Iyer LM, Wellems TE, Miller LH. Plasmodium Biology: Genomic Gleanings. Cell. 2003;115(7):771–85.
131. Alano P, Roca L, Smith D, Read D, Carter R, Day K. Plasmodium falciparum: Parasites Defective in Early Stages of Gametocytogenesis. Exp Parasitol. 1995;81:227–35.
132. Ribacke U, Mok BW, Wirta V, Normark J, Lundeberg J, Kironde F, et al. Genome wide gene amplifications and deletions in Plasmodium falciparum. Mol Biochem Parasitol. 2007;155(1):33–44.
133. Llinás M, Bozdech Z, Wong ED, Adai AT, Derisi JL. Comparative whole genome transcriptome analysis of three Plasmodium falciparum strains. Nucleic Acids Res. 2006;34(4):1166–73.
134. Lasonder E, Rijpma SR, van Schaijk BCL, Hoeijmakers WAM, Kensche PR, Gresnigt MS, et al. Integrated transcriptomic and proteomic analyses of P. falciparum gametocytes: molecular insight into sex-specific processes and translational repression. Nucleic Acids Res. 2016;1–15.
135. Griffiths A, Miller J, Suzuki D. Transcription: an overview of gene regulation in eukaryotes [Internet]. An Introduction to Genetic Analysis. 7th Edition. 2000 [cited 2017 Sep 12]. Available from: https://www.ncbi.nlm.nih.gov/books/NBK21780/%0A
136. Brick K, Watanabe J, Pizzi E. Core promoters are predicted by their distinct physicochemical properties in the genome of Plasmodium falciparum. Genome Biol. 2008;9(12):R178.
137. Adjalley SH, Chabbert CD, Klaus B, Pelechano V, Steinmetz LM. Landscape and Dynamics of Transcription Initiation in the Malaria Parasite Plasmodium falciparum. Cell Rep [Internet]. The Authors; 2016;14(10):2463–75. Available from: http://dx.doi.org/10.1016/j.celrep.2016.02.025
138. Young J, Johnson J, Benner C, Yan F, Chen K, Le Roch K, et al. In silico discovery of transcription regulatory elements in Plasmodium falciparum. BMC Genomics. 2008;9:70.
139. Russell K, Emes R, Horrocks P. Triaging informative cis -regulatory elements for the combinatorial control of temporal gene expression during Plasmodium falciparum intraerythrocytic development. Parasit Vectors. 2015;1–9.
140. Santos JM, Josling G, Ross P, Joshi P, Orchard L, Campbell T, et al. Red Blood Cell Invasion by the Malaria Parasite Is Coordinated by the PfAP2-I Transcription Factor. Cell Host Microbe [Internet]. 2017;21(6):731–741.e10. Available from: http://linkinghub.elsevier.com/retrieve/pii/S1931312817301993
141. Painter HJ, Carrasquilla M, Llinás M. Capturing in vivo RNA transcriptional dynamics from the

malaria parasite Plasmodium falciparum. Genome Res. 2017;1–21.
142. Campbell TL, de Silva EK, Olszewski KL, Elemento O, Llinás M. Identification and Genome-Wide Prediction of DNA Binding Specificities for the ApiAP2 family of regulators from the malaria parasite. PLoS Pathog. 2010;6(10):1–15.
143. Bird A. Perceptions of epigenetics. Nature [Internet]. 2007;447(7143):396–8. Available from: http://www.nature.com/doifinder/10.1038/nature05913
144. Workman JL, Kingston RE. Alteration of nucleosome structure as a mechanism of transcriptional regulation. Annu Rev Biochem. 1998;67:545–79.
145. Ay F, Bunnik EM, Varoquaux N, Vert J, Noble WS, Roch KG Le. Multiple dimensions of epigenetic gene regulation in the malaria parasite Plasmodium falciparum. BioEssays. 2014;37:182–94.
146. Silberhorn E, Schwartz U, Löffler P, Schmitz S, Symelka A, de Koning-Ward T, et al. Plasmodium falciparum Nucleosomes Exhibit Reduced Stability and Lost Sequence Dependent Nucleosome Positioning. PLoS Pathog. 2016;12(12):1–29.
147. Kensche PR, Hoeijmakers WAM, Toenhake CG, Bras M, Chappell L, Berriman M, et al. The nucleosome landscape of Plasmodium falciparum reveals chromatin architecture and dynamics of regulatory sequences. Nucleic Acids Res. 2015;44(5):2110–24.
148. Miao J, Fan Q, Cui L, Li J, Li J, Cui L. The malaria parasite Plasmodium falciparum histones : Organization , expression , and acetylation. Gene. 2006;369:53–65.
149. Cui L, Miao J. Chromatin-Mediated epigenetic regulation in the malaria parasite Plasmodium falciparum. Eukaryot Cell. 2010;9(8):1138–49.
150. Bunnik EM, Polishko A, Prudhomme J, Ponts N, Gill SS, Lonardi S, et al. DNA-encoded nucleosome occupancy is associated with transcription levels in the human malaria parasite Plasmodium falciparum. BMC Genomics. 2014;15(1):347.
151. Bischoff E, Vaquero C. In silico and biological survey of transcription-associated proteins implicated in the transcriptional machinery during the erythrocytic development of Plasmodium falciparum. BMC Genomics. 2010;11(1):34.
152. Gissot M, Briquet S, Refour P, Boschet C, Vaquero C. PfMyb1, a Plasmodium falciparum transcription factor, is required for intra-erythrocytic growth and controls key genes for cell cycle regulation. J Mol Biol. 2005;346(1):29–42.
153. Balaji S, Babu MM, Iyer LM, Aravind L. Discovery of the principal specific transcription factors of Apicomplexa and their implication for the evolution of the AP2-integrase DNA binding domains. Nucleic Acids Res. 2005;33(13):3994–4006.
154. Riechmann JL, Meyerowitz EM. The AP2 / EREBP Family of Plant Transcription Factors. Biol Chem. 1998;379(June):633–46.
155. Painter HJ, Campbell TL, Llinas M. The Apicomplexan AP2 family: Integral factors regulating Plasmodium development. Mol Biochem Parasitol. 2011;176(1):1–7.
156. Allen MD, Yamasaki K, Ohme-Takagi M, Tateno M, Suzuki M. A novel mode of DNA recognition by a beta-sheet revealed by the solution structure of the GCC-box binding domain in complex with DNA. EMBO J [Internet]. 1998;17(18):5484–96. Available from: http://www.pubmedcentral.nih.gov/articlerender.fcgi?artid=1170874&tool=pmcentrez&rendertype=abstract
157. Bunnik EM, Chung D-WD, Hamilton M, Ponts N, Saraf A, Prudhomme J, et al. Polysome profiling reveals translational control of gene expression in the human malaria parasite Plasmodium falciparum. Genome Biol. 2013;14(11):R128.
158. Foth BJ, Zhang N, Mok S, Preiser PR, Bozdech Z. Quantitative protein expression profiling reveals extensive post-transcriptional regulation and post-translational modifications in schizont-stage malaria parasites. Genome Biol. 2008;9(12):1–18.
159. Alberts B, Johnson A, Lewis J. Posttranscriptional Controls [Internet]. Molecular Biology of the Cell. 4th edition. 2002. Available from: https://www.ncbi.nlm.nih.gov/books/NBK26890/
160. Vembar SS, Droll D, Scherf A. Translational regulation in blood stages of the malaria parasite Plasmodium spp.: systems-wide studies pave the way. Wiley Interdiscip Rev RNA. 2016;7(6):772–92.
161. Baum J, Papenfuss AT, Mair GR, Janse CJ, Vlachou D, Waters AP, et al. Molecular genetics and comparative genomics reveal RNAi is not functional in malaria parasites. Nucleic Acids Res. 2009;37(11):3788–98.
162. Otto TD, Wilinski D, Assefa S, Keane TM, Sarry LR, Böhme U, et al. New insights into the blood-stage transcriptome of Plasmodium falciparum using RNA-Seq. Mol Microbiol. 2010;76(1):12–24.
163. López-Barragán MJ, Lemieux J, Quiñones M, Williamson KC, Molina-Cruz A, Cui K, et al. Directional gene expression and antisense transcripts in sexual and asexual stages of Plasmodium falciparum. BMC Genomics. 2011;12:587.
164. Sorber K, Dimon MT, Derisi JL. RNA-Seq analysis of splicing in Plasmodium falciparum uncovers new splice junctions , alternative splicing and splicing of antisense transcripts. Nucleic Acids Res.

2011;39(9):3820–35.
165. Hyde JE. Targeting purine and pyrimidine metabolism in human apicomplexan parasites. Curr Drug Targets [Internet]. 2007;8(1):31–47. Available from: http://www.ncbi.nlm.nih.gov/pmc/articles/PMC2720675/pdf/ukmss-27454.pdf
166. Miller C, Schwalb B, Maier K, Schulz D, Dumcke S, Zacher B, et al. Dynamic transcriptome analysis measures rates of mRNA synthesis and decay in yeast. Mol Syst Biol. 2011;7(458):1–13.
167. Gay L, Karfilis K V., Miller MR, Doe CQ, Stankunas K. Applying thiouracil (TU)-tagging for mouse transcriptome analysis. Nat Protoc. 2014;9(2):410–20.
168. Miller MR, Robinson KJ, Cleary MD, Doe CQ. TU-tagging : cell type – specific RNA isolation from intact complex tissues. Nat Methods [Internet]. Nature Publishing Group; 2009;6(6):439–41. Available from: http://dx.doi.org/10.1038/nmeth.1329
169. Munchel SE, Shultzaberger RK, Takizawa N, Weis K. Dynamic profiling of mRNA turnover reveals gene-specific and system-wide regulation of mRNA decay. Mol Biol Cell. 2011;22:2787–95.
170. Reddy N, Shrestha S, Hart K, Liang X, Kemirembe K, Cui L, et al. A bioinformatic survey of RNA-binding proteins in Plasmodium. BMC Genomics. BMC Genomics; 2015;16(890):1–26.
171. Mair GR, Lasonder E, Garver LS, Franke-Fayard BMD, Carret CK, Wiegant JCAG, et al. Universal features of post-transcriptional gene regulation are critical for Plasmodium zygote development. PLoS Pathog. 2010;6(2).
172. Kawahara H, Imai T, Imataka H, Tsujimoto M, Matsumoto K, Okano H. Neural RNA-binding protein Musashi1 inhibits translation initiation by competing with eIF4G for PABP. J Cell Biol. 2008;181(4):639–53.
173. Miao J, Fan Q, Parker D, Li X, Li J, Cui L. Puf Mediates Translation Repression of Transmission-Blocking Vaccine Candidates in Malaria Parasites. PLoS Pathog. 2013;9(4).
174. Vembar SS, Macpherson CR, Sismeiro O, Coppée J-Y, Scherf A. The PfAlba1 RNA-binding protein is an important regulator of translational timing in Plasmodium falciparum blood stages. Genome Biol [Internet]. 2015;16(1):212. Available from: http://genomebiology.com/2015/16/1/212
175. Cui L, Lindner S, Miao J. Translational regulation during stage transitions in malaria parasites. Ann N Y Acad Sci. 2015;1342(1):1–9.
176. Mair GR, Braks JAM, Garver LS, Dimopoulos G, Hall N, Wiegant JCAG, et al. Translational Repression is essential for Plasmodium sexual development and mediated by a DDX6-type RNA helicase. Science (80-). 2006;42(1):84–94.
177. Miao J, Li J, Fan Q, Li X, Li X, Cui L. The Puf-family RNA-binding protein PfPuf2 regulates sexual development and sex differentiation in the malaria parasite Plasmodium falciparum. J Cell Sci. 2010;123(Pt 7):1039–49.
178. Shock JL, Fischer KF, DeRisi JL. Whole-genome analysis of mRNA decay in Plasmodium falciparum reveals a global lengthening of mRNA half-life during the intra-erythrocytic development cycle. Genome Biol [Internet]. 2007;8(7):R134. Available from: http://genomebiology.biomedcentral.com/articles/10.1186/gb-2007-8-7-r134
179. Balu B, Maher SP, Pance A, Chauhan C, Naumov A V., Andrews RM, et al. CCR4-associated factor 1 coordinates the expression of Plasmodium falciparum egress and invasion proteins. Eukaryot Cell. 2011;10(9):1257–63.
180. Painter HJ, Chung NC, Sebastian A, Albert I, Storey JD, Llinás M. Genome-wide real-time in vivo transcriptional dynamics during Plasmodium falciparum blood-stage development. Nat Commun [Internet]. Springer US; 2018;9(1):2656. Available from: http://www.nature.com/articles/s41467-018-04966-3
181. Jackson KE, Habib S, Frugier M, Hoen R, Khan S, Pham JS, et al. Protein translation in Plasmodium parasites. Trends Parasitol. 2011;27(10):467–76.
182. Waters A, Syin C, McCutchan T. Developmental regulation of stage-specific ribosome populations in Plasmodium. Nature. 1989;342:438–40.
183. Tuteja R. Identification and bioinformatics characterization of translation initiation complex eIF4F components and poly (A) -binding protein from Plasmodium falciparum. Commun Integr Biol. 2009;2(3):245–60.
184. Tuteja R, Pradhan A. PfeIF4E and PfeIF4A colocalize and their double- stranded RNA inhibits Plasmodium falciparum proliferation. Commun Integr Biol. 2010;3(6):611–3.
185. Gebauer F, Hentze MW. Molecular mechanisms of translational control. Nat Rev. 2004;5:827–35.
186. Miao J, Chen Z, Wang Z, Shrestha S, Li X, Li R, et al. Sex-specific proteomes of human malaria parasite. Mol Cell Proteomics. 2017;33(1):1–36.
187. Tao D, Ubaida-Mohien C, Mathias DK, King JG, Pastrana-Mena R, Tripathi A, et al. Sex-partitioning of the Plasmodium falciparum Stage V Gametocyte Proteome Provides Insight into falciparum-specific Cell Biology. Mol Cell Proteomics. 2014;13(10):2705–24.
188. Doerig C, Rayner JC, Scherf A, Tobin AB. Post-translational protein modifications in malaria parasites. Nat Rev Microbiol [Internet]. Nature Publishing Group; 2015;13(3):160–72. Available

from: http://www.nature.com/doifinder/10.1038/nrmicro3402
189. Issar N, Roux E, Mattei D, Scherf A. Identification of a novel post-translational modification in Plasmodium falciparum: Protein sumoylation in different cellular compartments. Cell Microbiol. 2008;10(10):1999–2011.
190. Ponts N, Saraf A, Chung DWD, Harris A, Prudhomme J, Washburn MP, et al. Unraveling the ubiquitome of the human malaria parasite. J Biol Chem. 2011;286(46):40320–30.
191. de Macedo CS, Schwarz RT, Todeschini AR, Previato JO, Mendonça-Previato L. Overlooked post-translational modifications of proteins in Plasmodium falciparum: N- and O-glycosylation - A review. Mem Inst Oswaldo Cruz. 2010;105(8):949–56.
192. Kehr S, Jortzik E, Delahunty C, Yates JR, Rahlfs S, Becker K. Protein *S* -Glutathionylation in Malaria Parasites. Antioxid Redox Signal [Internet]. 2011;15(11):2855–65. Available from: http://www.liebertonline.com/doi/abs/10.1089/ars.2011.4029
193. Wang L, Delahunty C, Prieto JH, Rahlfs S, Jortzik E, Yates JR, et al. Protein *S* -nitrosylation in *Plasmodium falciparum*. Antioxid Redox Signal [Internet]. 2014;20(18):2923–35. Available from: http://online.liebertpub.com/doi/abs/10.1089/ars.2013.5553
194. Jortzik E, Becker K. Thioredoxin and glutathione systems in Plasmodium falciparum. Int J Med Microbiol [Internet]. Elsevier GmbH.; 2012;302(4–5):187–94. Available from: http://dx.doi.org/10.1016/j.ijmm.2012.07.007
195. Resh MD. Covalent Lipid Modifications of Proteins. Curr Biol. 2008;86(12):3279–88.
196. Jones ML, Collins MO, Goulding D, Choudhary JS, Rayner JC. Analysis of protein palmitoylation reveals a pervasive role in Plasmodium development and pathogenesis. Cell Host Microbe. 2012;12(2):246–58.
197. von Itzstein M, Plebanski M, Cooke BM, Coppel RL. Hot, sweet and sticky: the glycobiology of Plasmodium falciparum. Trends Parasitol. 2008;24(5):210–8.
198. Gerold P, Schofield L, Blackman MJ, Holder AA, Schwarz RT. Structural analysis of the glycosyl-phosphatidylinositol membrane anchor of the merozoite surface proteins-1 and -2 of Plasmodium falciparum. Mol Biochem Parasitol. 1996;75(2):131–43.
199. Tachado SD, Mazhari-Tabrizi R, Schofield L. Specificity in signal transduction among glycosylphosphatidylinositols of Plasmodium falciparum, Trypanosoma brucei, Trypanosoma cruzi and Leishmania spp. Parasite Immunol. 1999;21(12):609–17.
200. Doerig C, Grevelding CG. Targeting kinases in Plasmodium and Schistosoma: Same goals, different challenges. Biochim Biophys Acta - Proteins Proteomics. Elsevier B.V.; 2015;1854(10):1637–43.
201. Solyakov L, Halbert J, Alam MM, Semblat J-P, Dorin-semblat D, Reininger L, et al. Global kinomic and phospho-proteomic analyses of the human malaria parasite Plasmodium falciparum. Nat Commun. 2011;2(565):1–12.
202. Pease BN, Huttlin EL, Jedrychowski MP, Talevich E, Harmon J, Dillman T, et al. Global Analysis of Protein Expression and Phosphorylation of Three Stages of Plasmodium falciparum Intraerythrocytic Development. J Proteome Res. 2013;12:4028–45.
203. Treeck M, Sanders JL, Elias JE, Boothroyd JC. The Phosphoproteomes of Plasmodium falciparum and Toxoplasma gondii Reveal Unusual Adaptations Within and Beyond the Parasites ' Boundaries. Cell Host Microbe. Elsevier; 2011;10(4):410–9.
204. Gupta AP, Bozdech Z. Epigenetic landscapes underlining global patterns of gene expression in the human malaria parasite, Plasmodium falciparum. Int J Parasitol [Internet]. 2017;47(7):399–407. Available from: http://dx.doi.org/10.1016/j.ijpara.2016.10.008
205. Bannister AJ, Kouzarides T. Regulation of chromatin by histone modifications. Cell Res [Internet]. Nature Publishing Group; 2011;21(3):381–95. Available from: http://www.nature.com/doifinder/10.1038/cr.2011.22
206. Miao J, Lawrence M, Jeffers V, Zhao F, Parker D, Ge Y, et al. Extensive lysine acetylation occurs in evolutionarily conserved metabolic pathways and parasite-specific functions during Plasmodium falciparum intraerythrocytic development. Mol Microbiol. 2013;89(4):660–75.
207. Gupta AP, Chin WH, Zhu L, Mok S, Luah YH, Lim EH, et al. Dynamic Epigenetic Regulation of Gene Expression during the Life Cycle of Malaria Parasite Plasmodium falciparum. PLoS Pathog. 2013;9(2).
208. Peterson CL, Laniel M-A. Histones and histone modifications. Curr Biol. 2004;14:R546–51.
209. Cui L, Fan Q, Cui L, Miao J. Histone lysine methyltransferases and demethylases in Plasmodium falciparum. Int J Parasitol. 2008;38(10):1083–97.
210. Fan Q, An L, Cui L. Plasmodium falciparum. Eukaryot Cell. 2004;3(2):264–76.
211. Salcedo-Amaya AM, van Driel MA, Alako BT, Trelle MB, van den Elzen AMG, Cohen AM, et al. Dynamic histone H3 epigenome marking during the intraerythrocytic cycle of Plasmodium falciparum. Proc Natl Acad Sci U S A [Internet]. 2009;106(24):9655–60. Available from: http://www.ncbi.nlm.nih.gov/pubmed/19497874%5Cnhttp://www.pubmedcentral.nih.gov/articlerend

er.fcgi?artid=PMC2701018
212. Cui L, Miao J, Furuya T, Li X, Su XZ, Cui L. PfGCN5-mediated histone H3 acetylation plays a key role in gene expression in Plasmodium falciparum. Eukaryot Cell. 2007;6(7):1219–27.
213. Karmodiya K, Pradhan SJ, Joshi B, Jangid R, Reddy PC, Galande S. A comprehensive epigenome map of Plasmodium falciparum reveals unique mechanisms of transcriptional regulation and identifies H3K36me2 as a global mark of gene suppression. Epigenetics Chromatin [Internet]. BioMed Central; 2015;8(1):32. Available from: http://www.epigeneticsandchromatin.com/content/8/1/32%5Cnhttp://www.ncbi.nlm.nih.gov/pubmed/26388940%5Cnhttp://www.pubmedcentral.nih.gov/articlerender.fcgi?artid=PMC4574195
214. Jiang L, Mu J, Zhang Q, Ni T, Srinivasan P. PfSETvs methylation of histone H3K36 represses virulence genes in Plasmodium falciparum. Nature. 2014;499(7457):223–7.
215. Lopez-Rubio JJ, Mancio-Silva L, Scherf A. Genome-wide Analysis of Heterochromatin Associates Clonally Variant Gene Regulation with Perinuclear Repressive Centers in Malaria Parasites. Cell Host Microbe [Internet]. Elsevier Ltd; 2009;5(2):179–90. Available from: http://dx.doi.org/10.1016/j.chom.2008.12.012
216. Coetzee N, Sidoli S, van Biljon R, Painter H, Llinás M, Garcia BA, et al. Quantitative chromatin proteomics reveals a dynamic histone post-translational modification landscape that defines asexual and sexual Plasmodium falciparum parasites. Sci Rep [Internet]. 2017;7(1):1–12. Available from: http://www.ncbi.nlm.nih.gov/pubmed/28377601%5Cnhttp://www.pubmedcentral.nih.gov/articlerender.fcgi?artid=PMC5428830
217. Fraschka SA, Filarsky M, Hoo R, Preiser PR, Fraschka SA, Filarsky M, et al. Comparative Heterochromatin Profiling Reveals Conserved and Unique Epigenome Signatures Linked to Adaptation and Development of Malaria Parasites. Cell Host Microbe. 2018;1–14.
218. Josling GA, Petter M, Oehring SC, Gupta AP, Dietz O, Wilson DW, et al. A Plasmodium Falciparum Bromodomain Protein Regulates Invasion Gene Expression. Cell Host Microbe. 2015;17(6):741–51.
219. Iwanaga S, Kaneko I, Kato T, Yuda M. Identification of an AP2-family Protein That Is Critical for Malaria Liver Stage Development. PLoS One. 2012;7(11).
220. Yuda M, Iwanaga S, Shigenobu S, Kato T, Kaneko I. Transcription factor AP2-Sp and its target genes in malarial sporozoites. Mol Microbiol. 2010;75(4):854–63.
221. Berry A, Deymier C, Sertorio M, Witkowski B, Benoit-Vical F. Pfs 16 pivotal role in Plasmodium falciparum gametocytogenesis: A potential antiplasmodial drug target. Exp Parasitol. Elsevier Inc.; 2009;121(2):189–92.
222. Sinha A, Hughes K, Modrzynska K, Otto T, Pfander C, Dickens N, et al. A cascade of DNA-binding proteins for sexual commitment and development in Plasmodium. Nature. 2014;507:253–61.
223. Modrzynska K, Pfander C, Chappell L, Yu L, Suarez C, Dundas K, et al. A Knockout Screen of ApiAP2 Genes Reveals Networks of Interacting Transcriptional Regulators Controlling the Plasmodium Life Cycle. Cell Host Microbe. 2017;21(1):11–22.
224. Josling G, Llinás M. Sexual development in Plasmodium parasites: knowing when it's time to commit. Nat Rev Microbiol. 2015;13(9):573–87.
225. Arnot D., Gull K. The Plasmodium cell-cycle : facts and questions. Ann Trop Med Parasitol. 1998;92(4):361–6.
226. Jacobberger JW, Horan PK, Hare JD. Cell cycle analysis of asexual stages of erythrocytic malaria parasites. Cell Prolif. 1992;25:431–55.
227. Gritzmacher CA, Reese RT. Protein and Nucleic Acid Synthesis During Synchronized Growth of Plasmodium falciparumt. J Bacteriol. 1984;160(3):1165–7.
228. Mahajan B, Selvapandiyan A, Gerald NJ, Majam V, Zheng H, Wickramarachchi T, et al. Centrins , Cell Cycle Regulation Proteins in Human Malaria Parasite Plasmodium falciparum. 2008;
229. Grimberg BT, Erickson JJ, Sramkoski RM, Jacobberger JW, Zimmerman PA. Monitoring Plasmodium falciparum Growth and Development by UV Flow Cytometry Using an Optimized Hoechst-Thiazole Orange Staining Strategy. Cytometry. 2008;73A:546–54.
230. Spencer SL, Cappell SD, Tsai F, Overton KW, Wang CL, Meyer T. The Proliferation-Quiescence Decision Is Controlled by a Bifurcation in CDK2 Activity at Mitotic Exit. Cell [Internet]. Elsevier Inc.; 2013;155(2):369–83. Available from: http://dx.doi.org/10.1016/j.cell.2013.08.062
231. Foster DA, Yellen P, Xu L, Saqcena M. Regulation of G1 Cell Cycle Progression : Distinguishing the Restriction Point from a Nutrient-Sensing Cell Growth Checkpoint (s). Genes Cancer. 2011;1124–31.
232. Johnson A, Skotheim JM. Start and the Restriction Point. Curr Opin Cell Biol. 2014;25(6):1–12.
233. Voet D, Voet JG, Pratt CW. Fundamentals of Biochemistry. New Jersey: John Wiley & Sons, Inc.; 2013. 71-73 p.

234. Doerig C, Tobin AB. Previews Parasite Protein Kinases : At Home and Abroad. Cell Host Microbe. Elsevier Inc.; 2010;8(4):305–7.
235. Holton S, Merckx A, Burgess D, Doerig C, Noble M, Endicott J. Structures of P . falciparum PfPK5 Test the CDK Regulation Paradigm and Suggest Mechanisms of Small Molecule Inhibition. Structure. 2003;11:1329–37.
236. Doerig C, Billker O, Haystead T, Sharma P, Tobin AB, Waters NC. Protein kinases of malaria parasites : an update. Trends Parasitol. 2008;24(12):571–7.
237. Oredsson S. Polyamine dependence of normal cell-cycle progression. Biochem Soc Trans. 2003;31(2):366–70.
238. Landau G, Ran A, Bercovich Z, Feldmesser E, Horn-Saban S, Korkotian E, et al. Expression profiling and biochemical analysis suggest stress response as a potential mechanism inhibiting proliferation of polyamine-depleted cells. J Biol Chem. 2012;287(43):35825–37.
239. Hoppe H, Verschoor J, Louw AI. Plasmodium falciparum: A Comparison of Synchronisation for in Vitro Cultures. Exp Parasitol. 1991;72:464–7.
240. Allen RJW, Kirk K. Plasmodium falciparum culture : The benefits of shaking. Mol Biochem Parasitol. 2010;169:63–5.
241. Trager W, Jensen JB. Human Malaria Parasites in Continuous Culture. Science (80-). 1976;193(4254):673–5.
242. Lambros C, Vanderberg JP. Synchronization of Plasmodium falciparum erythrocytic stages in culture. J Parasitol. 1979;3:418–20.
243. Reader J, Botha M, Theron A, Lauterbach SB, Rossouw C, Engelbrecht D, et al. Nowhere to hide: interrogating different metabolic parameters of Plasmodium falciparum gametocytes in a transmission blocking drug discovery pipeline towards malaria elimination. Malar J. 2015;14(1):1–17.
244. Verlinden B, De Beer M, Pachaiyappan B, Besaans E, Andayi WA, Reader J, et al. Interrogating alkyl and arylalkylpolyamino (bis)urea and (bis)thiourea isosteres as potent antimalarial chemotypes against multiple lifecycle forms of Plasmodium falciparum parasites. Bioorg Med Chem. 2015;23(16):5131–43.
245. Kafsack BF, Painter HJ, Llinas M. New Agilent platform DNA microarrays for transcriptome analysis of Plasmodium falciparum and Plasmodium berghei for the malaria research community. Malar J. 2012;11(1):187.
246. Van Brummelen AC, Kellen L, Wilinski D, Llinás M, Louw AI, Birkholtz L, et al. Co-inhibition of Plasmodium falciparum S -Adenosylmethionine Decarboxylase / Ornithine Decarboxylase Reveals Perturbation-specific Compensatory Mechanisms by Transcriptome, Proteome, and Metabolome Analyses. J Biol Chem. 2009;284:4635–46.
247. Benjamini Y, Hochberg Y. Controlling the False Discovery Rate : A Practical and Powerful Approach to Multiple Testing. J R Stat Soc. 1995;57(1):289–300.
248. Gentleman RC, Carey VJ, Bates DM, Bolstad B, Dettling M, Dudoit S, et al. Bioconductor : open software development for computational biology and bioinformatics. Genome Biol. 2004;5(10):1–16.
249. Yang YH, Paquet A, Dudoit S. Exploratory analysis for two-color spotted microarray data. 2009. p. 1–84.
250. Hu G, Cabrera A, Kono M, Mok S, Chaal BK, Haase S, et al. Transcriptional profiling of growth perturbations of the human malaria parasite Plasmodium falciparum. Nat Biotechnol. Nature Publishing Group; 2010;28(1):91–8.
251. Friedlander G, Joseph-strauss D, Carmi M, Zenvirth D, Simchen G, Barkai N. Modulation of the transcription regulatory program in yeast cells committed to sporulation. Genome Biol. 2006;7(3):1–14.
252. Aragon AD, Quiñones GA, Thomas E V, Roy S, Werner-washburne M. Release of extraction-resistant mRNA in stationary phase Saccharomyces cerevisiae produces a massive increase in transcript abundance in response to stress. Genome Biol. 2006;7(2):1–13.
253. Szklarczyk D, Franceschini A, Wyder S, Forslund K, Heller D, Huerta-Cepas J, et al. STRING v10: Protein-protein interaction networks, integrated over the tree of life. Nucleic Acids Res. 2015;43(D1):D447–52.
254. Morrissey E. GRENITS: Gene Regulatory Network Inference Using Time Series. R package version 1.24.0. 2012.
255. Assaraf YG, Golenser J, Spira DT, Bachrach U. Polyamine levels and the activity of their biosynthetic enzymes in human erythrocytes infected with the malarial parasite , Plasmodium falciparum. Biochem J. 1984;222:815–9.
256. Toettcher JE, Loewer A, Ostheimer GJ, Yaffe MB, Tidor B. Distinct mechanisms act in concert to mediate cell cycle arrest. PNAS. 2009;106(3).
257. Khan T, Brummelen AC Van, Parkinson CJ, Hoppe HC. ATP and luciferase assays to determine

the rate of drug action in in vitro cultures of Plasmodium falciparum. Malar J. Malaria Journal; 2012;11(1):1–11.
258. Assaraf YG, Golenser J, Spira DT, Messer G, Bachrach U. Cytostatic effect of DL-a-difluoromethylornithine against Plasmodium falciparum and its reversal by diamines and spermidine. Parasitol Res. 1987;73:313–8.
259. Niemand J, Louw AI, Birkholtz L, Kirk K. Polyamine uptake by the intraerythrocytic malaria parasite , Plasmodium falciparum. Int J Parasitol. Australian Society for Parasitology Inc.; 2012;42(10):921–9.
260. Grimberg BT. Methodology and application of flow cytometry for investigation of human malaria parasites. J Immunol Methods. Elsevier B.V.; 2011;367(1–2):1–16.
261. Schmid I, Cole SW, Korin YD, Zack JA, Giorgi J V. Detection of Cell Cycle Subcompartments by Flow Cytometric Estimation of DNA – RNA Content in Combination With Dual-Color Immunofluorescence. Cytometry. 2000;116:108–16.
262. Rittershaus ESC, Baek SH, Sassetti CM. The normalcy of dormancy: Common themes in microbial quiescence. Cell Host Microbe. 2013;13(6):643–51.
263. Darzynkiewicz Z, Evenson D, Staiano-Coico L, Sharpless T, Melamed MR. Relationship between RNA content and progression of lymphocytes through S phase of cell cycle. Proc Natl Acad Sci U S A. 1979;76(1):358–62.
264. Hall N, Carlton J. Comparative genomics of malaria parasites. Curr Opin Genet Dev. 2005;15:609–13.
265. Aragon AD, Rodriguez AL, Meirelles O, Roy S, Davidson GS, Tapia PH, et al. Characterization of Differentiated Quiescent and Nonquiescent Cells in Yeast Stationary-Phase Cultures. Mol Biol Cell. 2008;19:1271–1280.
266. Liu H, Adler AS, Segal E, Chang HY. A transcriptional program mediating entry into cellular quiescence. PLoS Genet. 2007;3(6):0996-1008.
267. Sanderson T, Rayner JC. PhenoPlasm: a database of disruption phenotypes for malaria parasite genes. Wellcome Open Res [Internet]. 2017;2:45. Available from: https://wellcomeopenresearch.org/articles/2-45/v1
268. Wallace HM, Fraser A V, Hughes A. A perspective of polyamine metabolism. Biochem J. 2003;14:1–14.
269. Oredsson SM, Alm K, Dahlberg E, Holst CM, Johansson VM, Myhre L. Inhibition of cell proliferation and induction of apoptosis by N 1 , N 11 -diethylnorspermine-induced polyamine pool reduction. Heal Implic Diet Amin. 2007;35(2):405–9.
270. Alm K, Oredsson S. Cells and polyamines do it cyclically. Essays Biochem. 2009;46:63–76.
271. Kramer DL, Chang B-D, Chen Y, Diegelman P, Alm K, Black AR, et al. Polyamine Depletion in Human Melanoma Cells Leads to G 1 Arrest Associated with Induction of p21 WAF1/CIP1/SDI1 , Changes in the Expression of p21-regulated Genes, and a Senescence-like Phenotype. Cancer Res. 2001;61:7754–62.
272. Hartwell L, Weinert T. Checkpoints: controls that ensure the order of cell cycle events. Science (80-) [Internet]. 1989;246(4930):629–34. Available from: http://www.sciencemag.org/cgi/doi/10.1126/science.2683079
273. Wong JT. Protozoan Cell Cycle Control. Biol Signals. 1996;5:301–8.
274. Butler CL, Lucas O, Wuchty S, Xue B, Uversky VN, White M. Identifying Novel Cell Cycle Proteins in Apicomplexa Parasites through Co-Expression Decision Analysis. PLoS One. 2014;9(5):1–16.
275. Codd A, Teuscher F, Kyle DE, Cheng Q, Gatton ML. Artemisinin-induced parasite dormancy: a plausible mechanism for treatment failure. Malar J [Internet]. BioMed Central Ltd; 2011;10(1):56. Available from: http://malariajournal.biomedcentral.com/articles/10.1186/1475-2875-10-56
276. Krohn M, Skjolberg HC, Soltani H, Grallert B, Boye E. The G1-S checkpoint in fission yeast is not a general DNA damage checkpoint. J Cell Sci [Internet]. 2008;121(24):4047–54. Available from: http://jcs.biologists.org/cgi/doi/10.1242/jcs.035428
277. Dorin-Semblat D, Carvalho TG, Nivez M-P, Halbert J, Poullet P, Semblat J-P, et al. An atypical cyclin-dependent kinase controls Plasmodium falciparum proliferation rate. Kinome. 2013;1:4–16.
278. Tewari R, Dorin D, Moon R, Doerig C, Billker O. An atypical mitogen-activated protein kinase controls cytokinesis and flagellar motility during male gamete formation in a malaria parasite. Mol Microbiol. 2005;58(5):1253–63.
279. Carvalho TG, Doerig C, Reininger L. Nima- and Aurora-related kinases of malaria parasites. Biochim Biophys Acta. Elsevier B.V.; 2013;1834(7):1336–45.
280. Mitra P, Deshmukh AS, Dhar SK. DNA replication during intra-erythrocytic stages of human malarial parasite Plasmodium falciparum. Curr Sci. 2012;102(5):725–40.
281. Kahl CR, Means AR. Regulation of Cell Cycle Progression by Calcium/Calmodulin-Dependent Pathways. Endocr Rev. 2003;24(6):719–36.
282. Means AR. Calcium, calmodulin and cell cycle regulation. FEBS Lett. 1994;347:1–4.

283. Skelding KA, Rostas JAP, Verrills NM. Controlling the cell cycle: The role of calcium/calmodulin-stimulated protein kinases I and II. Cell Cycle. 2011;10(4):631–9.
284. Lei M, Tye BK. Initiating DNA synthesis: from recruiting to activating the MCM complex. J Cell Sci. 2001;114(Pt 8):1447–54.
285. Mehra P, Biswas AK, Gupta A, Gourinath S, Chitnis CE, Dhar SK. Expression and characterization of human malaria parasite Plasmodium falciparum origin recognition complex subunit 1. Biochem Biophys Res Commun. 2005;337(3):955–66.
286. O'Farrell PH. Quiescence: early evolutionary origins and universality do not imply uniformity. Philos Trans R Soc B Biol Sci [Internet]. 2011;366(1584):3498–507. Available from: http://rstb.royalsocietypublishing.org/cgi/doi/10.1098/rstb.2011.0079
287. Crest J, Oxnard N, Ji JY, Schubiger G. Onset of the DNA replication checkpoint in the early Drosophila embryo. Genetics. 2007;175(2):567–84.
288. Sinden R. The cell biology of malaria infection of mosquito: Advances and opportunities. Cell Microbiol. 2015;17(4):451–66.
289. Hughes KR, Philip N, Starnes GL, Taylor S, Waters AP. From cradle to grave : RNA biology in malaria parasites. WIREs RNA. 2010;1:287–303.
290. Tibúrcio M, Dixon MWA, Looker O, Younis SY, Tilley L, Alano P. Specific expression and export of the Plasmodium falciparum Gametocyte EXported Protein-5 marks the gametocyte ring stage. Malar J. 2015;14(334):1–12.
291. Ikadai H, Shaw Saliba K, Kanzok SM, McLean KJ, Tanaka TQ, Cao J, et al. Transposon mutagenesis identifies genes essential for Plasmodium falciparum gametocytogenesis. Proc Natl Acad Sci U S A. 2013;110(18):E1676-84.
292. Silvestrini F, Bozdech Z, Lanfrancotti A, Di Giulio E, Bultrini E, Picci L, et al. Genome-wide identification of genes upregulated at the onset of gametocytogenesis in Plasmodium falciparum. Mol Biochem Parasitol. 2005;143(1):100–10.
293. Lu X, Batugedara G, Lee M, Prudhomme J, Bunnik E, Le Roch K. Nascent RNA sequencing reveals mechanisms of gene regulation in the human malaria parasite Plasmodium falciparum. Nucleic Acids Res [Internet]. 2017;1–16. Available from: https://academic.oup.com/nar/article-lookup/doi/10.1093/nar/gkx464
294. Silvestrini F, Lasonder E, Olivieri A, Camarda G, van Schaijk B, Sanchez M, et al. Protein Export Marks the Early Phase of Gametocytogenesis of the Human Malaria Parasite Plasmodium falciparum. Mol Cell Proteomics. 2010;9(7):1437–48.
295. Adjalley SH, Johnston GL, Li T, Eastman RT, Ekland EH, Eappen AG. Quantitative assessment of Plasmodium falciparum sexual development reveals potent transmission- blocking activity by methylene blue. PNAS. 2011;108(47):E1214–23.
296. Clark K, Dhoogra M, Louw AI. Transcriptional responses of Plasmodium falciparum to a-difluoromethylornithine-induced polyamine depletion. Biol Chem. 2008;389(February):111–25.
297. Bozdech Z, Mok S, Gupta AP. DNA Microarray-Based Genome-Wide Analyses of Plasmodium Parasites. In: Ménard R, editor. Malaria: Methods and Protocols. Totowa, NJ: Humana Press; 2013. p. 189–211.
298. Painter HJ, Altenhofen LM, Kafsack BFC, Llinás M. Chapter 14 Whole-Genome Analysis of Plasmodium spp . Utilizing a New Agilent Technologies DNA Microarray Platform. In: Malaria: Methods and Protocols. 2013. p. 213–9.
299. Branham WS, Melvin CD, Han T, Desai VG, Moland CL, Scully AT, et al. Elimination of laboratory ozone leads to a dramatic improvement in the reproducibility of microarray gene expression measurements. BMC Biotechnol. 2007;7(1):8.
300. Broadbent K, Park D, Wolf AR, Van D, Sims JS, Ribacke U, et al. A Global Transcriptional Analysis of Plasmodium Falciparum Malaria Reveals A Novel Family of Telomere-Associated lncRNAs The Harvard community has made this article openly available . Please share how this access benefits you . Your story matters . Citati. Genome Biol. 2011;1–15.
301. Wei T, Simko V. Visualization of a correlation matrix. 2016. p. 1–17.
302. Meerstein-Kessel L, Van Der Lee R, Stone W, Lanke K, Baker DA, Alano P, et al. Probabilistic data integration identifies reliable gametocyte-specific proteins and transcripts in malaria parasites. Sci Rep. 2018;8(1):1–13.
303. Duffy PE. A Novel Malaria Protein , Pfs28 , and Pfs25 Are Genetically Linked and Synergistic as Falciparum Malaria Transmission-Blocking Vaccines. Infect Immun. 1997;65(3):1109–13.
304. Tiburcio M, Niang M, Deplaine G, Perrot S, Bischoff E, Ndour PA, et al. A switch in infected erythrocyte deformability at the maturation and blood circulation of Plasmodium falciparum transmission stages. Blood. 2012;119(24):172–81.
305. Reininger L, Billker O, Tewari R, Mukhopadhyay A, Fennell C, Dorin-Semblat D, et al. A NIMA-related protein kinase is essential for completion of the sexual cycle of malaria parasites. J Biol Chem. 2005;280(36):31957–64.

306. Mancio-Silva L, Lopez-Rubio JJ, Claes A, Scherf A. Sir2a regulates rDNA transcription and multiplication rate in the human malaria parasite Plasmodium falciparum. Nat Commun. 2013;4:1–6.
307. Ginsburg H. Progress in in silico functional genomics : the malaria Metabolic Pathways database. Trends Parasitol. 2006;22(6):238–40.
308. Kumar S, Kumar M, Ekka R, Dvorin JD, Paul AS, Madugundu AK, et al. PfCDPK1 mediated signaling in erythrocytic stages of Plasmodium falciparum. Nat Commun [Internet]. Springer US; 2017;8(1):1–12. Available from: http://dx.doi.org/10.1038/s41467-017-00053-1
309. Sebastian S, Brochet M, Collins MO, Schwach F, Jones ML, Goulding D, et al. A Plasmodium Calcium-Dependent Protein Kinase Controls Zygote Development and Transmission by Translationally Activating Repressed mRNAs. Cell Host Microbe [Internet]. 2012;12(1):9–19. Available from: http://linkinghub.elsevier.com/retrieve/pii/S1931312812002004
310. Gupta AP, Zhu L, Tripathi J, Kucharski M, Patra A, Bozdech Z. Histone 4 lysine 8 acetylation regulates proliferation and host – pathogen interaction in Plasmodium falciparum. Epigenetics Chromatin. BioMed Central; 2017;1–17.
311. Miao J, Fan Q, Cui L, Li X, Wang H, Ning G, et al. The MYST family histone acetyltransferase regulates gene expression and cell cycle in malaria parasite Plasmodium falciparum. Mol Microbiol. 2010;78(4):883–902.
312. Lin Q, Zhou H, Wurtele H, Zhiguo Z. Acetylation of Histone H3 Lysine 56 Regulates Replication-Coupled Nucleosome Assembly. Cell. 2008;134(2):244–55.
313. Florens L, Washburn MP, Raine JD, Anthony RM, Grainger M, Haynes JD, et al. A proteomic view of the Plasmodium falciparum life cycle. Nature. 2002;419(October):520–6.
314. Petter M, Bonow I, Klinkert MQ. Diverse expression patterns of subgroups of the rif multigene family during Plasmodium falciparum gametocytogenesis. PLoS One. 2008;3(11).
315. Yuda M, Iwanaga S, Shigenobu S, Mair GR, Janse CJ, Waters AP, et al. Identification of a transcription factor in the mosquito-invasive stage of malaria parasites. Mol Microbiol. 2009;71(6):1402–14.
316. Elemento O, Slonim N, Tavazoie S. A Universal Framework for Regulatory Element Discovery across All Genomes and Data Types. Mol Cell. 2007;28(2):337–50.
317. Garcia CRS, Azevedo MF De, Wunderlich G, Budu A, Young JA, Bannister L. Plasmodium in the Postgenomic Era : New Insights into the Molecular Cell Biology of Malaria Parasites. Int Rev Cell Mol Biol. 2008;266(07):85–156.
318. Delves M, Plouffe D, Scheurer C, Meister S, Wittlin S, Elizabeth A, et al. The Activities of Current Antimalarial Drugs on the Life Cycle Stages of Plasmodium : A Comparative Study with Human and Rodent Parasites. PLoS Med. 2012;9(2).
319. Dyer M, Day K. Expression of Plasmodium falciparum trimeric G proteins and their involvement in switching to sexual development. Mol Biochem Parasitol. 2000;108(1):67–78.
320. Lasonder E, Green J, Camarda G, Talabani H, Holder A, Langsley G, et al. The Plasmodium falciparum Schizont Phosphoproteome Reveals Extensive Phosphatidylinositol and cAMP-Protein Kinase A Signaling. J Proteome Res. 2012;11:5323–37.
321. Srivastava A, Philip N, Hughes KR, Georgiou K, MacRae JI, Barrett MP, et al. Stage-Specific Changes in Plasmodium Metabolism Required for Differentiation and Adaptation to Different Host and Vector Environments. PLoS Pathog. 2016;12(12):1–30.
322. Rowe JA, Claessens A, Corrigan RA, Arman M. Adhesion of Plasmodium falciparum-infected erythrocytes to human cells: molecular mechanisms and therapeutic implications. Expert Rev Mol Med [Internet]. 2009;11(May):e16. Available from: http://www.journals.cambridge.org/abstract_S1462399409001082
323. Teng R, Lehane AM, Winterberg M, Shafik SH, Summers RL, Martin RE, et al. H-NMR metabolite profiles of different strains of Plasmodium falciparum. Biosci Rep. 2014;34:685–99.
324. Ginsburg H, Atamna H. The redox status of malaria-infected erythrocytes : An overview with an emphasis on unresolved problems. Parasite. 1994;1:5–13.
325. Atamna H, Pascarmona G, Ginsburg H. Hexose-monophosphate shunt activity in intact Plasmodium falciparum-infected erythrocytes and in free parasites. Mol Biochem Parasitol. 1994;67:79–89.
326. Gardiner DL, Trenholme KR. Plasmodium falciparum gametocytes : playing hide and seek. Ann Transl Med. 2015;3(8):8–10.
327. Duffy S, Avery VM. Identification of inhibitors of Plasmodium falciparum gametocyte development. Malar J. 2013;12(408):408.
328. Lucantoni L, Duffy S, Adjalley SH, Fidock DA, Avery VM. Identification of MMV Malaria Box Inhibitors of Plasmodium falciparum Early-Stage Gametocytes Using a Luciferase-Based High-. Antimicrob Agents Chemother. 2013;57(12):6050–62.
329. Lian L, Al-helal M, Roslaini AM, Fisher N, Bray PG, Ward SA, et al. Glycerol : An unexpected

major metabolite of energy metabolism by the human malaria parasite. Malar J. 2009;8(38):1–4.
330. Mohanty S, Srinivasan N. Identification of “Missing” Metabolic Proteins of Plasmodium falciparum: A Bioinformatics Approach. Protein Pept Lett. 2009;16:961–8.
331. Sana TR, Gordon DB, Fischer SM, Tichy SE, Kitagawa N, Lai C, et al. Global Mass Spectrometry Based Metabolomics Profiling of Erythrocytes Infected with Plasmodium falciparum. PLoS One. 2013;8(4):1–14.
332. Kirk K, Howitt SM, Bröer S, Saliba KJ, Downie MJ. Purine uptake in Plasmodium: transport versus metabolism. Trends Parasitol. 2009;25(6):246–9.
333. Mata-cantero L, Lafuente MJ, Sanz L, Rodriguez MS. Magnetic isolation of Plasmodium falciparum schizonts iRBCs to generate a high parasitaemia and synchronized in vitro culture. Malar J. 2014;13(112):1–9.
334. Coronado LM, Tayler NM, Correa R, Giovani RM, Spadafora C. Separation of Plasmodium falciparum Late Stage-infected Erythrocytes by Magnetic Means. J Vis Exp. 2013;73:2–5.
335. Biolog Inc. Biolog Redox Dye Mixes for Enumerating Mammalian Cells in Proliferation and Chemosensitivity Assays. 2007.
336. Makler MT, Hinrichs DJ. Measurement of the lactate dehydrogenase activity of Plasmodium falciparum as an assessment of parasitemia. Am J Trop Med Hyg. 1993;48(2):205–10.
337. Bochner BR, Siri M, Huang RH, Noble S, Lei X, Clemons PA, et al. Assay of the Multiple Energy-Producing Pathways of Mammalian Cells. PLoS One. 2011;6(3):1–8.
338. Vehkala M, Shubin M, Connor TR, Thomson NR, Corander J. Novel R pipeline for analyzing biolog phenotypic microarray data. PLoS One. 2015;10(3):1–14.
339. Vaas LAI, Sikorski J, Hofner B, Buddruhs N, Fiebig A, Klenk H-P, et al. opm : An R Package for Analysing Phenotype Microarray and Growth Curve Data. Phenotype Microarray Data. 2014;1–31.
340. Galardini M, Mengoni A, Biondi EG, Semeraro R, Florio A, Bazzicalupo M, et al. DuctApe: A suite for the analysis and correlation of genomic and OmniLog™ Phenotype Microarray data. Genomics. Elsevier Inc.; 2014;103(1):1–10.
341. Bochner BR, Gadzinski P, Panomitros E. Phenotype MicroArrays for High-Throughput Phenotypic Testing and Assay of Gene Function. Genome Res. 2001;11:1246–55.
342. Geary TG, Divo AA, Jensen JB. Nutritional Requirements of Plasmodium falciparum in Culture. II. Effects of Antimetabolites in a Semi Defined Medium1. J Protozool. 1985;32(1):65–9.
343. Eisenberg F, Dayton PG, Burns JJ. Studies on the glucuronic acid pathway of glucose metabolism. J Biol Chem. 1959;234(2):250–3.
344. BeMiller JN. An Introduction to Pectins: Structure and Properties. In: Chemistry and Function of Pectins [Internet]. 1986. p. 2–12. Available from: http://pubs.acs.org/doi/abs/10.1021/bk-1986-0310.ch001
345. Kirk K, Horner HA, Kirk J. Glucose uptake in Plasmodium falciparum-infected erythrocytes is an equilibrative not an active process. Mol Biochem Parasitol. 1996;82(2):195–205.
346. Elford BC, Cowan GM, Ferguson DJ. Parasite-regulated membrane transport processes and metabolic control in malaria-infected erythrocytes. Biochem J. 1995;308:361–74.
347. Ginsburg HAGAI. Transport pathways in the malaria - infected erythrocyte Their Characterization And Their Use As Potential Targets ForChemotherapy. Biochem Pharmacol. 1994;48(10):1847–56.
348. Woodrow CJ, Penny JI, Krishna S. Intraerythrocytic Plasmodium falciparum Expresses a High Affinity Facilitative Hexose Transporter. J Biol Chem. 1999;274(11):7272–7.
349. Woodrow CJ, Burchmore RJ, Krishna S. Hexose permeation pathways in Plasmodium falciparum-infected erythrocytes. PNAS. 2000;97(18):2–7.
350. Bochner BR. Sleuthing out bacterial identities. Nature. 1989 May 11;339(6220):157–8.
351. Geary TG, Divo a a, Bonanni LC, Jensen JB. Nutritional requirements of Plasmodium falciparum in culture. III. Further observations on essential nutrients and antimetabolites. J Protozool. 1985;32(4):608–13.
352. Martin RE, Kirk K. Transport of the essential nutrient isoleucine in human erythrocytes infected with the malaria parasite Plasmodium falciparum. Blood. 2007;109(5):2217–25.
353. Ginsburg H, Tilley L. Plasmodium falciparum metabolic pathways (MPMP) project upgraded with a database of subcellular locations of gene products. Trends Parasitol. Elsevier Ltd; 2011;27(7):285–6.
354. Shears MJ, Botté CY, McFadden GI. Fatty acid metabolism in the Plasmodium apicoplast: Drugs, doubts and knockouts. Mol Biochem Parasitol. 2015;199(1–2):34–50.
355. Le Roch KG, Zhou Y, Blair PL, Grainger M, Moch JK, Haynes JD, et al. Discovery of Gene Function by Expression Profiling of the Malaria Parasite Life Cycle. Science (80-). 2003;301(September):1503–9.
356. Aravind L, Iyer LM, Anantharaman V. The two faces of Alba: the evolutionary connection between proteins participating in chromatin structure and RNA metabolism. Genome Biol [Internet].

2003;4(10):R64. Available from: http://www.ncbi.nlm.nih.gov/pubmed/14519199%5Cnhttp://genomebiology.com/content/pdf/gb-2003-4-10-r64.pdf%5Cnhttp://genomebiology.com/2003/4/10/R64%5Cnhttp://www.ncbi.nlm.nih.gov/pubmed/14519199%5Cnhttp://www.pubmedcentral.nih.gov/articlerender.fcgi?artid=

357. Lasonder E, Treeck M, Alam M, Tobin AB. Insights into the Plasmodium falciparum schizont phospho-proteome. Microbes Infect. Elsevier Masson SAS; 2012;14(10):811–9.
358. Graeser R, Wernli B, Franklin RM, Kappes B. Plasmodium falciparum protein kinase 5 and the malarial nuclear division cycles. Mol Biochem Parasitol. 1996;82(1):37–49.
359. Eksi S, Suri A, Williamson KC. Molecular & Biochemical Parasitology Sex- and stage-specific reporter gene expression in Plasmodium falciparum. Mol Biochem Parasitol. 2008;160:148–51.
360. Eksi S, Morahan BJ, Haile Y, Furuya T, Jiang H, Ali O, et al. Plasmodium falciparum Gametocyte Development 1 (Pfgdv1) and Gametocytogenesis Early Gene Identification and Commitment to Sexual Development. PLoS Pathog. 2012;8(10).
361. Coleman BI, Duraisingh MT. Transcriptional control and gene silencing in Plasmodium falciparum. Cell Microbiol. 2008;10(10):1935–46.